REDUCING OPEN CELL LANDFILL METHANE EMISSIONS WITH A BIOACTIVE ALTERNATIVE DAILY COVER

Final Scientific Report
August 1, 2005-March 31, 2009

Principal Author(s)
Helene Hilger, UNC Charlotte Civil and Environmental Engineering
James Oliver, UNC Charlotte Biology
Jean Bogner, Landfills+
David Jones, TenCate Geosynthetics North America

June 2009

DOE Award Number: DE-FC26-05NT42433

Submitted by:
University of North Carolina Charlotte
9201 University City Blvd
Charlotte, North Carolina 28223

with subcontractors:

Landfills+
1144 N. President
Wheaton, IL 60187

and

TenCate[tm] Geosynthetics North America
365 S. Holland Drive
Pendergrass GA 30567

DISCLAIMER

ABSTRACT

Methane and carbon dioxide are formed in landfills as wastes degrade. Molecule-for-molecule, methane is about 20 times more potent than carbon dioxide at trapping heat in the earth's atmosphere, and thus, it is the methane emissions from landfills that are scrutinized. For example, if emissions composed of 60% methane and 40% carbon dioxide were changed to a mix that was 40% methane and 60% carbon dioxide, a 30% reduction in the landfill's global warming potential would result. A 10% methane, 90% carbon dioxide ratio will result in a 75% reduction in global warming potential compared to the baseline. Gas collection from a closed landfill can reduce emissions, and it is sometimes combined with a biocover, an engineered system where methane oxidizing bacteria living in a medium such as compost, convert landfill methane to carbon dioxide and water. Although methane oxidizing bacteria merely convert one greenhouse gas (methane) to another (carbon dioxide), this conversion can offer significant reductions in the overall greenhouse gas contribution, or global warming potential, associated with the landfill. What has not been addressed to date is the fact that methane can also escape from a landfill when the active cell is being filled with waste. Federal regulations require that newly deposited solid waste to be covered daily with a 6 in layer of soil or an alternative daily cover (ADC), such as a canvas tarp. The aim of this study was to assess the feasibility of immobilizing methane oxidizing bacteria into a tarp-like matrix that could be used for alternative daily cover at *open* landfill cells to prevent methane emissions. A unique method of isolating methanotrophs from landfill cover soil was used to create a liquid culture of mixed methanotrophs. A variety of prospective immobilization techniques were used to affix the bacteria in a tarp-like matrix. Both gel encapsulation of methanotrophs and gels with liquid cores containing methanotrophs were readily made but prone to rapid desiccation. Bacterial adsorption onto foam padding, natural sponge, and geotextile was successful. The most important factor for success appeared to be water holding capacity. Prototype biotarps made with geotextiles plus adsorbed methane oxidizing bacteria were tested for their responses to temperature, intermittent starvation, and washing (to simulate rainfall). The prototypes were mesophilic, and methane oxidation activity remained strong after one cycle of starvation but then declined with repeated cycles. Many of the cells detached with vigorous washing, but at least 30% appeared resistant to sloughing. While laboratory landfill simulations showed that four-layer composite biotarps made with two different types of geotextile could remove up to 50% of influent methane introduced at a flux rate of 22 g m^{-2} d^{-1}, field experiments did not yield high activity levels. Tests revealed that there were high hour-to-hour flux variations in the field, which, together with frequent rainfall events, confounded the field testing. Overall, the findings suggest that a methanotroph embedded biotarp appears to be a feasible strategy to mitigate methane emission from landfill cells, although the performance of field-tested biotarps was not robust here. Tarps will likely be best suited for spring and summer use, although the methane oxidizer population may be able to shift and adapt to lower temperatures. The starvation cycling of the tarp may require the capacity for

intermittent reinoculation of the cells, although it is also possible that a subpopulation will adapt to the cycling and become dominant. Rainfall is not expected to be a major factor, because a baseline biofilm will be present to repopulate the tarp. If strong performance can be achieved and documented, the biotarp concept could be extended to include interception of other compounds beyond methane, such as volatile aromatic hydrocarbons and chlorinated solvents.

TABLE OF CONTENTS

Executive Summary 9
Introduction 12
Landfill Alternative Daily Covers 13
Statement of Work 15
Immobilization 15
Adsorption 15
Entrapment 17
Experimental Methods 19
Methanotroph Population Isolation and Identification 19
Site and Sampling 19
Soil Enrichment 19
Methanotrophs by Adsorption from Enriched Soil 19
DNA Isolation and Methanotrophic Diagnostic Microarray Analysis 20
Evaluation of Three Cell Immobilization Techniques 22
Synthesis of Alginate Beads 22
Synthesis of Liquid-Core Gel Capsules. 23
Adsorption of Cells to Various Materials. 24
Accumulation of Biomass on Supports 24
Evaluation of Environmental Factors of Influence on Adsorbed Cells 24
Effects of Temperature on Methane Oxidation 24
Effects of Long-term Methane Starvation on Renewed Methane Oxidation. 24
Effect of Intermittent Methane Starvation on Methane Uptake 25
Cell Stability Assay 25
Geotextile Selection 26
Water Holding Capacity 26
Methane Oxidation Capacity 26
Phosphate Release by Geotextiles with a Phosphate Additive. 27
Laboratory Evaluation of Prototypes 28
Methanotroph Culture Preparation for Biotarp 28

Bench-Scale Continuous Flow Chamber 28
Synthetic Landfill Gas Flux 31
Biotarp Test Sample Preparation 31
Continuous Flow Chamber Sample Collection and Analysis 31
Batch Test After Continuous Flow Incubation 32
Chamber Smoke Tests 33
Visualization of Methanotrophs and Biotarp after Chamber Incubations 33
Field Evaluation of Prototypes 35
Flux Chambers 35
Flux Measurements 36
Gas Chromatography. 37
Statistical Analysis 38
Results and Discussion 38
Cell Immobilization 38
Methanotroph Population Isolation and Identification 38
Evaluation of Three Cell Immobilization Techniques 40
Evaluation of Environmental Factors of Influence on Adsorbed Cells 44
Laboratory Evaluation of Prototypes 48
Water Holding Capacity 48
Methane Oxidation Capacity 49
Phosphorus Release 50
Bench Scale Continuous Flow Chambers 51
Methanotroph Architecture in the Biotarp 54
Field Evaluation of Biotarp Prototypes 60
Experiment 1: Baseline Flux Conditions (11/9-12/07/07) 60
Experiment 2: Biotarps tested over buried waste (12/13-12/20/2007) 60
Experiment 3: Biotarps tested over intermediate cover (1/15-1/16/08) 61
Experiment 4: Biotarps tested over intermediate cover (2/7-2/15/08) 62
Experiment 5: Biotarps tested recessed in intermediate cover (2/20-2/21/08) 63
Experiment 6: Biotarps tested recessed over intermediate cover (2/28-2/29/08) 64
Experiment 7: Composite biotarps with soil (4/17/08) 64

Experiment 8: Composite biotarps with compost (4/25-4/28/08)..... 65
Experiment 9: Composite biotarps and two types of controls (5/22-6/6/08)..... 66
Experiment 10: Effect of longer acclimation time on biotarp performance (6/27-7/22/08)..... 67
Experiment 11: Composite biotarps with shale (7/28-7/31/08)..... 68
Experiment 12: Shale amendment and in-situ methanotroph tarp (8/7-8/25/08) 69
Experiment 13: Multiple treatments on the same chamber in one day (9/19/08 and 10/3/08)..... 70
Experiment 14: Multiple treatments on the same chamber in one day (10/23-11/24/08) 71
Experiment 15: Replicate methane flux readings at a single chamber(4/27/09 and 6/22/09) 72
Conclusions and Recommendations 74
References..... 77

TABLE OF FIGURES

Figure 1: Schematic of typical landfill cell formation..... 10
Figure 2: Five supports incubated in enriched landfill soil..... 19
Figure 3: Gas-tight incubation bottles..... 19
Figure 4: Immobilization by entrapment in alginate beads..... 20
Figure 5: Apparatus for synthesis of alginate beads..... 21
Figure 6: Fixed and moveable frames to position biotarp samples in chamber..... 27
Figure 7: Laboratory-scale continuous flow reactor for biotarp testing..... 27
Figure 8: Sampling and flow measurement locations for mass balance analysis..... 30
Figure 9: Flux chamber design and testing configuration..... 34
Figure 10: Landfill cover soil enriched in a 9% or 45% methane-in-air headspace..... 36
Figure 11: Isolation of methanotrophs from enriched landfill cover soil by adsorption..... 37
Figure 12: Average daily methane uptake by cells adsorbed to supports..... 37
Figure 13: Methane oxidation by alginate beads..... 38
Figure 14: Methane uptake by a mixed methanotroph culture adsorbed to various supports..... 40
Figure 15: Biomass accumulation on various supports..... 41
Figure 16: Methane uptake by cells adsorbed to a geotextile at various temperatures..... 42
Figure 17: Methane uptake rates under starvation conditions..... 44
Figure 18: Methane uptake rates under starvation cycles..... 45
Figure 19: Stability of adsorbed methanotrophs..... 45
Figure 20: Methane oxidation with various geotextile candidates..... 47
Figure 21: Phosphate release by treated geotextile..... 49
Figure 22: Batch study of methane oxidation after continuous flow incubation..... 50
Figure 23: Four-layer composite tarps with soil and compost amendments..... 51
Figure 24: Performance comparison of four layer biotarp prototypes with additives..... 52
Figure 25: Concanavalin A probes for methanotroph EPS..... 53
Figure 26: Fluorescent *In Situ* Hybridization for methanotrophs on geotextile..... 54
Figure 27: Biotarp prototype probed for Type I methanotrophs..... 56
Figure 28: Biotarp prototype probed for Type II methanotrophs..... 57
Figure 29: Repeated measures on a single flux chamber..... 71

EXECUTIVE SUMMARY

.Landfills are one of the largest global anthropogenic sources of methane, contributing 12% of worldwide anthropogenic methane emissions.[1] In the U.S., 2007 figures put landfill methane emissions from the nation's approximately 1800 operating landfills[2] second only to those from livestock operations. While there are strict regulations that guide the final landfill capping to prevent methane emissions, any methane created during the filling of an open landfill cell escapes unabated. The Resource Conservation and Recovery Act requires that solid waste deposited in an open cell be covered daily with a 15 cm (6 in) layer of soil or alternative daily cover (ADC), such as newspaper slurry, foam, or a canvas tarp to prevent windblown trash from getting out and vermin from getting in.

The aim of this study was to assess the feasibility of immobilizing methane oxidizing bacteria into a tarp-like matrix that could be used for alternative daily cover at open landfill cells. The purpose of this "biotarp" would be to mitigate fugitive methane emissions during the time that the open cell is being filled, a period that can last up to one year. Methane is about 20 times as potent as carbon dioxide in terms of its ability to retain heat in the earth's atmosphere; therefore, even though methane oxidizing bacteria merely convert one greenhouse gas (methane) to another (carbon dioxide), this conversion can offer significant reductions in the overall greenhouse gas contribution, or global warming potential, associated with the landfill. For example, if a baseline landfill gas has a composition of 60% methane and 40% carbon dioxide, changing this ratio to 40% methane and 60% carbon dioxide will result in a 30% reduction in the landfill's global warming potential. A 10% methane, 90% carbon dioxide ratio will result in a 75% reduction in global warming potential compared to the baseline.

The specific research objectives were to:

- Isolate methanotrophs from landfill soil and create a culture of mixed methane oxidizing (methanotrophs) bacteria
- Identify a suitable immobilization technique to embed methane oxidizers in a matrix that could be used for ADC
- Visualize and verify methane oxidizer immobilization in the matrix
- Evaluate biotarp prototypes in batch and in continuous flow chambers that simulate landfill conditions
- Determine the response of immobilized methane oxidizers to temperature variation, methane starvation, and washing (to simulate heavy rainfall).
- Evaluate biotarp prototypes under field conditions

The purpose of the first objective, creation of a mixed methanotroph culture, was to provide a source of bacteria for inoculating a potential biotarp matrix. Although methanotroph isolation can be challenging, a modification of previously published methods was used here that

proved to be relatively straightforward procedurally and successful for generating liquid cultures of methanotrophs from soil samples. The liquid cultures were used to inoculate a variety of potential supports that were either suitable for creating a tarp (e.g. geotextile) or suitable for incorporation into a tarp (e.g. glass beads). The cultures were also used to embed the cells in alginate gel beads and to immobilize them in the core of liquid core gel capsules. Testing of the methane oxidation activity of cells immobilized in all of these ways showed that the adsorption of the cells into a synthetic geotextile matrix was the preferable method based on batch methane oxidation capacity studies. The key factor among the materials that performed well as a methanotroph support appeared to be good water holding capacity. Hence, geotextile and natural sponge outperformed glass beads and plastic trickling filter supports. When a series of candidate geotextiles was compared, two were identified that had good water holding capacity and good methane oxidation activity (140-294 mL $CH_4/10^8$ cells inoculated.)

Methane oxidizers adsorbed to geotextile to create a biotarp showed a typical mesophilic response to temperature, which means they will likely be less active in a biotarp during colder months of the year. There is some evidence that population shifts may allow biotarp cultures to adapt to changing temperature, but that phenomenon was not investigated here. Biotarps showed a distinct drop in activity during batch starvation experiments, where they were exposed to alternating conditions of 12 h with and without methane in the headspace. When biotarp swatches were exposed to strenuous washing (to simulate heavy rainfall), about 70% of the cells detached. However, the 30% that remained proved to be quite resistant to removal, suggesting that a biotarp could repopulate after heavy rainstorms. Molecular staining of biotarp specimens to examine the microbial architecture of methane oxidizers in the tarp showed that there was a notable build up of exopolymer substances (EPS), which is known to encase the methanotrophs and inhibit their methane oxidation capacity. It is possible that under field conditions, this EPS may be sloughed off during rain events and serve to revitalize the underlying biofilm.

In laboratory simulations of landfill conditions, where biotarp prototypes were exposed to a continuous flow of methane (22 g m^{-2} d^{-1}) and carbon dioxide from below and air from above, the highest methane uptake observed was 50%, and this was with a four-layer composite biotarp made with two types of geotextile and a layer of methanotroph-inoculated shale layered with the geotextiles. Without an external amendment, methane uptake was high initially and then tapered off as the days of incubation increased. Amendments such as landfill soil, compost, and shale appeared to maintain steadier uptake rates over nine days of incubation.

In field tests, biotarp prototype samples were tested in static flux chambers installed in intermediate cover at a nearby landfill. Control tarps were dry tarps or tarps wetted with either DI or NMS media. The measured bare soil fluxes generally fell in the range of 100-200 g m^{-2} d^{-1}. Six chambers were used within a 6.1 x 6.1 m area (20 x 20 ft) area. It was difficult to draw reliable conclusions from the field experiments because of high flux variability and frequent rain events during the field testing campaign. Another experimental paradigm will likely be needed to obtain more conclusive data about biotarp performance. Specifically, an engineered system to deliver subsurface synthetic landfill gas at known concentrations upward through a field scale

prototype tarp will be needed to eliminate all of the confounding variables of active field conditions.

Overall, the findings suggest that a methanotroph embedded biotarp appears to be a feasible strategy to mitigate methane emission from landfill cells, although the performance of field-tested biotarps was not robust here. If strong performance can be achieved and documented, the biotarp concept could be extended to include interception of other compounds beyond methane. Landfills are well-known for emitting a variety of non-methane organic compounds, and there is evidence that methanotrophs can cometabolize them. Also, the biotarp concept offers a unique opportunity for sensor applications.

INTRODUCTION

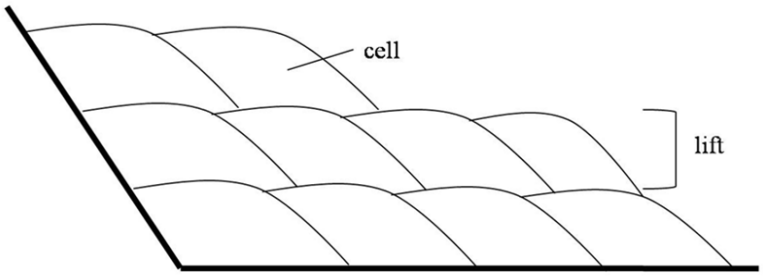

Figure 1: Schematic of typical landfill cell formation

.Landfills are one of the largest anthropogenic sources of methane in the U.S. and throughout the world. Globally, they contribute about 653 million metric tons (720 million U.S. tons) of methane to the atmosphere annually, which represents about 12% of worldwide anthropogenic methane emissions[1]. As of 2007, U.S. landfill methane emissions were estimated at 6.3 million metric tons (7.0 million U.S. tons), making them the second largest anthropogenic source after livestock sources.[2] Despite increased U.S. recycling and composting, 54.3% of U.S. municipal solid wastes (MSW) (121 million metric tons; 133.3 million U.S. tons) were buried in landfills, and there were about 1800 operating U.S. landfills as of 2005[3].

Not surprisingly, landfills have been targeted as a technology where methane mitigation efforts can have substantial impact in reducing greenhouse gas emissions. A ton of deposited municipal solid waste produced about 160 to 250 m^3 of landfill gas, which typically contains 50 to 60% methane and 40 to 50% carbon dioxide[4]. After waste deposition, certain bacteria can breakdown much of the solid organic matter into simpler and more soluble compounds. This process occurs quickly and is accompanied by rapid consumption residual oxygen and nitrate entrained in the waste. This aerobic phase is followed by anaerobic conditions under which volatile fatty acids (VFAs), including acetic acid, butyric acid and propionic acid accumulate, causing the pH to decrease. Using several different pathways, bacteria can use acetic acid and other decomposition products for food, generating methane and carbon dioxide as by-products. As substrates for methane production accumulate, the rate of methane production rises. Methane concentrations of 50% to 60% by volume are typical of this phase[5].

Most landfill methane mitigation efforts center on gas collection, with systems typically installed upon landfill closure, and gas can be collected for as much as 20 years after a landfill has been capped. However, as many practitioners know, landfill methane emissions can begin soon after waste placement, because the depth of waste buried per day, coupled with the practice of daily cover, quickly yields an anaerobic environment followed by methanogen activity. In 2001, using static closed chambers, methane emissions of up to several hundred g $m^{-2}d^{-1}$ were measured on an open active cell at a French landfill[6]. The refuse was compacted approximately 10 m deep and had been in place for a maximum of 40 days. Given that the total range of landfill methane emissions measurements using small scale chamber techniques encompasses seven orders of magnitude (0.0004 – 4000 g m^{-2} d^{-1})[7], this indicates that fully methanogenic

conditions can be developed very quickly and that emissions approaching the highest measured values can occur very early in the life cycle of landfilled waste.

The basic unit of a landfill is a "cell", which includes daily deposits of compacted waste and daily layers of cover material. A cell is typically 3 m (9.8 ft) high, although heights of 10 m (30 ft) have been employed. Cells typically have a rectangular surface area and steeply sloping sides. Waste is deposited into a cell each day and compacted to 710-950 kg/m$^{3)}$ (4679-6260 lb/ft^2).[4] At the end of each work day, the waste is covered by soil, which serves to exclude disease vectors, rodents, and some rainwater, and minimize odor and windborne litter. A given cell is filled to a designated height, after which a new cell is begun. After adjacent cells in a sector are filled to the same height, they are collectively referred to as a lift (Fig. 1). A lift is often covered with an additional 15 cm (6 in) layer of soil or combination of soil and compost that provides a more permanent barrier to odor and stormwater. New cells are then established over the intermediate cover until the landfill section has reached a pre-determined height.

LANDFILL ALTERNATIVE DAILY COVERS

Title 40, Part 258 of the Code of Federal Regulations, Solid Waste Disposal Facility Criteria, requires landfill owners or operators to cover compacted waste with 15 cm (6 in) of earthen material at the end of each operating day, and more frequent coverage is required if there are problems with disease vectors, fires, odors, wind-blown litter or scavengers. This type of daily landfill cover consumes valuable landfill space and reduces the landfill operating life. In cases where soil is not available on site, it must be purchased and delivered, which significantly increases the cost of operations. As a result, several types of alternative daily covers (ADC) have been developed, and they have been well-reviewed by Haughey[8]. Some of the information provided in the review is summarized below.

ADCs can be generally categorized as blankets, sprays, and slurries of waste materials. Blanket ADCs are large tarps that cover the working surface of a landfill. This type of ADC is placed at the end of each operating day, and although many are placed by landfill staff, some are applied with dedicated motorized roller machines. Reusable tarps made of various types of polypropylene or polyethylene geomembranes are taken up each morning, while non-reusable blanket ADCs are composed of thin polyethylene, polypropylene, or polyvinyl chloride. Some non-reusable blankets will thermally degrade in 4-6 weeks; however, others must be perforated to allow them to be left in place without acting as an impermeable layer.

Spray ADC may be applied as either a slurry or a foam. Slurries are solids, such as newspaper, mixed paper, wood fiber, cement kiln dust or fly ash, mixed with water and sprayed over the working landfill surface. The slurry is applied in a thin layer and is designed to harden over the waste after 20 min to 2 h. Foams are composed of synthetic materials such as resins or soaps, and they are mixed with water and applied in a thin layer with a specialized foam sprayer. However, unlike a slurry ADC, the foam does not harden. Compared to daily soil cover, both blanket and spray ADCs take up negligible landfill volume. Waste ADCs may employ yard waste, municipal or industrial wastewater sludge, auto shredder waste, shredded tires, cement

kiln dust, and impacted soil. Although the waste material consumes fill capacity that is approximately equal to that of traditional daily soil cover, it does generate some tipping fee revenue.

After a series of lifts has been completed, but before final capping occurs, it is common practice to place a layer of intermediate cover on top of the cells. This typically a 12 in (30 cm) layer of soil that is seeded for erosion control. A final cover is a highly engineered system that overtops the intermediate cover of a completed landfill sector to minimize infiltration of rain water and dispersion of waste. This final cover also aids in the long-term maintenance of the landfill. The particular composition of the final cover is regulation and site dependent. It will typically consist of a gas control layer that routes gas to flares or a collection system, a filter and drainage layer, and a layer of seeded topsoil for erosion control.

One of the emerging companion strategies to gas collection in Europe is the use of a 1 meter (3.3 ft) deep compost biocover overlain on completed cells either before capping or as part of a modified cap design[9]. Methane passing through biocovers is converted to biomass, carbon dioxide and water. Furthermore, it has also been shown that these microbial populations are successful at removing a number of problematic volatile organic compounds and hazardous air pollutants.[10] Biocovers can be used alone during new landfill start up or as a supplement to gas collection in order to capture fugitive methane emissions. They are also suitable at small landfills where gas collection is not technically or economically feasible[11]. Three basic types of biogas collection systems have been designed and piloted: biocovers, biofilters, and biowindows.

The earliest biocover investigated was a compost cover that was employed to reduce methane emissions from a closed landfill site in Austria[12]. Methane was found to be emitted from control plots without compost covers, but no methane was detected from plots where either sewage sludge compost or municipal solid waste compost was underlain with gravel. The authors concluded that the gravel layer was important for gas distribution and porosity, while the compost provided the proper water-holding capacity and good thermal insulation properties. Subsequent laboratory investigations found that a mature and porous compost enhanced methane uptake over that achieved in conventional landfill cover soil[13].

Biofilters are also designed to host a methanotroph population as well as other microbes that can remove odor and non-methane organic compounds (NMOCs), but they are confined to a smaller area and require an active or passive system to feed the landfill gases into the filter. Oxygen is obtained from the air diffusing downward into the media, so a particular biofiltration medium must have high gas permeability, large surface area, and proper environmental conditions to promote methanotrophic growth and methane oxidation.[10]. Various types of media have been investigated under laboratory conditions, including assorted composts[14,15,16] wood chips, bark mulch, peat, or glass[17] , bottom ash[18], porous clay pellets[19], sand and soils[20,21] and mixtures of organic and inert materials[22,23].

Temperature[24,25], moisture holding capacity[26] and exopolymeric substance (EPS) formation[20] are also important influences in biofilter functioning. EPS is a polysaccharide and water gel produced by some bacteria under certain environmental conditions. It has been

suggested that other stressors, such as nutrient imbalance[27] can promote EPS formation, which can be problematic in bio-based systems because it tends to clog the system and slow the rate of methane oxidation.

STATEMENT OF WORK

The purpose of the work described here was to build on existing biocover technology to devise a method to mitigate methane releases that occur early in the life of a landfill before capping, gas collection or biocovers are implemented. Unlike biocovers or biofilters, the method would require daily emplacement and removal of the bioactive unit so that waste filling could occur during landfill operating hours. Therefore, materials were sought that could be used to support methane oxidizing bacteria, and methods were sought that could immobilize the bacteria in the tarp without sacrificing their capacity for methane oxidation. The goal was to incorporate methane oxidizers into an overnight tarp matrix (ADC) that could be removed each morning and replaced each evening. The following sections will summarize prior work on bacterial immobilization

IMMOBILIZATION

Immobilization techniques have been widely explored over the last 30 years and have been applied to all types of cells, organelles, as well as enzymes, proteins, and other subcellular structures[28,29,30]. An immobilized cell is defined as a cell or remnant thereof that by natural or artificial means is prevented from moving independently of its neighbors to all parts of the aqueous phase of the system under study[31]. Numerous investigations have demonstrated the advantages associated with the use of immobilized cells. Pashova *et al.*[32] found pectinolytic enzyme activity levels were greatly increased in immobilized cells of *Aspergillus niger* compared to free cells. Others report that when Pseudomonas sp. and *Xanthomonas maltophilia* were immobilized, the degradation rate for acrylamide increased over that of sessile cell cultures[33]. Three distinct types of general immobilization methods were considered here: adsorption, confinement in a liquid-liquid emulsion, and entrapment[34].

ADSORPTION

Adsorption involves nonspecific interactions between cells and a surface support material. Bhamidimarri[35] describes three types of forces involved in microbial adsorption: short range forces, interfacial reactions, and long range forces. Short range forces are thought to be the most important[36] and include dipole-dipole interactions and hydrogen bonding. Interfacial reactions are those involved in the conditioning of the surface by microbial production of EPS. Long-range forces consist of Van der Waals forces and electrostatic interactions. The electrostatic forces result from the charges associated with the cell and the surface of the support. Mozes *et al.*[37] presented evidence that adsorption of microorganisms to a support was the result of electrostatic interactions. Adsorption has been optimized by altering the electrostatic charges of cells and a

support surface to increase the immobilization yield[38]. The role of Van der Waals forces in adsorption has been shown empirically by Klotz *et al.*[39]. They demonstrated the adherence of *Candida albicans* and other *Candida* spp. to inert plastic surfaces was a result of Van der Waals attractive forces. In addition to cells being attached to a surface by adsorption, a portion of the cell population may remain physically trapped within the support but dispersed in the liquid phase and not physically attached[40].

In addition to physio-chemical attachments, cellular structures can contribute to adsorption. Three types of cellular mediated attachments to surfaces have been identified: extracellular adhesions, holdfasts, and lipopolysaccharide attachment[35]. Furthermore, flagella are thought to aid in chemotactic responses and hold cells in close proximity to the surface.
It is likely that some combination of cellular, physical and chemical factors mediate the passive attachment of cells to surfaces, depending on the particular microbe and surface involved. What is clear is that cell adsorption if a fairly common phenomenon, and it has even been shown to increase the activity of cells[41].

Use of adsorbed cells has proven to have many practical applications. *Pseudomonas putida* cells were immobilized by adsorption onto magnetite in order to treat Cu^{2+}-containing municipal wastewater[42]. A strain of blue green microalgae was immobilized on a loofa sponge in a continuous flow fixed bed column reactor to efficiently remove heavy metal ions from aqueous solution[43]. Tse and Yu[44] adsorbed a *Pseudomonas* strain capable of degrading synthetic dyes to porous glass beads to increase degradation efficiency from an initial rate of less than 10% to 80%.

Adsorption has several advantages over other immobilization techniques. It is considered the most gentle option because it is passive, and only the natural properties of the cells and support surface are involved[31]. It typically requires no changes in cultivation conditions[40]. Although most investigations of adsorbed cells show increased cellular activity[45,46] this is not always the case[47,48,49]. It has been suggested that adsorbed cells benefit from a localized concentration of nutrients[50]. One of the problems reported with adsorption is that it can be relatively non-specific, so that cells may desorb from a surface as readily as they attach[31]. Furthermore, changes in ionic strength[30,51]or pH[30] can lead to cell desorption[31].

The type of support used for cell adsorption is also critical. The support must be nontoxic and have a high surface area accessible to the cells[52]. Atkinson *et al.*[53] expanded the description of a desirable support material to include the ability to withstand heat sterilization, a resistance to microbial degradation, a cost appropriate to the application, and the ability to be reused. A variety of organic and inorganic supports have been explored, including polyurethane foam[54], wood shavings[55], stainless steel wire meshes[56], natural cellulose sponge[43], ceramics[57], brick[58], porous glass[46], and alumina[59].

In addition to retention, many applications require that the cells be able to grow and replicate. Microorganisms attached to a surface by more than physio-chemical interactions often results in the formation of biofilm[60]. Biofilm formation is actually quite common in nature, with attached microorganisms vastly out-numbering planktonic organisms in natural environments[61].

In a review exploring the incentives for bacterial biofilm production, Jefferson[62] suggests that biofilms play a protective role by allowing the cells within it to withstand shear forces, nutrient deprivation, pH changes, oxygen radicals, disinfectants, and antibiotics better than planktonic organisms. However, there can also be some limitations for cells deep in a biofilm if substrate cannot easily diffuse through the sugar-water gel[63]. A portion of cells within a biofilm can become nutrient and oxygen deprived, leading to lowered cellular activity.

ENTRAPMENT

Cell entrapment is the most frequently used immobilization technique, wherein cells are contained in a three-dimensional gel matrix. There are many different methods to entrap cells, and they are typically independent of the natural properties of the cells themselves[64]. There are also many different materials that can be used to entrap cells, with the most common ones including alginate, polyvinyl alcohol, and proteins.

Poly vinyl alcohol (PVA) is a hydrophilic polymer in which hydrogen bonding occurs between neighboring hydroxyl groups of the polymer chain to form a non-covalent network[65]. At temperatures below 0°C, this bonding is enhanced and is considerably stronger[66]. PVA is very stable and resists biodegradation, making it ideal for nonsterile conditions. The gel strength can be modified by the degree of deacetylation, polymer chain length, concentration, and thaw time[65]. In 1998, Jekel *et al.*[67] introduced a new method that allowed gelation at room-temperature, which avoided much of the cell loss that occurred during the freezing process. Applications of PVA-entrapped cells include ethanol production[68], wastewater nitrification[69], enzyme production[70], nucleoside synthesis[71,72] and gasoline desulfurization[73] .

Proteins have many properties that make them excellent candidates for use in entrapment techniques. The type of film they form depends on their composition (proportion of hydrophobic and hydrophilic residues) and the degree of unfolding they undergo, with the film forming as the unfolded protein separates from the solvent phase. Most protein films are moisture sensitive but provide an excellent barrier to nonpolar substances, such as oxygen and fats[74]. Good film performance correlates with good surface active properties, film forming and mechanical properties, high gas barrier properties, and a high resistance to organic solvents and fats[75]. Other beneficial properties are that it be biodegradable, and easily modifiable. Each protein film type may have unique properties that make it suitable for a particular application. Both animal and plant proteins are available, and include collagen, gelatin, and keratin, wheat gluten, soy and pea protein[76].

One common method used to entrap cells is spray drying, where a cell suspension is atomized using compressed air or nitrogen. The product is collected in a desiccation chamber and dried under a current of hot air[76]. Entrapment by extrusion disburses cells within a molten mass, which is then cooled and solidified[77]. A third method, coacervation, precipitates the protein as a coating onto the cell[76]. Recent applications include the use of whey protein to immobilize probiotics[78], the use of a starch-milk-gluten matrix to co-immobilize lactic acid-

producing bacteria[79], and the conversion of sucrose (via intracellular invertase) by cells immobilized in gelatin[80].

A fourth common technique is to entrap cells in alginate beads or sheets[81]. Alginates are natural marine polymers that have been used in various applications for emulsification, thickening, film formation and gelation[82]. They are composed of copolymers of d-mannuronic and l-glucuronic acid joined in a blockwise fashion by a glycosidic bond, allowing for three possible configurations: M-blocks, MG-blocks, and G-blocks. Some applications of alginate entrapment include the use of immobilized organisms to deliver probiotic organisms[83], to remove contaminants in wastewater treatment[84] and to degrade soil contaminants[85].

Bead preparation involves two main steps: first, the formation of an alginate bead with an internal cell-containing core; and then gelation of alginic acid by multivalent cations[31], which solidifies the droplet surface. Cells are added to a solution of alginate and added dropwise into a bath of dilute aqueous $CaCl_2$. The Ca^{2+} ions react with the alginate molecules, causing them to cross-link[81]. The alginate gels and traps the cells inside a solid-gel bead. The bead size is an important element in a successful entrapment procedure. Beads should be large enough to contain the cells and be handled with ease. The exact size depends on the type of nozzle used, the viscosity of the alginate solution, and the fall distance to the $CaCl_2$ bath.

Alginate entrapment tends to be one of the mildest entrapment methods for cells, so that high viability is maintained[31]. The method is easily performed, and the alginate itself is inert and nontoxic[86,87,88,89]. However, the ionotrophic nature of the alginate makes it highly susceptible to chelating agents, such as phosphate, lactate, and citrate[81]. Also, cells that are located at the bead surface are likely to proliferate more rapidly, leading to mass transfer resistance and bead leakage at the surface[90,91,92]. The alginate bead has a gel polymeric matrix pore size of approximately 10 nm[93], which reduces the space in which cells can proliferate and prevents high cell densities from being reached. Furthermore, as the cell density increases within the bead, the strength of the matrices decreases[90].

Entrapment of cells using liquid core alginate gel (also referred to as hydrogel membrane) capsules is similar to the formation of alginate beads. Similar components are used, but the capsule formation is accomplished by reversing the use of key solutions: cells are mixed in a dilute $CaCl_2$ solution and then added dropwise to an alginate solution. Calcium ions will diffuse from the center of the droplet and bind alginate chains at the surface, with an alginate membrane ultimately forming around a soft gel core of $CaCl_2$/cell mixture. The gel core will not solidify, as it does in the alginate bead[94]. This technique has several advantages over the use of alginate beads, primarily that the cells or other biological materials never contact the gel-forming polymers of the alginate solution[95]. Furthermore, capsule size, membrane thickness, and pore-size can be modified. Capsule size can be changed from a diameter of 100 μm to several mm by adjusting the microdroplet generator. The length of incubation will determine the membrane thickness. Finally, adding various molecular weights and concentration of non-gelling polymer, such as dextran, to the $CaCl_2$ solution can create different specific pore sizes within the capsule. After capsule formation, the non-gelling polymer will diffuse out.

In order to develop and determine the feasibility of a methanotroph embedded biotarp, the following specific research objectives were investigated:

- Isolation of a mixed methanotroph population from landfill cover soil
- Identification a feasible immobilization technique that enhanced methane oxidation
- Determination of immobilized methanotroph responses to temperature variation, methane starvation, and washing
- Evaluation and selection of biotarp prototype components
- Construction and evaluation of biotarp prototypes using continuous flow chambers
- Visualization and verification of immobilized methanotrophs in prototypes
- Evaluation of biotarp prototypes under field conditions

EXPERIMENTAL METHODS

METHANOTROPH POPULATION ISOLATION AND IDENTIFICATION

Site and Sampling

To obtain a culture containing a mixture of methanotrophs, fresh landfill cover soil samples (24.5 cm x 4 cm; 9.6 in x 1.6 in) were collected from a closed landfill in Charlotte, NC. This site has a history of methane production, and soil regions with high methane emissions had previously been identified[8], and the soil was a likely source of methanotroph populations.

Soil Enrichment

The soil was incubated with methane to grow the population of methanotrophs. Large stones and debris were manually removed, and multiple samples of the landfill soil were mixed. The mix was divided into duplicate 50 g subsamples, each of which was placed in a 1L gas-tight jar with a threaded cap. Each jar cap had a Swage-lok compression fitting that held a silicone septum for headspace adjustments and sampling. Various optimal methane headspace concentrations have been offered in the literature for optimal methanotroph enrichment from environmental samples[96,97,98]. Therefore, low and high initial enrichment methane headspace concentrations were tested. A gas-tight syringe was used to prepare a 9% or 45% methane-in-air headspace[99]. This headspace concentration was monitored by gas chromatography and maintained for 21 days at room temperature, with the headspace replenished as needed.

Methanotrophs by Adsorption from Enriched Soil

Once active methane oxidation was observed in the enriched soil, steps to separate the bacteria from the soil were undertaken to obtain a population of mixed methanotrophs in a liquid medium. An alternative to previously published methods of isolating methanotrophs was devised

whereby some potential attachment supports were placed directly within soil samples incubated under methane headspace. Specifically, the moisture content of 20 subsamples of the landfill cover soil was adjusted to 15% (w/w), and the soil was placed in 100 mL gas-tight bottles. Five materials were tested for their ability to adsorb and host methanotrophic cells present in the soil. The supports were selected because they possessed one or more of the following properties: (i) high surface area; (ii) good water holding capacity; and/or (iii) a known propensity for methanotroph or bacterial biofilm attachment. The supports included natural sponge (Florida Sponge, Pinellas Park, FL); a 0.95 cm x 2 cm x 4 cm (0.37 in x 0.79 in x 1.6 in) sample of a highly wettable polypropylene (PP) nonwoven geotextile (TenCate^{tm} Geosynthetics North America, Pendergast, GA); a small sub-section of injection molded polypropylene plastic tower packing material (AceChemPack Tower Packing Co, Hangzhou, China); a 9 cm (3.5 in) diameter circle of polycarbonate membrane with a 0.22 μm pore size (GE Osmonics, Minnetonka, MN); and glass beads with a 20-30 cm (8-12 in) diameter (Polysciences, Warrington, PA) (Fig. 2).

Each support material was placed in the midst of the enriched soil, and the jars were incubated for 20 d at room temperature under a 20% methane-in-air headspace. Methane uptake was monitored by gas chromatography, and headspace methane was replenished as needed. After the 20 d incubation, supports from bottles with the highest methane oxidation capacity were removed to fresh 100 mL gas-tight jars containing 10 mL of Whittenbury's Nitrate Mineral Salts (NMS)[100] (Fig. 3). The samples were shaken at room temperature for 21 d under a 20% methane-in-air headspace, replacing the headspace as needed. The spent media was collected, pooled, and diluted 1:1 in fresh NMS to create liquid cultures containing a mix of soil methanotrophs released from the supports. The fresh liquid cultures were shaken at room temperature in100 mL gas-tight bottles in a 10% methane-in-air headspace. Methane uptake was monitored by gas chromatography, and the resulting mixed methanotroph stock was maintained by fresh inoculations into NMS as the methane headspace was depleted. This cell population was used in subsequent laboratory investigations, including the population characterization described in the following sections.

DNA Isolation and Methanotrophic Diagnostic Microarray Analysis

In order to confirm that the mixed methanotroph culture derived in this way did, in fact, contain methanotrophic cells, DNA was extracted from the enriched sample and a diagnostic microarray was performed. DNA was extracted according to manufacturer instructions from an overnight mixed methanotroph liquid culture using a DNeasy Tissue Kit (Qiagen, Inc.). DNA microarray analysis was conducted as previously described[101] by Dr. Levente Bodrossy at the Austrian Research Centers in Seibersdorf, Austria. Briefly, the *pmoA*/*amoA* genes were amplified from the samples to obtain RNA transcripts. The purified RNA was fragmented and tested sequences specific to various types of methanotrophs with diverse origins. Hybridized slides were scanned, and the results were normalized to a positive control for hybridization with a variety of molecular probes. These probes were derived from sequences specific to various types of

methanotrophs with diverse origins. Hybridized slides were scanned, and the results were normalized to a positive control.

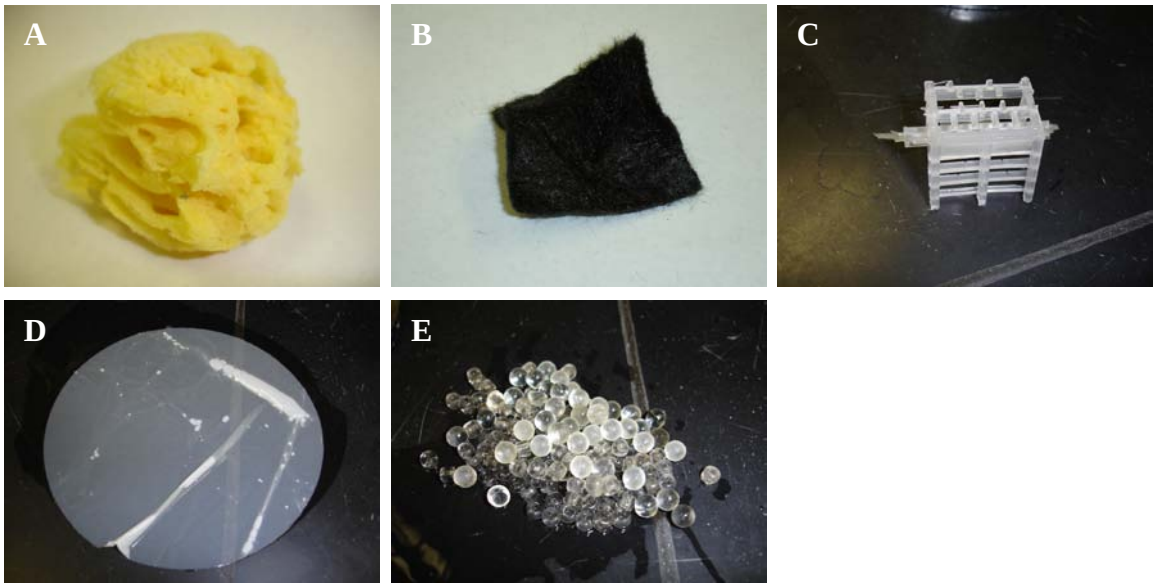

Figure 2.Five supports incubated in enriched landfill soil for isolating methanotrophs by adsorption. A **natural sponge;** B **highly wettable PP nonwoven geotextile;** C **subsection of injected molded polypropylene plastic tower packing material;** D **polycarbonate membrane; and** E **glass beads.**

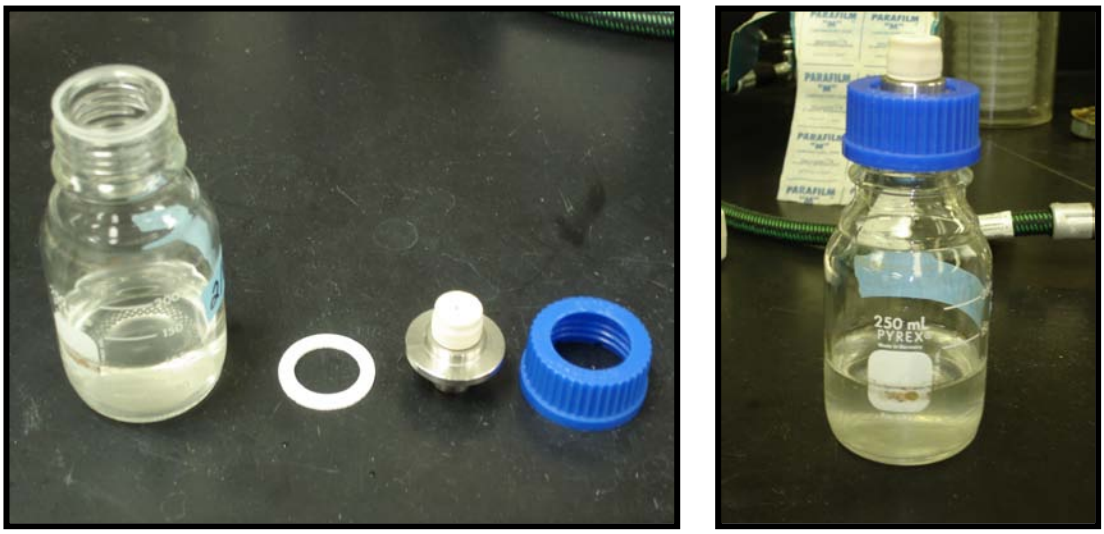

Figure 3. Gas-tight bottle sealed with metal port fittings and capped with a white plastic septum underlain with an additional silicone septum.

EVALUATION OF THREE CELL IMMOBILIZATION TECHNIQUES

Three methods of immobilizing methanotrophs for use in a biotarp were studied. The first was to embed the cells in a gel matrix. The typical matrix is made with alginate, and the resulting gel is gas permeable. The second method was to entrap the cells in a gel coating that had a liquid center containing the cells. It was thought this might offer more opportunity for cell growth and methane uptake. The third method was to adsorb the cells to a matrix so that they would exist as a biofilm on the support material. The rationale for this method was that it might offer less resistance to gases diffusing to and from the cells.

Synthesis of Alginate Beads

Alginate beads were prepared using a modification of the method described by Knaebel et al.[102] (Fig. 4). A 50 mM HEPES solution was prepared and pre-heated to 80°C and divided into 30 mL, 25 mL, and 20 mL aliquots. Sodium alginate (Sigma Aldrich, St. Louis, MO) was added to each solution aliquot under continuous stirring and heat, such that the final concentration after the addition of cells was 6% (w/v). The alginate solutions and a 500 mL 0.1 mM $CaCl_2$ bath solution were then sterilized by autoclaving and allowed to cool to room temperature overnight.

The 30 mL aliquot with alginate served as the control. A 5 mL portion of an overnight methanotroph culture was added to the 25 mL alginate solution to yield a 17% cell suspension containing approximately 5.0×10^8 colony forming units (cfu)/mL and a 10 mL portion of

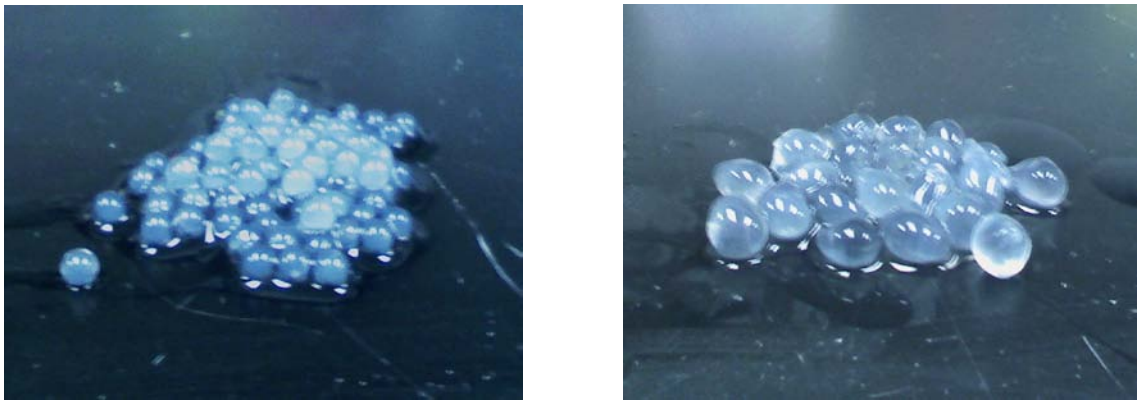

Figure 4. **Immobilization of a mixed methanotroph population by entrapment in alginate beads (left) or liquid-core gel capsule beads (right).**

methanotroph culture was added to the 20 mL alginate solution to yield a 33% cell suspension bead solution containing approximately $2.5x10^7$ cfu/mL The mixtures were gently stirred.

Beads were synthesized by feeding droplets of the solution into a continuously stirred 0.1mM $CaCl_2$ bath (Fig. 5). Droplets were created using a low-flow peristaltic pump that fed the alginate solution through 2 mm (0.08 in) diameter silicone tubing with a 1mm (0.04 in) diameter connector fitted at the end. The droplets fell from a height of approximately 17 cm (6.7 in) above the $CaCl_2$ bath. Beads were formed at a rate of 1 bead/5 seconds, and the mixtures were stirred for an additional 30 min after beads formed, and then the beads were removed by straining through a sterile mesh. The beads from each cell concentration were divided into duplicate 100 mL gas-tight bottles with a 10% methane-in-air headspace. Beads were incubated at room temperature for 3 d, with the headspace methane concentration monitored each day by gas chromatography.

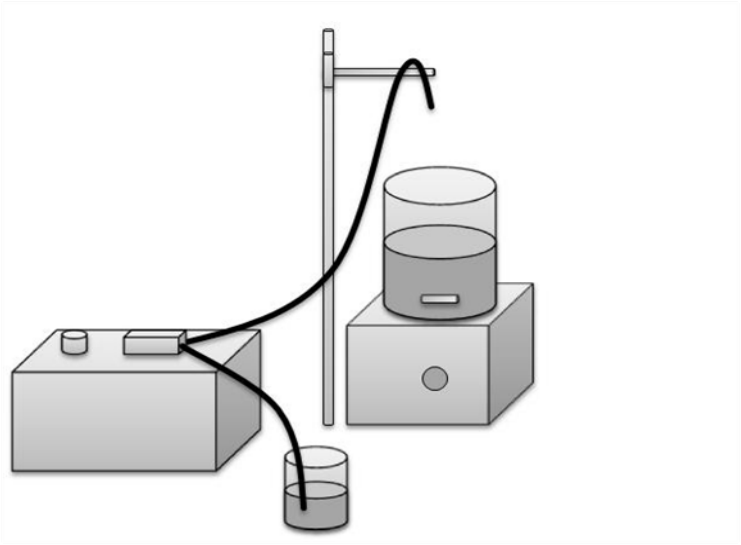

Figure 5. Apparatus for synthesis of alginate beads. The alginate/cell mixture was pumped and added dropwise to a $CaCl_2$ bath.

Synthesis of Liquid-Core Gel Capsules.

Synthesis of liquid-core gel capsules was based on a method described by Koyama and Seki[103], and the same kind of apparatus was employed. A sterile solution containing 2% (w/v) $CaCl_2$ and 20% (w/v) PEG 8000 was prepared. Either 5 mL or 10 mL aliquots of an overnight mixed methanotroph population were added to the solutions to bring the final volumes to 30 mL. This yielded a 33% cell suspension bead solution containing approximately 5.3×10^7 cfu/mL and a 17% cell suspension bead solution containing approximately $1.1x10^8$ cfu/mL. A 30 mL $CaCl_2$-PEG solution served as a negative control. A 1.92 % (w/v) alginate solution was prepared by slowly adding the sodium alginate to a 0.1% (w/v) Tween 60 solution that was pre-warmed to approximately 70°C. The solution was incubated overnight in a 70°C water bath to completely dissolve the alginate before autoclave sterilization.

Beads were synthesized using a peristaltic pump as described previously, but here $CaCl_2$ droplets were dispensed into an alginate bath. Beads were formed at a rate of 1 bead/45 sec, and after 10-15 beads were formed, they were removed with sterile forceps and placed in a sterile 2% (w/v) $CaCl_2$ gelation solution (pH 6.0) for 10 minutes. This process was repeated until 30 mL of

gel capsule beads were synthesized. After formation, each batch was divided between two sterile gas-tight bottles and incubated under a 10% methane-in-air headspace at room temperature. The methane concentration in each bottle was monitored by gas chromatography for 3 d.

Adsorption of Cells to Various Materials.

Six different support types were tested for their ability to maintain a robust population of methanotrophs. These included all of the materials used in the isolation study and one additional material: a 2.5 x 3 x 4 cm (1 in x 1.2 in x 1.6 in) piece of synthetic foam padding with a 19.2 kg m^{-3} (1.2 lb ft^{-3}) density (Foamorder, San Francisco, CA). An overnight mixed methanotrophs population was diluted 1:10 in fresh NMS, and 5 mL aliquots were added to each gas-tight bottle containing a sterile support material. Positive controls consisted of 5 mL portions of culture without the addition of a support. All samples were incubated under a 10% methane-in-air headspace concentration and incubated at room temperature. After 24 h, the methane headspace concentration was analyzed by gas chromatography.

Accumulation of Biomass on Supports

All supports were sterilized, dried for 6 h in a pre-warmed 105°C (221°F) oven, and cooled in a desiccator before pre-weighing. Overnight mixed methanotrophs were diluted 1:10 in fresh NMS, and 10 mL were placed in a gas-tight bottle with each support type in triplicate. The headspace gases were initially adjusted to 10% methane-in-air, and readjusted to this concentration every 2-3 d for 15 d during incubation at room temperature. After this incubation period, supports were then placed in a pre-warmed, 105°C oven to dry for 6 h, cooled in a desiccator, and re-weighed. The biomass accumulation on each support was calculated as the increased weight of the supports after incubation.

Evaluation of Environmental Factors of Influence on Adsorbed Cells

Effects of Temperature on Methane Oxidation

An overnight mixed methanotroph cell population was diluted 1:10 into fresh NMS and 5 mL aliquots were placed into gas tight bottles containing a 38 x 63.5 mm (1.5 in x 2.5 in) piece of TenCate**tm** 567 g/0.84 m^2 (20 oz/yd^2) (osy) wettable PP geotextile. A 10% methane-in-air headspace was prepared and replicate samples were incubated at 5, 15, 25 or 35°C (41, 59, 77, and 95°F) for 24 h. Sterile NMS incubated at room temperature served as a negative. The initial and finial methane headspace concentrations were determined by gas chromatography.

Effects of Long-term Methane Starvation on Renewed Methane Oxidation.

An overnight mixed methanotroph population was diluted 1:10 in fresh NMS, and 5 mL aliquots were added to gas tight bottles containing a 38 x 63.5 mm (1.5 in x 2.5 in) piece of TenCate**tm** 20

osy wettable PP geotextile. A negative control was prepared with sterile NMS. All bottles were prepared with a 10% methane-in-air headspace and the initial methane headspace concentration was measured using gas chromatography. Samples were incubated at room temperature for 24 h, after which the methane concentration was measured and used to calculate the initial methane oxidation rate.

Samples were starved by opening the bottles and allowing atmospheric air to enter and replace the headspace gases. After recapping, gas chromatography was used to confirm that no methane was present, the samples were incubated at room temperature and a 10% methane-in-air headspace was reintroduced after 2, 5, 7, or 9 d. The methane headspace concentration was measured by gas chromatography after a 24 h incubation and the final methane uptake rate calculated.

Effect of Intermittent Methane Starvation on Methane Uptake

An overnight mixed methanotroph population was diluted 1:10 in fresh NMS and a 5 mL aliquot added to gas-tight bottles containing a 38 x 63.5 mm (1.5 in x 2.5 in) piece of 20 osy wettable PP geotextile. A negative control was prepared with sterile NMS. A 10% methane-in-air headspace was established in each bottle, and the initial methane headspace concentration was determined by gas chromatography. All samples were incubated with methane for 18 h, and then the headspace was sampled to determine the final methane concentration and the methane oxidation rate.

All sample headspace volumes were then refreshed, with positive control samples adjusted to a 10% methane-in-air headspace and samples in the starvation treatment receiving air only. After 12 h, methane was reintroduced into bottles in the starved treatment set, and all samples were further incubated for 12 h and then tested for methane oxidation activity. After this 24-h cycle, all headspace gases were refreshed and the 12-hour starvation cycle was repeated 5 times over 5 d.

Cell Stability Assay

In addition to temperature and starvation stress, biotarp methanotrophs will also be subjected to the effects of precipitation in the field. For this reason, the firmness of cell attachment to the geotextile was determined by monitoring methane uptake after washing. An overnight mixed methanotroph population was diluted 1:10 in fresh NMS to a final volume of 35 mL in 250 mL gas-tight bottles in triplicate. Seven pieces of 38 x 63.5 mm (1.5 in x 2.5 in) TenCate^{tm} 20 osy wettable PP geotextile were placed in each of seven bottles and incubated for 15 d under a 10% methane-in-air headspace. The methane headspace was refreshed every 2-3 d. After incubation, three geotextile sections were placed directly into sterile gas-tight bottles with a 10% methane-in-air headspace as positive controls. The remaining 18 geotextile sections were removed to 50 mL conical tubes containing 40 mL sterile DI water. The sections were shaken at 450 rpm, and

each hour, three samples were removed to gas-tight bottles, for a total of 5 h. The initial and finial methane headspace concentrations at 24 and 48 h were determined by gas chromatography.

GEOTEXTILE SELECTION

TenCate^{tm} Geosynthetics (Pendergrass, GA) provided nine geotextiles that were tested as candidates for a biotarp matrix. The criteria that were considered in the evaluation were water holding capacity, ability to support methanotrophs, and ability to support high methane oxidation rates. Some of the specimens were manufactured specifically for this project, while others were among TenCate^{tm}'s standard commercial products. The samples differed in thickness, fiber density, water affinity, and chemical composition (Table 1).

Water Holding Capacity

Triplicate 7.5 cm (3 in) squares of each geotextile were cut. The thickness of each piece was measured, and the swatches were weighed. Each was then soaked in deionized (DI) water for 10 min and weighed to obtain the water-saturated weight. Finally, each swatch was soaked again in DI for 10 min, squeezed until no further water could be removed, and reweighed. Each weight was expressed as g/m^2 by dividing the dry, saturated or wrung out weight of a swatch by its surface area.

Methane Oxidation Capacity

A fresh culture of methanotrophs was grown for 24 h. Three 7.5 cm (3 in) squares of geotextiles were cut and washed thoroughly in DI. Washing consisted of three sequences of soaking in DI for 10 min followed by rinsing in running DI water. The wash process was important because several of the materials tested produced soap-like foam when wetted. The washing process was performed to ensure that the bacteria would not be affected by any chemical originally present in the geotextile. Preliminary trials showed that this wash procedure was adequate for removing all traces of foam. After washing, the swatches were autoclaved for 20 min.

Clean and sterile geotextile pieces were inoculated with 10 mL of freshly prepared mixed methanotroph culture. The liquid absorption by the piece was confirmed by the change in color of the geotextile (the geotextile darkens when wet). The pieces were then tested in 100 mL gas-tight bottles containing about 8% methane-in-air headspace. Methane concentrations in the bottles were measured initially and again after 24 h to evaluate the relative methane oxidation rates associated with each geotextile. The initial oxygen concentration was about 19% of the headspace.

Table 1. Geotextile Candidate Types and Characteristics

TYPE	THICKNESS (cm)	COLOR	CHARACTERISTICS
20 osy wettable PP	0.81 ± 0.04	White	Polypropylene; high water holding capacity
160N	0.30 ± 0.06	Black	Nonwoven polypropylene fibers (64)
20 osy wettable PP 3 denier	0.97 ± 0.01	White	Like 20 osy wettable PP with a lighter thread
6 osy wettable PP 3 denier	0.46 ± 0.04	White	Like 160N with a lighter thread
FR 60	0.36 ± 0.05	White	Treated with a polyphosphate-based additive. Releases inorganic phosphate when wetted.
160N + FR 60	0.61 ± 0.05	White and Black	Composite of two geotextiles
30 osy PP	1.27 ± 0.01	White	A thicker version of 20 osy wettable PP
S1600	0.50 ± 0.01	Grey	Needle-punched nonwoven geotextile made of PP fibers, inert to biological degradation (64)
IR 26	0.70 ± 0.01	Black	High water holding capacity. One side fused during fabrication, inducing a skin-like surface on one side.

Phosphate Release by Geotextiles with a Phosphate Additive.

Candidate geotextile material E (FR60) with phosphate incorporated and FR120, which is composed of two thicknesses of FR60 fused together, were evaluated for their phosphate release rate. It was thought that the phosphate, if released slowly and continually, might enhance methanotroph performance. However, if the phosphate leached rapidly and at high concentrations, it could challenge the osmotic stability of the microbes. Therefore, the phosphate release rates of these geotextiles were assessed.

Newly cut 4 cm x 4 cm (1.5 in x 1.5 in) square sections of geotextiles FR60 and FR120 (with FR120 being twice as thick as FR60) were placed in a flask containing 100mL DI water, and they were shaken at 400 rpm. After 5, 10, 20, and 30 min, 5 mL water samples were removed and diluted 1:10 in fresh DI water. The phosphate concentration was measured using the PhosVer® 3 method (Hach Co., Loveland, CO) for reactive phosphorous (orthophosphate) and a HachDR2500 colorimeter. The geotextile swatches were then transferred to 100 mL fresh DI water to determine if additional phosphate release would occur. After shaking for 5 min, 5

mL of liquid were removed and the phosphate concentrations of the undiluted samples were measured.

LABORATORY EVALUATION OF PROTOTYPES

Continuous flow chambers were designed to simulate landfill conditions more closely than was possible in batch experiments.

Methanotroph Culture Preparation for Biotarp

Stock liquid cultures of the mixed methanotroph population were used to grow methanotrophs for inoculating prototype biotarps in the laboratory-scale reactors. A 100 mL portion of liquid culture was mixed with 900 mL of sterile NMS in a 2 L Erlenmeyer flask with a gas tight stopper and septum. All incubations were conducted at room temperature under a 10% methane-in-air headspace. A sterile magnetic stirrer was used to stir and aerate the cultures overnight before use. The cells were allowed to grow for about 24 h, and then the liquid culture was apportioned among multiple 50 mL plastic centrifuge tubes and spun down at 4500 rpm (Centra GP8R, Thermo Electron Company) for 12 min at 4500rpm at 5 °C. The supernatant was decanted, and an equal volume of fresh NMS was added atop each pellet. After remixing, this preparation was used to inoculate the test geotextiles. Aliquots of the cultures were withdrawn for cell counts on NMS agar before the cultures were used to inoculate the tarps.

Bench-Scale Continuous Flow Chamber

Bench-scale continuous flow chambers were fabricated from cylindrical acrylic plastic (Fig. 6). The cylinders were oriented horizontally so that each chamber was 25.4 cm (10 in) high and 45.7 cm (18 in) long. The chambers were sealed closed at one end and equipped with a gas-tight removable lid at the other end. Two 0.32 cm (0.125 in) diameter brass bulkhead tube fittings (Swagelok, Solon, OH) passed through the sealed wall, spaced 7.6 cm (3 in) apart horizontally from the wall center. A 0.32 cm (0.125 in) brass union tube fitting (Swagelok, Solon, OH.) was fitted at the center of the lid.

The lower bulkhead fittings on the closed end of the chamber were used to accommodate an 8 in piece of 0.32 cm (1/8 in) diameter perforated stainless steel tubing that delivered synthetic landfill gas to the chamber. A bed of gravel was spread beneath the bottom pipe to distribute the gas evenly as it entered test biotarps that would be mounted above the gas tube. Similarly, the upper bulkhead fitting was used to introduce air into the top of the chamber through a 38 cm (15 in) length of 0.32 cm (0.125 in) diameter perforated stainless steel tubing formed into a U-shape.

A circle of 2.5 cm (1 in) thick rectangular commercial furnace filter (E-Z flow II, Flanders Precicionaire, St-Petersburg, FL) was cut to snugly cover the cross-section of the cylindrical chamber. The filter was installed near the open (exit) end of the chamber to function as a gas mixing device. It was important that the gases sampled through the septum-covered

outlet of the chamber were representative of chamber conditions. The lid was fitted with a butyl rubber gasket and secured with six bolts and wing nuts that were tightened to ensure a gas-tight seal.

Inside the bioreactor, a rectangular acrylic frame (0.95 cm; 3/8 in thickness) was installed to hold the biotarp samples in place and prevent gas short-circuiting during testing (Fig. 7). The frame was sealed in place with silicone (Silicone II, GE), and its upper surface had a rubber gasket. Biotarp samples were sandwiched between two gasketed smaller frames, stacked vertically atop the larger fixed frame in the chamber, and secured in place with threaded bolts and wing nuts. The large frame was 30 cm (12 in) long and 17.8 cm (7 in) wide with a 17.8 cm by 11.4 cm (7 in x 4.5 in) opening in the center to accommodate the smaller biotarp frame. The screws were 5 cm (2-in) long and 0.32 cm (0.125 in) diameter, and they were distributed evenly around the larger fixed inside frame. The two small frames were 25.4 cm x 16.5 cm (10 in x 6.5 in) and made from 0.64 cm (0.25 in) thick acrylic plastic. The opening in the small frame was 17.8 cm x 11.4 cm (7 in x 4.5 in), matching the opening of the larger frame.

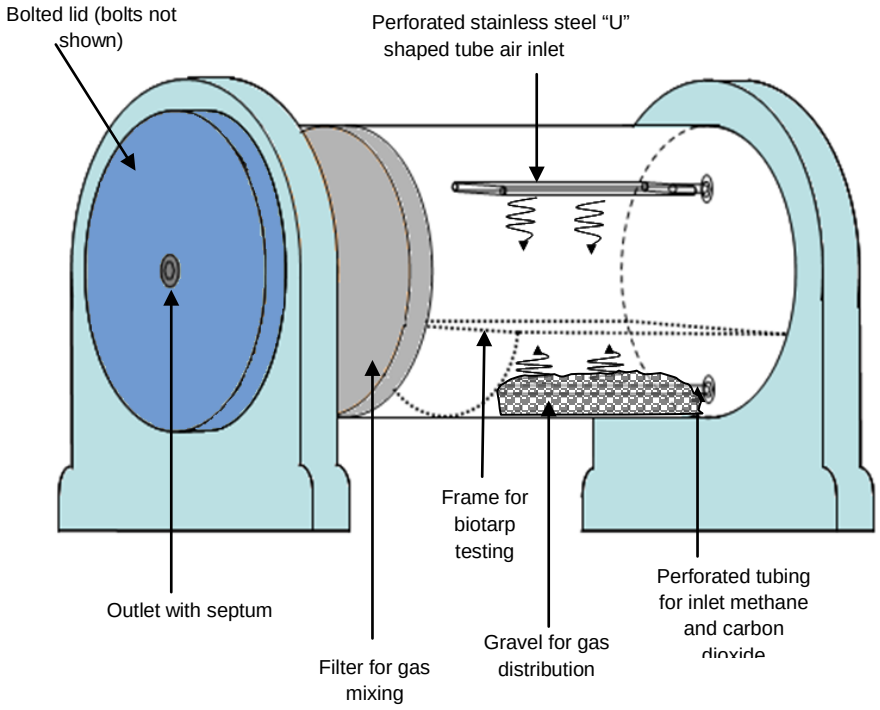

Figure 6. Laboratory continuous flow reactor for landfill simulation

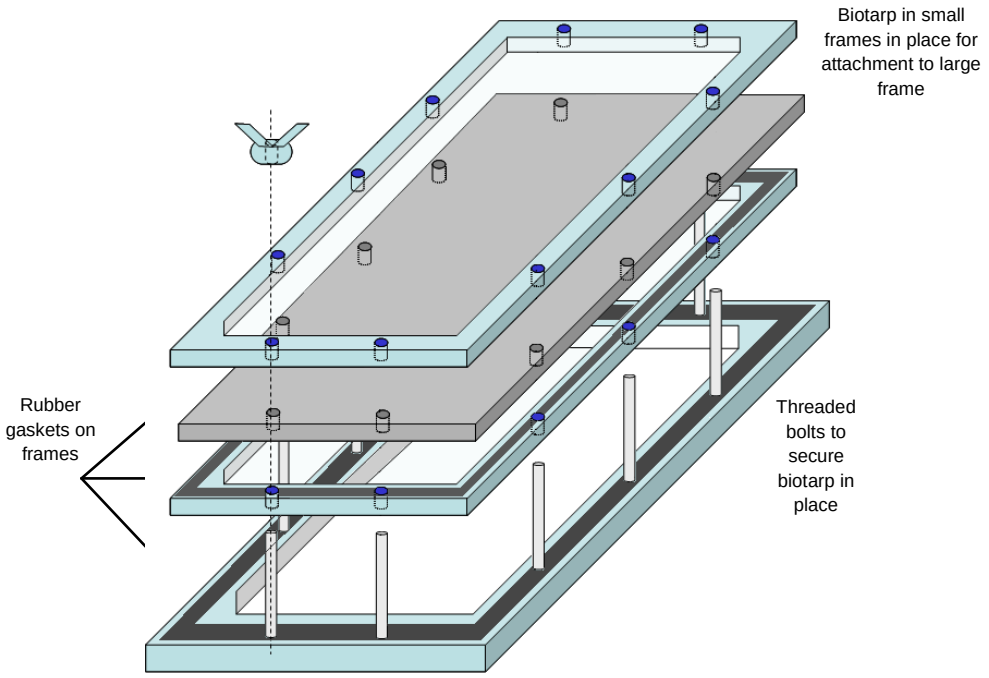

Figure 7. Fixed and moveable frames used to position biotarp samples in the chamber

The synthetic landfill gas was a 1:1 mix of ultra pure methane (National/Specialty Gases, Durham, NC) and bone dry carbon dioxide (National/Specialty Gases, Durham, NC). The gases were combined in a mixing tube before being fed into the chamber. The mixing tube was a 45.7 cm (18 in) length of 5.7 cm (2.25 in) diameter PVC pipe filled with glass wool to enhance mixing and fitted with a gas-tight septum for gas sampling. The gas delivery system was plumbed with stainless steel tubing and Swagelok fittings. Each gas was metered through flow controllers (0-5 mL/min range, VCD 1000, Porter Instrument Inc.) before entering the mixing tube, and then effluent from the mixing tube fed the stainless steel sparging tube inside and near the bottom of the continuous flow chamber. Medical grade air (Linde Gas, Independence, OH) passed through a flow controller (range 0-25 mL/min) before entering the perforated tubing at the top of the test chamber.

Exit flows from the chamber were monitored with a mass flow meter (Amidal 2000, Humonics J&W Scientific, Folson CA) that could be attached to the outlet end via the gas tight silicone septum (Sheet Maot 250c, Alltech, Deerfield, IL). The mass flow meter was also used to calibrate and monitor the flow controllers and conduct preliminary to ensure that the sum of the inlet flows equaled the outlet flow from an empty chamber.

Synthetic Landfill Gas Flux

The continuous flow chambers were operated to create a synthetic landfill gas flux of about 20-25 g m^{-2} d^{-1}. For the 17.8 cm by 11.4 cm (7 in x 4.5 in) test swatch surface area, a 1 mL/min inlet landfill gas flow was used, which for a 1:1 methane and carbon dioxide mix, required 0.5 mL/min of methane and 0.5 mL/min of carbon dioxide. . The flux was calculated according to Eq. 1:

$$F = \frac{f}{1000} * \frac{P}{1 * R * T} * 16 * \frac{1}{A} * 60 * 24 \qquad \text{Eq. 1}$$

Where,

F = methane flux in g m^{-2} d^{-1}

f = methane flux in mL/min

P = atmospheric pressure in Pa

R = ideal gas law constant

T = temperature in degrees Kelvin

A = surface area on the material used in meter

At room temperature (21.1 ^{o}C; 70 ^{o}F), the flux through the tarp was 23.2 g m^{-2} d^{-1}. The air flow was set at 5 mL/min to simulate atmospheric conditions. The flow of methane and carbon dioxide constituted 8.33% of the total flow into the continuous flow chamber, and more oxygen was delivered than methane.

Biotarp Test Sample Preparation

Geotextile pieces were cut to 16.5 cm x 25.4 cm (6.5 in x 10 in) and were tested singly or in various combinations. All were prewashed and autoclaved. The swatches were soaked in the resuspended methanotroph cultures for at least 10 min, removed, and allowed to drain until no further liquid dripped from them. The edges of a test sample were covered with duct tape to prevent short circuiting, which was a particular concern with thicker combinations. As noted above, the taped biotarp sample was then “sandwiched” between the two small Plexiglas frames and anchored to the larger frame inside the continuous flow chamber. All biotarp samples were tested against control samples that were similarly prepared except the geotextile unit was soaked in NMS without methanotrophs.

Continuous Flow Chamber Sample Collection and Analysis

A mass balance of gases into and out of the chamber was conducted (Fig. 8). A 50µl syringe (Hamilton syringe, Reno, Nevada) was used for gas sampling, and duplicate samples were collected to measure gas concentrations in the mixing tube (reactor influent, a mix of pure methane and pure carbon dioxide) and in the reactor effluent (a mix of methane, carbon dioxide, water vapor, nitrogen, and oxygen). The reactor outlet was a Swagelok fitting that

accommodated a length of 0.32 cm (1/8 in) diameter stainless steel tubing. About mid-way along the length of the tubing was a Swagelok "T" fitting with a septum for gas sampling. The flow meter could attach to the end of the tube for flow measurements.

A difference between the inlet and exit flows was expected if methane oxidation was occurring. The reactants are two gases – methane and oxygen. The products are carbon dioxide and water, but the water tends to exist both as liquid water and as water vapor. The result is that there are less gas molecules produced than reacted, so that a slight vacuum develops in the chamber and the exit flow rate is lower than the inlet flow rate.

Methane uptake was calculated by comparing the mass of methane entering the chamber to the mass of methane exiting (Eq. 2).

$$\%CH_4 uptake = \frac{CH_4 in - CH_4 out}{CH_4 in} \times 100 = \frac{\%CH_{4in} \times Flow_{in} - \%CH_{4out} \times Flow_{out}}{Flow_{in} CH_{4in}} \times 100 \qquad \text{Eq. 2}$$

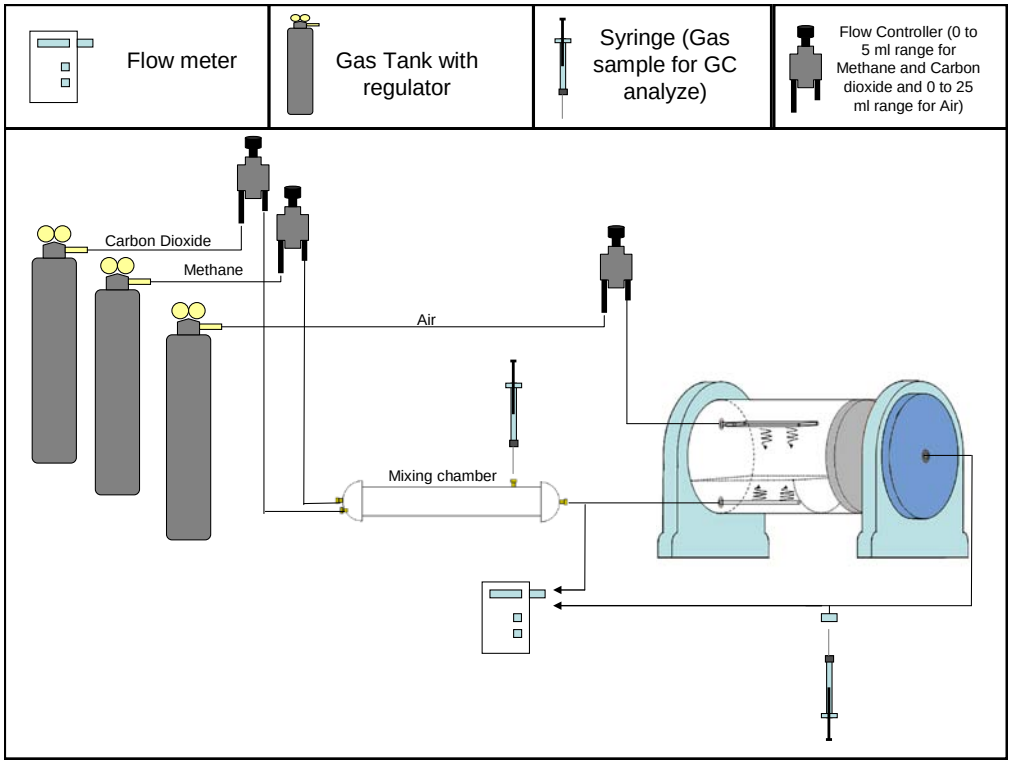

Figure 8. Sampling and flow measurement locations for mass balance analysis.

Batch Test After Continuous Flow Incubation

If no methane oxidation activity was observed in the continuous flow chamber, then upon dismantling, small pieces of the incubated tarp were tested in batch for methane uptake. Tarp pieces were cut into small 4 cm by 4 cm (1.6 in x 1.6 in) squares and incubated in a 100 ml gas-tight bottle under a 10% headspace. The methane concentration was measured (using the Shimadzu GC) just after filling the bottle and then 24 h later. The methane consumption by

control and biotarps were compared. Activity by the biotarp but not by the control would show that (i) the methanotrophic bacteria embedded in the tarp were still oxidizing methane but (ii) the continuous flow chamber experiments did not reveal such activity.

Chamber Smoke Tests

Before any continuous flow studies of biotarp performance were conducted, smoke tests were used to confirm that the gas flow was following the intended path and not short-circuiting. A smoke candle (National Safety Products Incorporated) that emitted smoke for 30 sec was lighted above a funnel, and the funnel outlet was connected to the bottom inlet of the chamber using flexible tubing. A vacuum was applied to the outlet of the chamber just before the candle was lit, so that the smoke was drawn into and through the chamber. Visual inspection of the smoke confirmed that the delivery system provided an even distribution of gas and that no short circuiting occurred.

Visualization of Methanotrophs and Biotarp after Chamber Incubations

A unique protocol was devised to permit visualization of the methanotroph architecture within the geotextile. Specifically, a method was developed to ascertain whether the cells were adsorbed to the geotextile or merely held in liquid droplets within it. Methanotrophs are known to excrete exopolymeric substances (EPS) when attached to surfaces,[104,105,106,107] so the method was also used to determine whether or not EPS was being produced here and interfering with optimum methane oxidation. The technique developed involved first embedding small samples of biotarp and then probing them with fluorescent Concanavalin A to detect EPS and fluorescent oligonucleotides to reveal methanotrophic cells. Concanavalin A binds to glucose and mannose residues[108,109] to reflect the presence of EPS, which is largely a polymer of sugars. The target sugars are among those in methanotroph EPS, although methanotroph EPS contains other sugars as well[110,111,112]. Methanotrophs are known for their ability to synthesize copious EPS, with as much as 62% of their cell biomass due to extracellular polysaccharide[111]. The use of fluorescently labeled oligonucleotides constitutes a method called FISH, fluorescent in situ hybridization. Briefly, the oligonucleotides are configured to attach to short sequences of RNA that are unique to Type I and Type II methanotrophs. The probes are introduced to the sample in a solution that is then washed away. If the probe finds a target and hybridizes, it will remain after washing and be visible via the fluorescent molecule attached to it.[113] The validity of each staining protocol was first established, and then the two techniques were applied.

Biotarp Samples. After a complete trial in a continuous flow chamber one of the four-layer composite biotarp prototypes containing shale was sectioned into 4 cm by 4 cm (1.6 in x 1.6 in) squares. The shale pieces were removed to improve embedding and slicing. Two types of negative controls were prepared; one from a prototype sample that was not exposed to cells and another that was formalin fixed just after soaking in a cell preparation.

Cell Fixation, Embedding, and Slicing. Each geotextile section was fixed in 50 mL of a 5% formalin solution for 5 min. At the North Carolina State School of Veterinary Medicine Histology Laboratory, the geotextile samples were further cut to fit 12 x 16 x 5 mm (0.47 x 0.63 x 0.20 in)(plastic molds (ES Sciences, East Granby, CT). Samples were dehydrated in a series of increasing ethanol concentrations (70%, 80%, 95% and 100%) for one hour each under gentle vacuum. Samples were then transferred to Technovit 7100 (Heraeus Kulze, Wehrheim) infiltrate with a 30-60 min vacuum treatment during infiltration, followed by infiltration overnight at room temperature. After 24 h, the infiltrate was changed again, and samples remained in infiltrate until embedded. Samples were embedded in Technovit 7100 glycol methacrylate resin (Heraeus Kulze, Wehrheim) according to manufacturer instructions. Hardened blocks were placed in a 65°C (150°F) oven for 1 h and stored in a desiccator box prior to microtoming. A glass knife was used to cut 2.5 micron sections, which were then placed on charged slides.

Fluorescent In Situ Hybridization (FISH). A hybridization buffer was prepared from 720 µL 5M NaCl, 80µL Tris-HCl, 4 µL 10% SDS, and 800 µL deionized formamide, and the volume was brought to 4 mL with RNase free water. A moist chamber was created by placing a Kim-Wipe dampened with hybridization buffer in a Petri dish and applying 200 µL of hybridization buffer to each geotextile section. The chamber was placed in a pre-heated 46°C (115°F) incubator for 30 min.

Two probes, Gm705 and Gm633[114], were synthesized with a CY3 tag (MWG Biotech, High Point, NC) and applied to each section at a concentration of 0.01µg/µL. They were mixed well with the hybridization buffer in the dark and further incubated in a 47°C (117°F) pre-warmed oven hybridization chamber for 90 min. A wash buffer was prepared by the addition of 2000 µL 1M Tris-HCl, 4300 µL 5M NaCl, 1000 µL 0.5M EDTA, and 100 µL 10% SDS and brought to 100 mL with RNase free water. The wash buffer was prewarmed to 51°C (124°F) in a water bath before use. Slides were rinsed well with the wash buffer and then flooded before being incubated for 10 min at 51°C (124°F). Slides were rinsed with DI water and dried overnight at room temperature.

Biofilm Staining. A 1mg/mL stock solution of Concanavalin A conjugated to Alexa Fluor 488 (Invitrogen, Eugene, OR) was prepared in a 0.1M sodium bicarbonate (pH 8.3) solution. Sections were stained by diluting 10 µL of the Concanavalin stock in 90 µL sodium bicarbonate solution and incubated in the dark at room temperature for 30 min. Slides were rinsed with DI water and dried overnight. Type I RNA probes were utilized in combination with Alexa Fluor 488 tagged-Concanavalin and Type II probes were used with Alexa Fluor 594 tagged-Concanavalin.

Microscopy. Slides were examined on an inverted fluorescent microscope (Olympus 1X71) with the appropriate filters and images captured using a digital camera (Olympus DP70) mounted atop the microscope.

FIELD EVALUATION OF PROTOTYPES

Flux Chambers

The flux chambers, consisting of a base and dome cover, were designed by Dr. Jean Bogner of Landfills +, who has used such chambers successfully at other sites. The basic design was modified slightly here so that fluxes with and without a biotarp present could be measured. Each chamber had a 40.6 cm (16 in) diameter 0.64 cm (0.25 in) in thick stainless steel cylindrical base that was 22.9 cm (9 in) high (Fig. 9). To accommodate the biotarp, a 2.5 cm (1 in) wide stainless steel ring was welded to the inside circumference of the cylinder 7.6 cm (3 in) from the bottom, and a stainless steel ring was provided to weight down tarp samples placed on the inner ring to prevent short circuiting. At the top of the cylinder, and there was a 1 in wide channel. The chamber lids were made using 0.32 cm (0.125 in) thick stainless steel bowls that when inverted, created a removable dome. At the top of each dome, a gas-tight septum was installed using open-cap stainless steel union tube fittings (Swagelok, Solon, OH) and silicone septum material cut to fit the cap (Sheet Maot 250c, Alltech, Deerfield, IL).

The base of each flux chamber was set firmly into the soil, and additional soil was tamped tightly down to seal the interface between the base and the soil. Then the test sample was emplaced and topped with the rings to hold it in position. The chamber cover was set in the channel just before a flux measurement was taken. Spring clamps were used (four per chamber) to anchor the cover to the base, and then water was poured on the channel to seal the two parts together and prevent gas escape. On a given sampling date if water was present, the chamber was allowed an additional day to thoroughly dry. No testing occurred when the soil was damp. A methane flux measurement method was standardized and used for all testing

Vials and Evacuation Manifold. Samples from the flux chambers were collected in 20 mL pre-evacuated vials (Serum bottles, Fisher Scientific). The vials were closed with a septum stopper (Bellco Glass Inc., Vineland, NJ) and secured with an aluminum cap. Pre-evacuation of the vials was accomplished using a vacuum pump (Welch GEM 1.0) fitted with a digital gauge (OVG64, Omega). A manifold was constructed so that seven vials could be evacuated at one time. The manifold was constructed using stainless steel tubing and connectors (Swagelok, Solon, OH). Valves were included to control the flow to each vial. The manifold had 1 mL plastic syringes (Becton Dickinson & Co.)with needles (22g, Becton Dickinson & Co) adapted to connect to the manifold and accept the bottles. A vacuum of 50 millitorrs (0.0001 psi) was applied to the vials. Pretests showed that the vials could hold the vacuum perfectly for at least three days.

Flux chamber siting and placement. Concord Motor Speedway (CMS) Landfill (Concord, NC), managed by Allied Waste Industries, Inc., provided an area of about 100 m^2 (1080 ft^2) on the landfill for the flux chamber experiments. Six chambers were installed to allow multiple tests to be conducted simultaneously. The site had 60-90 cm (2-3 ft) of intermediate cover atop municipal waste that had been in place about one year. The cover was clay overlain with top soil

in about equal proportions. Since the aim of the chamber experiments was to test prototype biotarps at typical methane flux levels, different chamber depths were tried. By mounting the chambers higher or lower in the intermediate cover, different flux levels, ranging from 30 to 5000 g m^{-2} d^{-1} could be measured. First, the intermediate cover was removed, and the flux chambers were installed directly on the waste layer. In a second configuration, the flux chambers were put on top of the intermediate cover. In a third configuration, about 20 cm (8 in) of intermediate cover soil was removed before the chambers were emplaced.

Flux Measurements

Sample collection for methane flux measurements took about15 min. After the base and the top were clamped and the water seal was poured, a timer was turned on, and the first sample was collected. Samples were subsequently collected over 3 to 5 min timed intervals and put in evacuated vials.

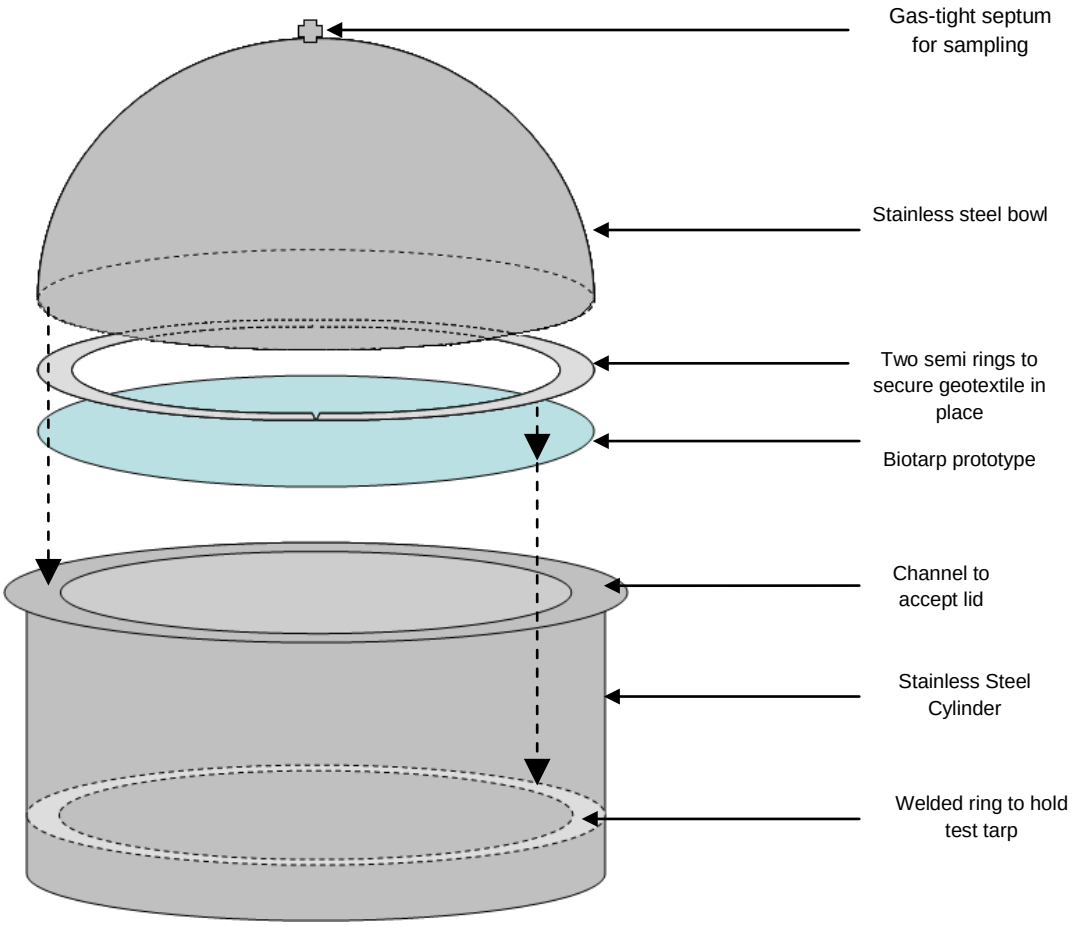

Figure 9: Flux chamber design and testing configuration.

Samples were withdrawn using 60 mL plastic syringes (Becton Dickinson & Co.) equipped with a needle (22g) and a valve. A 50 mL sample was collected at each time point and

immediately injected into in an evacuated vial. Each vial was labeled with the flux chamber number, the time at which the sample was taken, and a sign"-"or "+" to indicate the presence or absence of biotarp in the chamber. During sampling, the site temperature was measured, and atmospheric pressure data was obtained for each sampling date from the "weather.com" website. After a session of sampling, the vials were analyzed using the SRI gas chromatograph that passed the sample through FID and TCD detectors plumbed in series. A graph of the methane concentration versus time was plotted, and a linear regression model was used to calculate an R^2 "goodness of fit" value. If the R^2 value was greater than 0.9, the data was considered acceptable, and the slope of the best fit line was used to calculate the methane mass flow rate from the soil in ppm/min. This volumetric flux was converted to units of g m^{-2} d^{-1} (Eq. 3).

$$F = \frac{f * V}{1000} * \frac{P}{1000 * 1 * R * T} * 16 * \frac{1}{A} * 24 * 60 \qquad \text{Eq.3}$$

Where,

F is the methane flux in g m^{-2} d^{-1}

f is the methane flux in ppm/min

V is the flux chamber volume in m^3

P is the atmospheric pressure in Pa

R is the ideal gas law constant

T is the temperature in degrees Kelvin

A is the surface area of the flux chamber base in meters

Gas Chromatography.

Two gas chromatographs were used. A Shimadzu 14A equipped with a thermal conductivity detector (TCD) was used to measure gas headspace concentrations in batch sample jars. For the continuous flow landfill simulation studies and the field trials an SRI Model 8610c GC from SRI Instruments (Torrance, CA) with a flame ionization detector (FID) and TCD detector plumbed in series. Both instruments were fitted with a CTRI column (Alltech, Deerfield, IL) that yielded distinct peaks for methane, oxygen, carbon dioxide, and nitrogen passing through the TCD detector and a methane peak when the gas sample passed through the FID detector. Helium carrier gas was used for both instruments.

For the Shimadzu 14-A the helium carrier gas was set at a flow rate of 60 cm^3/min, and the detector temperature was set to 75ºC (167 ºF). The injector and oven temperature were both maintained at 60ºC (140ºF). Standard curves were generated using ultra-high purity methane and carbon dioxide (National Welders, Augusta, GA), and oxygen and nitrogen were obtained from atmospheric air sampling each time the GC was employed. The SRI injector was operated near 100ºC (212ºF), the oven at 60ºC, the column at 60ºC, and the TCD at 100ºC. The GC provided ambient air at 6 psi (41.4 MPa) (via an internal pump), as well as hydrogen and helium (via tanks

from National/Specialty Gases, Durham, NC) at 25 psi (172 MPa) and 30 psi (207 MPa), respectively. The GC included a 1 mL injection loop for precise sample measurement, allowing a 5mL syringe to be used to inject approximately 2.5 mL of gas. The GC would automatically inject precisely 1mL of sample. GC calibration was performed using small custom-made tanks from Matheson Tri-Gas (Twinsbug, Ohio); a 10ppm methane/air standard tank, 100ppm methane/nitrogen tank, and a 10% methane in nitrogen tank.

Statistical Analysis

Data were compared using appropriate t-tests or analysis of variance (one-way ANOVA) with a Tukey's multiple comparison test and a two-way ANOVA. Statistical analysis was performed with Microsoft Excel or Prism GraphPad software (GraphPad Software Inc., San Diego, CA).

RESULTS AND DISCUSSION

CELL IMMOBILIZATION

Methanotroph Population Isolation and Identification

Soil Enrichment. Throughout the 21 d soil enrichment, jars with both headspace concentrations showed declining methane and oxygen concentrations and a concomitant rise in carbon dioxide concentrations. These changes are indicative of methane oxidation and suggest that an active methanotroph population was present. Methane oxidation rates in soil enriched in a 9% methane-in-air headspace showed significantly ($p < 0.05$) more methane uptake (47 g CH_4/day) than soil incubated at 45% methane-in-air (5 g CH_4/day). (Fig. 10). Despite having a lower initial methane concentration, the 9% methane headspace samples contained more oxygen. Although some methanotrophs are microaerophiles[115], these data suggest that methanotrophs present exerted enough oxygen demand in the 45% methane-in-air headspace to quickly deplete the oxygen supply, so that no further methane uptake was possible.

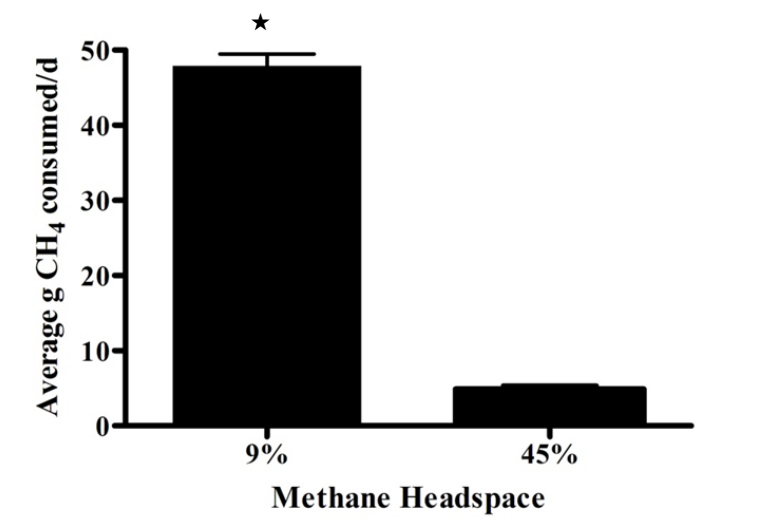

Figure 10. Average daily methane uptake of landfill cover soil enriched in a 9% or 45% methane-in-air headspace. Error bas represent the standard deviation of two replicate samples. ★ indicates a statistically significant difference ($p<0.05$) compared to soil enriched in a 45% methane headspace.

Joergensen and Degn[116] measured an oxygen to methane uptake ratio of 1.7 for Type I methanotroph, *Methylosinus trichosporium*, and a ratio of 1.5 for a Type II methanotrophic

strain. Similarly, environmental samples containing methanotrophs (wetland, agricultural, and forest soil, as well as lake sediment) were found to have an oxygen to methane ratio of 1:1.57-1:1.97. In sediments, methanotrophs will grow at the horizon that best satisfies the ratio ratio demanded by its metabolic pathways.[117]. Czepiel *et al.*[118] showed that methane oxidation rates were independent of oxygen concentrations at compositions greater than 3%. Based on the observed experimental data and reported oxygen levels, a methane headspace concentration of 20% methane was employed, which prevented oxygen concentrations from falling below 3% during subsequent enrichment attempts.

Methanotroph Isolation by Adsorption. Methane oxidation was observed to increase in all samples containing supports as well as in soil-only controls. After 20 days of incubation, only the sponge and synthetic geotextile samples had methane uptake rates significantly different from the controls (Fig. 11). The geotextile and natural sponge consumed 17 g CH_4/day consumed by the soil only control and other supports.

Sustained methane uptake was observed after transferring the sponge and geotextile to fresh NMS (Fig. 12). An average methane uptake of 1.1 g CH_4/day was observed in samples containing the natural sponge and 0.85 g CH_4/day was observed in samples containing the geotextile. There was no statistically significant difference ($p<0.05$) found between the methane uptake by samples containing the natural sponge and geotextile. Furthermore, this observed rate of methane uptake was sustained over the 21 days of enrichment for both supports (data not shown). Negative controls, containing NMS alone, showed negligible methane uptake.

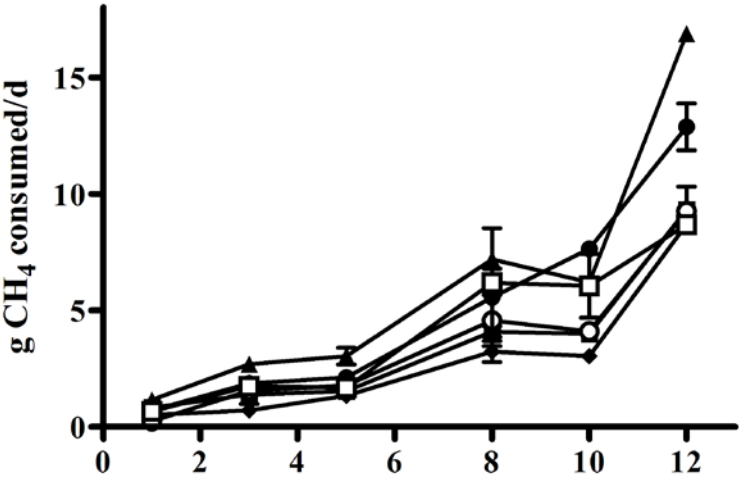

Figure 11. Isolation of methanotrophs from enriched landfill cover soil by adsorption onto natural sponge (▲), synthetic geotextile (●), glass beads (♦), plastic filter packing (□), polycarbonate membrane (○), and negative control (■). Error bars represent the standard deviation of two replicate samples.

There was also evidence that continued enrichment of the supports in liquid media (with aeration) allowed microbes to move from the supports into the solution. The NMS was observed to increase in turbidity, and the pooling of spent media from these samples yielded a liquid culture capable of consuming methane and producing carbon dioxide. As cultures were further

enriched by dilution in fresh NMS over several weeks, a rapid and high methane oxidation rate of nearly 100% methane oxidation in 24 hours was obtained.

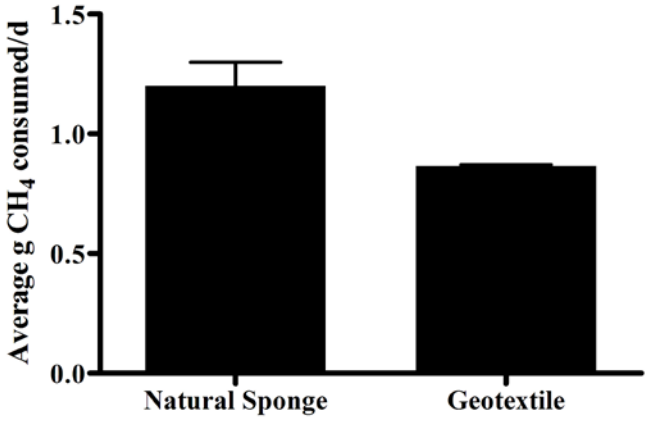

Figure 12. Average daily methane uptake by cells adsorbed to supports placed in NMS. Error bars represent the standard deviation of two replicates

Microarray Analysis. The microarray analysis of extracted DNA confirmed the presence of methanotrophs belonging to the *Methylobacter, Methylosinus,* and *Methylocystis* genera. *Methylobacter* species are Type I methanotrophs, while *Methylosinus* and *Methylocystis* species are Type II methanotrophs. Hybridization with probe Peat264, designed against pmoA sequences derived from a peat soil sample[119], was also observed. The genera found in the enrichment culture are among those that grow optimally under mesophilic conditions[120]. Various studies of methanotroph populations in environmental samples have also found that only a few genera dominate[120,121,122,123,124]. The species found here are consistent with those commonly found together[125], although they represent two very different optimal growth conditions. Type I methanotrophs tend to be found in low methane, high oxygen conditions, while the opposite conditions promote growth of Type II methanotrophs[117,126]. Additionally, the DNA sequence, from which Peat264 probe was derived, was found to be closely related to *Methylocystis parvus*[119]. This is consistent with the positive *Methylocystis* probe results in the microarray assay.

EVALUATION OF THREE CELL IMMOBILIZATION TECHNIQUES

Alginate Beads. Alginate beads were successfully synthesized with a 4 mm diameter and a solid inner core. Methane oxidation by alginate beads containing both of the cell concentrations tested was initially very low but increased over several days. After three days, the 5.0 x 10^8 cfu/mL beads consumed an average of 0.72 g CH_4/day and the 2.5x10^7cfu/mL beads consumed an average of 0.3 g CH_4/day. The cell free control beads had an average methane oxidation rate of 0.15 g CH_4/day (Fig.13). There was a statistically significant ($p<0.05$) difference between the methane uptake by the 5.0x10^8 cfu/mL beads relative to the 2.5x10^7 cfu/mL beads and the cell-free control beads, but no significant difference between the latter two treatments. Methane removal in bottles with control beads was likely due to some methane dissolution into the carry-over liquid surrounding the beads, since no accompanying carbon dioxide production was observed. Carbon dioxide production with concomitant methane and oxygen consumption was observed in beads containing methanotrophic cells.

Although the results clearly indicate that embedded methanotrophic bacteria can successfully oxidize methane, and that the methane uptake rate is proportional to the number of cells embedded, it should be noted that there is a limit to the number of cells that can be embedded per bead. Beads composed of a 50% methanotroph culture were attempted but were unsuccessful. Once dissolved in the HEPES, the bead solution was too viscous for bead formation.

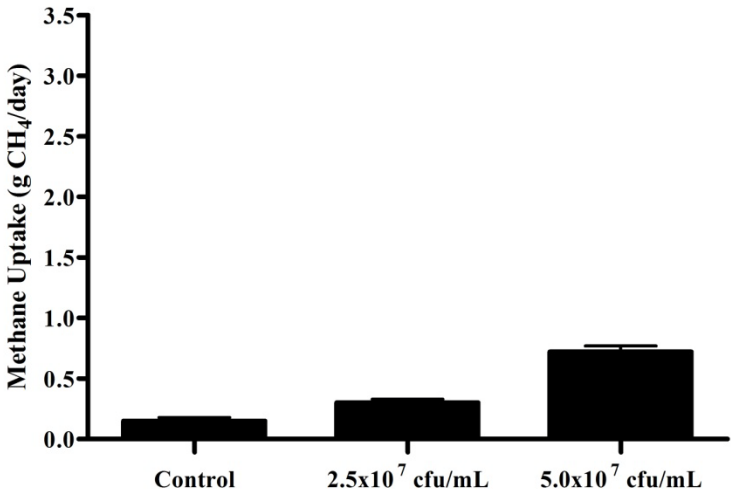

Figure 13. Methane oxidation by liquid-core gel capsules synthesized with various amounts of a mixed methanotroph population and negative control capsules containing no cells. Error bars represent the standard deviation of two replicates.

The lack of significant methane oxidation during the first two days of bead incubation suggests that an acclimatization period was necessary. This may be due to a delay in the transfer of methane molecules into the beads or an adjustment of the methanotrophic cells to growth conditions and methane oxidation within the alginate beads. There was also likely some cell replication during this period, although it was not possible to obtain a final cell count. A more serious problem with the beads was their rapid desiccation rate in open air. They also failed to rehydrate when soaked in water or HEPES. This propensity to desiccate could not be overcome.

Liquid Core Gel Capsules. During the synthesis of liquid-core gel capsule beads, gelation and proper bead formation was found to be highly influenced by the $CaCl_2$ concentration and the shear forces of the stirring alginate solution. At lower $CaCl_2$ concentrations, gelation occurred too slowly and spherical beads did not form. The stirring rated needed to be slow enough to prevent the formation of comet-shaped bodies, but fast enough to prevent beads from aggregating and fusing. Further, bead detention time in the alginate solution affected the thickness of the capsule. Multiple trials led to a detention time of 40 min, and formation of 10-15 beads at a time allowed batches of liquid-core gel capsules to be formed with relatively similar capsule thickness.

Unfortunately, the successfully prepared methanotrophic liquid-core gel capsules showed no statistically significant increased methane oxidation beyond that of controls (data not shown)) or that of cells embedded in solid core alginate beads. Addition of NMS to the incubation bottles did not stimulate activity. Also, like the alginate beads, the liquid core gel capsules quickly desiccated in air and were not considered a suitable immobilization vehicle for biotarp

development. One explanation may be that the higher levels of calcium ion exposure introduced by the 2% $CaCl_2$ solution were inhibitory. A typical methanotroph culture medium contains only 0.02% $CaCl_2$[100]. No reports on calcium homeostasis or calcium toxicity in methanotrophs have been published, but Rosch et al.[127] and King[128] found that increased calcium levels were toxic to *Streptococcus pneumoniae* cells, and a calcium efflux pump was required to survive under such conditions. Also, the alginate gel capsule may have been too thick to allow for sufficient gas exchange or nutrient transfer.

Adsorption to Supports. When the mixed methanotroph culture was applied to various support materials and monitored for activity, the natural sponge showed the greatest methane uptake rate (2.9 g CH_4/day), which was 7.5-fold higher than the positive control (planktonic methanotrophs) and significantly different ($p<0.001$) from all other supports tested (Fig. 14). The geotextile and synthetic foam padding also supported high methane oxidation (1.4 and 2.0 g CH_4/day, respectively) at rates that were significantly higher than the positive control ($p<0.001$) but significantly lower than that of the sponge. Differences in methane uptake activity between the other support materials examined and the control were not statistically significant.

The materials tested had a variety of physical properties that may have made some more successful than others in this testing paradigm. While cell-surface to support surface interactions can be important, the larger factor hereappeared to be the water absorbancy of the support. This is not a surprising factor, but the experiment confirmed that cell-to-support surface interactions was not a limiting factor for any of the high water absorbance materials.

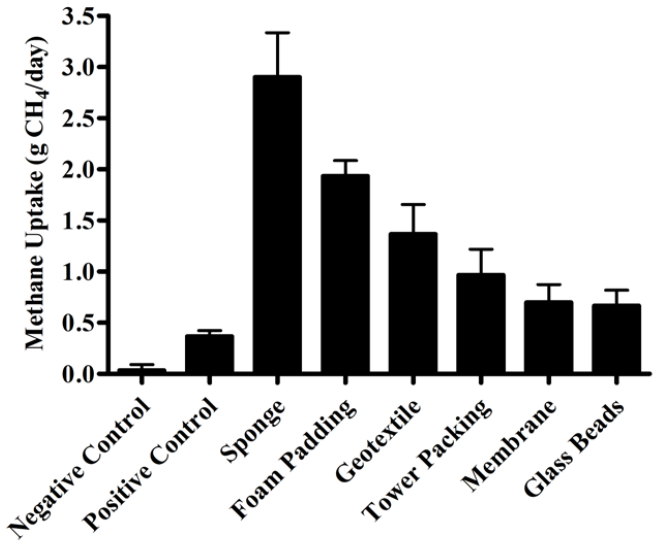

Figure 14. Methane uptake by a mixed methanotroph culture adsorbed to various supports. Negative controls contained sterile NMS (no cells) and positive controls contained an aliquot of liquid methanotrophs culture in NMS. Error bars are the st. dev. of triplicate samples. * indicates a $p<0.05$; ** a $p<0.001$ for means compared to all other conditions.

Accumulation of Biomass on Supports. Clearly, the greater methane uptake by higher methane oxidation was likely due to more cells having attached to the more absorbent material. Therefore, the amount of attached biomass on each material surface was measured. Geotextile samples were found to have a higher average

biomass accumulation than the sponge (87 mg vs. 57 mg); however, the sponge replicates showed high variability, and overall, there was no significant difference between the biomass accumulated on any of the various supports (Fig. 15). These data suggest that the methane oxidation levels observed was not merely a function of the number of attached cells on a particular surface. Furthermore, this indicates that differences in previously observed methane oxidation rates between materials were not due to differences in cell numbers. The enhanced performance by methanotrophs incubated with the natural sponge, geotextile or foam padding is likely due to properties of these materials themselves, with that property being higher water holding capacity.

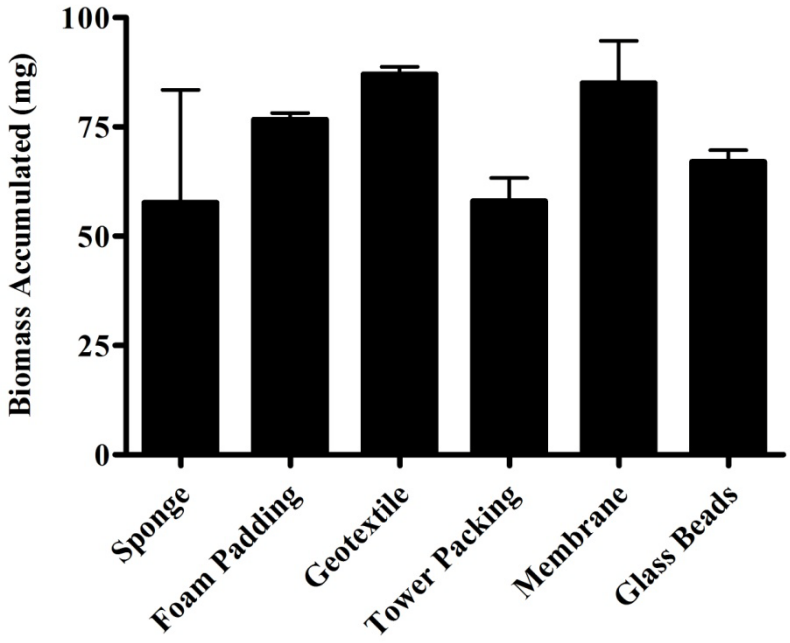

Figure 15. Biomass accumulation on various supports after incubation in a mixed methanotroph population for 15 days. Error bars represent the standard deviation of three replicate samples.

As screening experiments were concluded, several of the support matrices (plastic filter packing, glass beads, and polycarbonate membrane) were eliminated from further consideration due to their low methane uptake performance, handling difficulties, and low water holding capacities. The sponge and foam showed good potential for supporting methane oxidizing organisms, but it was felt that gas permeability through them would be limited, especially at high water content. Additionally, the natural sponge was found to be subject to degradation over time. The synthetic geotextile was selected for further study because of its low propensity for biological degradation, good performance in the methane uptake capacity comparisons, and its ability to hold water but still maintain good gas permeability. It was also much thinner than both the natural sponge and foam padding, making it more suitable for handling under field conditions.

EVALUATION OF ENVIRONMENTAL FACTORS OF INFLUENCE ON ADSORBED CELLS

Temperature Effects. Methane uptake was highly influenced by temperature (Fig 16). Samples held at 5°C (41°F) performed similarly to negative controls, with 0.1 g CH_4/day removed. Samples incubated at 15°C (59 °F) had slightly higher methane oxidation rates; however this increase was not statistically significant. Samples incubated at 25°C (77 °F) and 35 °C (95 °F) had average methane uptake rates of 2.2 g CH_4/day and 3.3 g CH_4/day, respectively. These rates were significantly higher ($p<0.001$) than those at the lower temperatures. Additionally, the 35°C oxidation rates were significantly higher ($p<0.01$) than the 25°C rates.

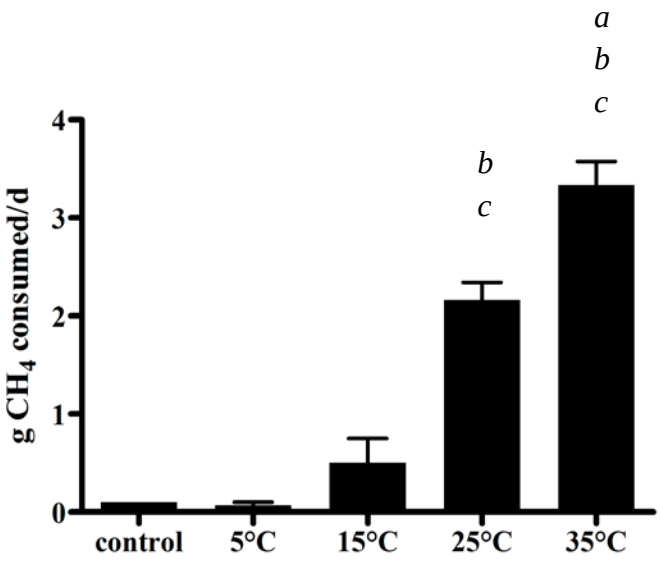

Figure 16. Methane uptake by cells adsorbed to a geotextile at various temperatures. Error bars represent the standard deviation of three replicate samples. Control samples contained planktonic cells held at room temperature. *a* indicates a $p<0.01$ for means compared to 25°C. *b* indicates a $p<0.001$ for means compared to 15°C. *c* indicates a $p<0.001$ for means compared to 5°C.

Increased methane oxidation with increasing temperature is consistent with landfill cover field observations [129],, laboratory landfill soil investigations [130], [131], [132], and laboratory investigations involving pure methanotroph cultures[133]. Maximum methane oxidation for the immobilized mixed methanotroph population in this investigation occurred at 35°C, however methane oxidation may be maintain at temperatures higher than 35°C[134]. Such temperatures were not examined, as they are unlikely to be encountered under field conditions.

These data suggest that, neglecting other factors, a methanotroph immobilized biotarp will function optimally at higher temperatures and may not provide much mitigation at lower temperatures. The methanotroph population employed was enriched and maintained at room temperature, and the optimal growth conditions were likely the moderate temperatures of 25 and 35°C. However, there is evidence that mixed methanotroph populations can shift to meet altered growth conditions. Gebert *et al.*[135] enriched biofilter media samples containing a mixed methanotroph population at 28°C (82°F) and found a methane oxidation temperature optimum of 38°C (100°F). However, when the media samples were enriched at 10°C (50°F), the optimal temperature for methane oxidation was 22°C (72°F). Examination of the methanotrophs in each

sample revealed that the dominant methanotrophic species had shifted. This was later supported by diagnostic microarray analysis, which confirmed the population shift was due to temperature[136].

The mixed methanotroph population utilized in this investigation was maintained at 25°C, favoring mesophilic methanotrophs. The culture was incubated at low temperatures for only 24 h. If incubated at low temperature for a longer time, a population shift like the one observed by Gebert *et al.* may allow the population to adapt.

Starvation Effects. Methanotrophs absorbed to a geotextile had an initial average methane uptake rate of 1.9 g CH_4/day before starvation. After each of the starvation durations tested, renewed methane uptake was observed (Fig. 17). After two days, a mean renewed methane uptake of 3.4 g CH_4/day was observed, which is almost a two-fold increase over the baseline uptake rate. However, after 5, 7, and 9 d of methane starvation,, uptake rates declined 2.3, 1.7, and 12.5-fold, respectively. Negative controls showed no methane uptake.

The increased methane uptake rate observed in the two day starved samples indicated that cell growth took place during the starvation period. As methane is soluble in both distilled water and seawater[137], it is also likely soluble in NMS. It is possible that the methanotrophs used methane that dissolved during the initial incubation period. It is also possible that cell growth did not occur, but that the stress of starvation induced a physiological response that increased the subsequent methane uptake rate. These data indicate that immobilized cells can tolerate a two day period of methane starvation and that short periods of starvation may enhance the oxidation rate.

Although methane uptake rates were much lower in samples exposed to five days of starvation, detection of some methane oxidation indicated that a portion of the cells survived and were metabolically active when methane was added to the headspace. Other cells in these populations may have been dying or entering a dormant state[138]. *Methylosinus trichosporium* forms exospores when methane starved[139], while other methanotrophs, such as *Methylobacter, Methylococcus, and Methylomonas*, form cysts[138]. If these survival structures were present in the longer starved samples, the 24-h period after methane re-introduction may not have been sufficient to allow for germination[138]. Whittenbury, et al.[138] noted that older exospores (7 d to 18 months) required 7-15 d to germinate. Longer recovery incubations with methane may be required for methane oxidation to return to its initial oxidation rate. This evidence also suggests that a methanotroph embedded biotarp could be stored off the landfill surface for short periods of time, without causing a loss of methane uptake potential.

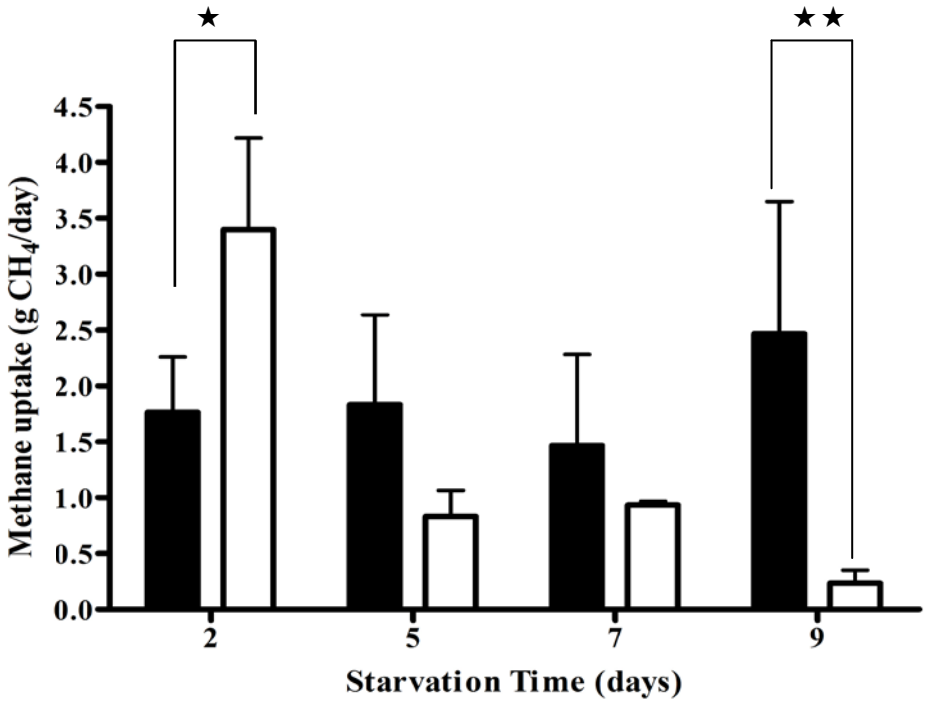

Figure 17. Initial (■) and final (□) methane uptake rates by a mixed methanotroph population adsorbed to a geotextile and methane starved for various amounts time. Error bars represent the standard deviation of three replicate samples. ★ indicates a $p<0.05$ and ★★ indicates a $p<0.01$ as compared to the means specified.

Conceptually, a biotarp would be methane starved approximately every 12 h while a landfill cell is being filled; therefore, the effects of methane starvation cycles were investigated. After the first 12-h starvation cycle, there was no difference in the methane uptake by starved and control cells (Fig. 18). However, after the second cycle of starvation, methane oxidation levels began to decline, and methane uptake fell to only 0.5 g CH_4/day after the fifth cycle. Control samples that received methane every 24 h with no starvation period, showed an initial methane uptake increase, but it was not sustained. By day three, uptake in controls began to decline as well. This was unexpected, as methane was plentiful in these samples, and a steady state rate was anticipated by day 3 or 4. The results suggest that multiple 12 h cycles of on-off methane cycling had a more significant effect on renewed methane uptake than a single 24 h interruption of continuous methane provision.

On the other hand, the decline in methane uptake rates by control samples suggested that methane starvation was not the only factor influencing oxidation rates. Although the methane headspace was refreshed every 24 h in the controls, the inorganic nutrients were not. The depletion of the inorganic salts in the NMS medium may have caused the decline in methane uptake by controls and amplified the effects of starvation in the methane cycled samples. Subsequent experiments were conducted in which additional NMS was added to the samples (data not shown). However, no increase in methane uptake was observed.

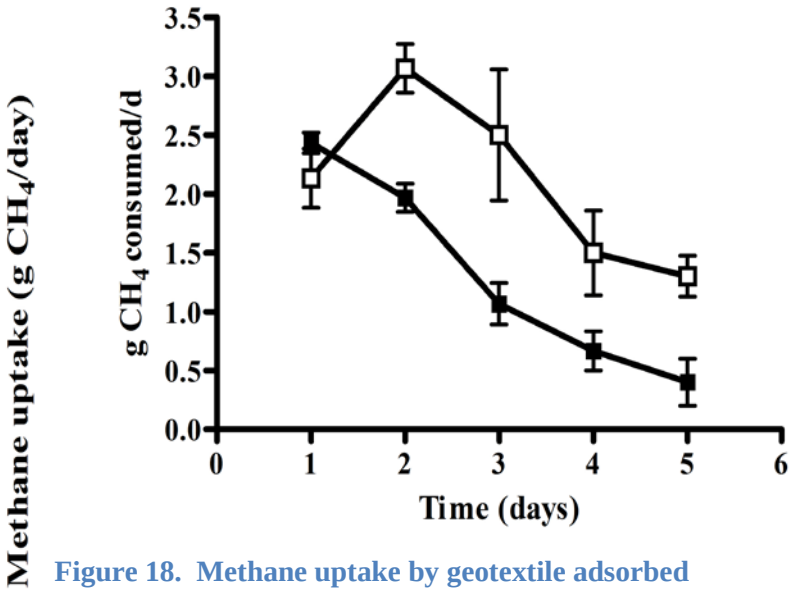

Figure 18. Methane uptake by geotextile adsorbed methanotrophs under a constant methane atmosphere (□) or cycle of 12 h methane, then 12 h air (■). Error bars represent the standard deviation of triplicate samples.

Cell Stability. Baseline methane uptake of samples used for cell stability testing was 2.3 g CH_4 after 24 h. This rate generally decreased over the 5 h of washing (Fig. 19). Initial oxidation rates declined by approximately 74% at the one hour mark, however there was no further decline in methane oxidation thereafter. These data suggest that despite a significant cell loss initially, a population of cells remains attached and capable of continuing to oxidize methane. Methane uptake increased further after 48 h post- washing in all samples (with a daily methane uptake similar to the 24 h post-washing rate), indicating continued activity of the remaining cells. These data suggest the biotarp may be capable of repopulation following cell during a precipitation event.

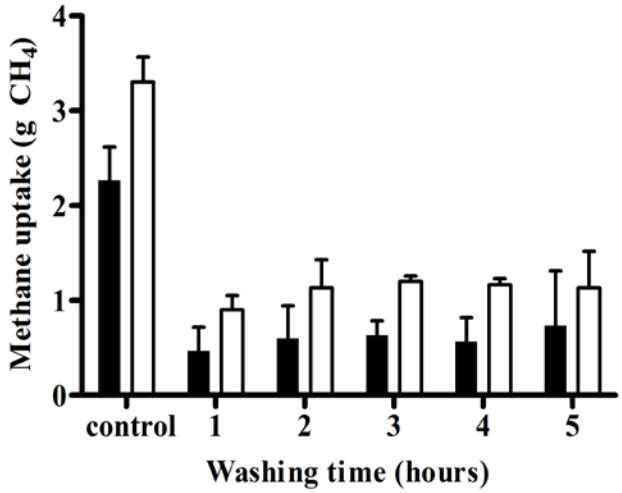

Figure 19. Methane uptake by a mixed methanotroph population adsorbed to geotextile sections at 24 h (■) and 48 h (□) after washing in DI water for various durations. Controls were unwashed geotextiles sections. The error bars represent the st. dev. of triplicate samples.

LABORATORY EVALUATION OF PROTOTYPES

Water Holding Capacity

The water holding capacity (WHC) of the nine geotextiles varied widely (Table 2). Geotextiles A, H and had the best WHC of the nine materials tested after being allowed to drain. Sample I held the maximum amount of water, with A and H holding 99.3% and 92.5% as much as I, respectively. None of the other drained samples retained more than 70% of the water retained by I. When wrung dry, material H had the maximum WHC of the group, with I and A retaining 88.5% and 82.8% as much water as material H. Based on their water holding performance and thinness relative to the other materials, geotextiles H (S1600) and I (IR 26) were judged to be excellent candidates for further study.

Table 2: Water Holding Capacity of Geotextiles Tested Drained and Wrung Dry

	Thickness (m) and volume (m^3) of a 1 m^2 swatch	Manufacturer's Designation	Dry Density	Water Retained Drained	Water Retained Wrung Dry	Relative Water Holding Capacity Drained	Relative Water Holding Capacity Wrung Dry
			g/cm^3	g/cm^3	g/cm^3	% of max	% of max
A	0.0081	20 osy wettable PP	0.120	0.803	0.378	99.3	82.8
B	0.0028	160N	0.104	0.237	0.176	29.3	38.7
C	0.0097	20 osy wettable PP 3 denier	0.079	0.300	0.068	37.1	15.0
D	0.0041	6 osy wettable PP 3 denier	0.052	0.571	0.211	70.7	46.4
E	0.0041	FR 60	0.055	0.456	0.139	56.4	30.5
F	0.0064	160N + FR 60	0.083	0.529	0.203	65.5	44.6
G	0.0127	30 osy PP	0.075	0.522	0.260	64.6	56.9
H	0.0050	S1600	0.144	0.748	0.456	92.5	100.0
I	0.0070	IR 26	0.165	0.808	0.403	100%	88.5

Methane Oxidation Capacity

Of the nine geotextiles, G,H, and I (30 osy PP, S1600 and IR26) supported in excess of 700 mg CH_4 uptake/m^2 d^{-1} (Fig.20), which was significantly higher ($p<0.05$) than the rates of any of the other materials. The uptake rate of S1600, one of the thinner materials tested, was also significantly higher than that of 30 osy PP and IR26. It is important to note that for these

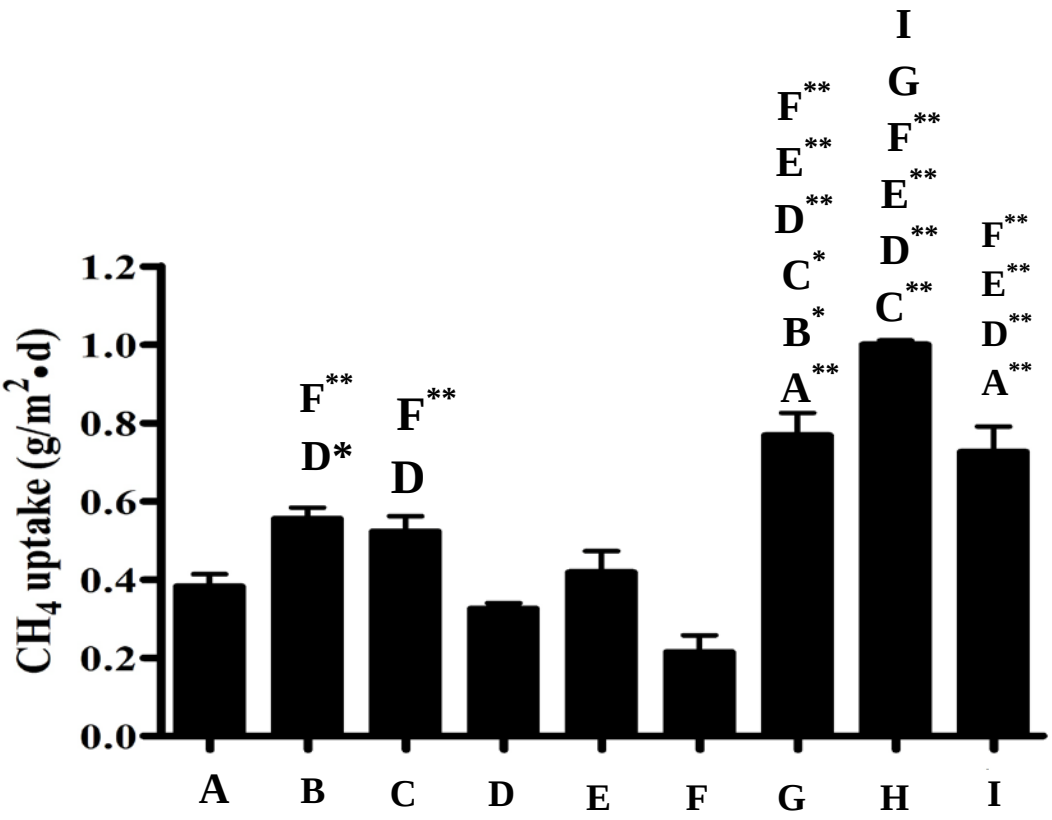

Figure 20. Comparison of the methane uptake by methanotrophic cells immobilized in various geotextiles materials, as described in Table 3. A statistically significant difference (p< 0.05) between two geotextile materials is indicated by the letter designation. * indicates p<0.01, and ** indicates p<0.001. Error bars represent the standard deviation of three replicate samples.

experiments, each material was allowed to adsorb an NMS+cells suspension and then drain. Therefore, the number of cells contributing to the performance shown here varied depending on a material's WHC. If it is assumed that the WHCs in Table 4 are applicable, and the culture contained 10^8 cells/mL, then the cells present in each test swatch can be calculated, and the results can be normalized for the number of cells contributing to the uptake (Table 3). From this

perspective, material B had a rate more than two-fold higher than material H, the next highest performer. The performance of material I was about half that of H.

Table 3: Batch Methane Oxidation Rates for Samples Normalized for the Number of Cells Adsorbed

	Volume/swatch	Manufacturer's Designation	Culture Retained (est.'d)	Methane Consumed in 24 h.
	(cm^3)		mL	mL $CH^4/10^8$ cells inoculated
A	0.0081	20 osy wettable PP	5.69	67.1
B	0.0028	160N	0.73	760
C	0.0097	20 osy wettable PP 3 denier	2.80	186
D	0.0041	6 osy wettable PP 3 denier	1.95	167
E	0.0041	FR 60	1.60	261
F	0.0064	160N + FR 60	2.99	71.6
G	0.0127	30 osy PP	5.77	133
H	0.0050	S1600	3.40	294
I	0.0070	IR 26	5.19	140

Phosphorus Release

Results from tests of the phosphate-impregnated tarps indicated that both types tested released most of the leachable phosphate they contained within five minutes of being placed in excess DI water (Fig 21).The thinner FR60 material yielded a mean diluted rinse water concentration of 3.87mg PO_4-P/L, while the thicker FR120 geotextile rinsing yielded a mean concentration of 20.52 mg PO_4-P/L).There was a very high phosphate release within the first 5 min of contact

with DI water . It was judged that such rapid release could cause osmotic stress for the methanotrophic bacteria, and use of these tarp candidates was discontinued.

Bench Scale Continuous Flow Chambers

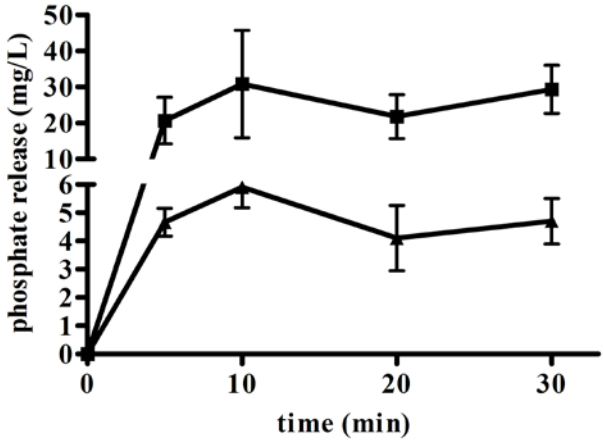

Figure 21. Phosphate release by FR60(▲) and FR120 (■). Error bars represent the SEM of triplicate samples.

A number of pilot trials were conducted in the laboratory chambers before the experiments described here were conducted. The pilot trials showed that a single or even double layer of biotarp tested with fluxes of 22 g m^{-2} d^{-1} had no discernable impact on methane concentrations in the chamber. To test for whether or not the bacteria were not alive and active in the geotextiles, swatches from the control and biotarps were tested in batch after the tarps were removed from the continuous flow chambers. Triplicate swatches from each tarp were incubated in 100ml bottles under 10% headspace methane (10 mL of methane added) and monitored for 3 d. While the control showed negligible methane uptake or carbon dioxide production over the three days, the biotarp swatches consumed almost all of the methane (Fig.22). Also, carbon dioxide production was evident in the biotarp bottles, but not in the controls.

Ultimately four layer biotarps were required to yield good methane uptake activity. It is not clear whether the improved performance was due to the higher number of methanotrophs present in the four-layered biotarps or to the increased retention time the greater thickness offered, though both likely contributed.

Composite Biotarp Trials. The average methane uptake rate of two independent evaluations of a four-layered biotarp was 16%, with a maximum removal of 23% attained during one trial (Table 4, Fig 23(a)). Overall, methane uptake remained constant for the first 4 d, after which it decreased regularly each day until reaching 3% uptake on the ninth day. Condensation was evident on the walls of biotarp chambers, but not on the walls of the controls. This is noteworthy because water is a product and indicator of the methane oxidation reaction. The negative control showed a negligible methane uptake, and carbon dioxide production was only observed in the biotarp chamber, suggesting that microbially mediated methane oxidation took place and the methane was not merely dissolved into the NMS or adsorbed to the geotextile fibers.

Although greater depth improved methane oxidation activity, no thicker prototypes were tested because it was judged that they would be too bulky for storage and handling under field conditions. Therefore, rather than increase the number of geotextile layers, some amendments were investigated that might stimulate more methane consumption

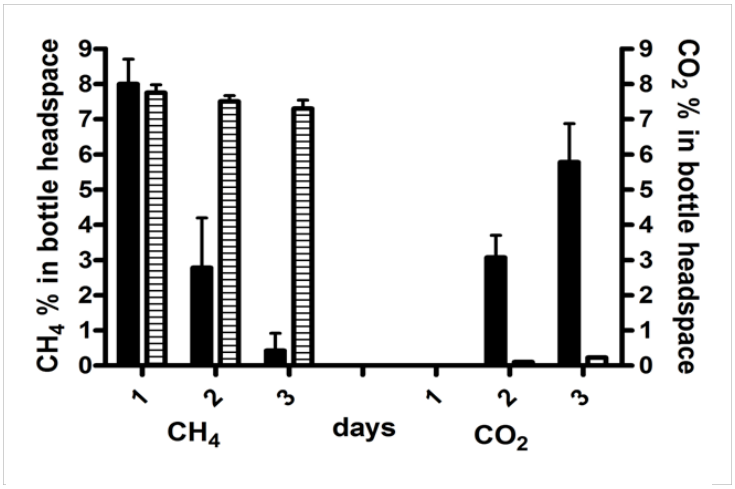

Figure 22. Methane uptake (left axis) and carbon dioxide production (right axis) by biotarp (solid bar) and control (striped bar) swatches of S1600 geotextile pieces after 25 day incubation in continuous flow chambers (n=3, error bars are st. dev.)

Composite Biotarps with Soil Amendment. The addition of landfill soil to the biotarp proved beneficial, increasing the average methane uptake rate of three independent trials to 26% removal (Table 4, Fig 34(b)), a value found to be statistically higher than the four-layered prototype ($p<0.05$). There was also considerable variation between replicates, ranging from 21% to 31%, particularly early in the time course. Unlike the unamended four-layered biotarp, performance was sustained, with little change overall during the nine days of monitoring. As observed in previous experiments, condensation accumulated on the walls of the biotarp chambers, and carbon dioxide production was robust. There was negligible change in methane and carbon dioxide, and no condensation was present in the negative control chamber.

Table 4: Biotarp Prototype Performance in Continuous Flow Chambers

Prototype	**Incubation (days)**	**Methane Uptake Rate (%)**		
		Mean	***Maximum***	***Steady-State***
Composite (S1600 + I26)	9	16	23	None reached
Composite + landfill soil	9	26	31	25
Composite + compost	9	27	31	25
Composite + shale	8	32	50	32

It is well known that soil microbes often require trace micronutrients from the soil or by-products from other microbes to flourish. Since the methanotroph population used here was enriched from landfill soil, the addition of the soil may have provided nutrients or other factors

that enhanced the methane oxidation capacity. The soil itself also contained methanotrophs, and the pre-incubation likely further increased the number of methanotrophs present in the biotarp.

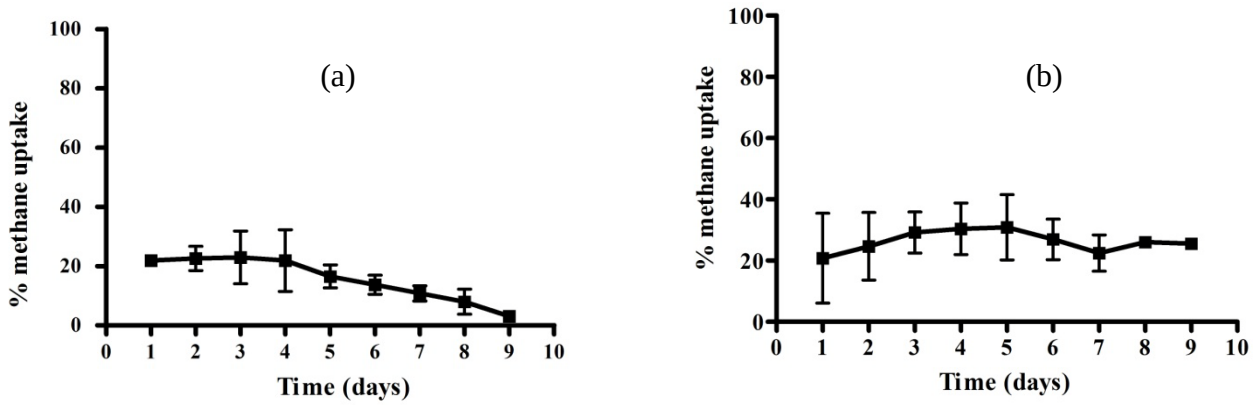

Figure 23. Comparison of four-layer composite tarps tested (a) without and with (b) landfill cover soil amendment. Error bars represent the standard deviation of duplicates.

Composite Biotarps with Compost Amendment. When compost amendment was tested as amid-layer in the four-layer composite biotarp, the average methane uptake rate of two independent compost-amended multilayered biotarps was 27% removal (Table 4), although the variability between replicates was very high, ranging from 20% to 35% removal. This average was statistically higher than the four-layered biotarp ($p<0.01$) and essentially equal to the methane removal rate of the soil additive biotarp In addition to methane consumption, carbon dioxide production and condensation formation were evident. The negative control showed negligible methane uptake, and no carbon dioxide production.

Compost has been shown to be a good host matrix for methanotrophs[140] and has been used in various types of experimental landfill covers to successfully reduce methane emissions[141]. This success is likely due, in part, to its excellent water holding capacity, which is a property previously indicated to be important for biotarp performance. It is, therefore, not surprising that the addition of compost to the biotarp led to increased methane uptake over the unamended multilayered biotarp. Like the intermediate landfill cover soil, methanotrophs were also likely to be present in the compost samples, particularly after enrichment.

Composite Biotarps with Shale Amendment. Shale is a very light, small rock used to lighten concrete. It is extremely porous, and it is akin to the expanded clay particles, which have been used as effective methanotroph supports in methane biofilters[142]. The addition of shale to the multilayer biotarp produced an overall average of 32% methane removal for three independent evaluations, and was found to be statistically higher than the four-layered ($p<0.001$), soil amended ($p<0.001$), and compost amended ($p<0.01$) prototypes (Table 4). Although methane removal began at 50%, it was observed to decline to 28% by day eight. As observed in other

prototype evaluations, there was large variability between the biotarp replicates, and values ranged from 59% to 21%. Both carbon dioxide production and condensation formation were present in biotarp chambers but absent in the negative controls. A comparison of all of the composites tested showed that the biotarp amended with shale outperformed all other treatments in the laboratory simulation experiments (Fig 24).

Methanotroph Architecture in the Biotarp

To detect methanotrophs in the biotarp two techniques were combined to show both the cells and any exopolymeric substances (EPS) produced. To establish that the method would work, a biotarp was incubated in batch and then removed for application of the fluorescent probes. One probe was attached to Concanavalin A to detect EPS, and another probe was attached to an oligonucleotide chain that binds with methanotrophs so that the cells could be identified.

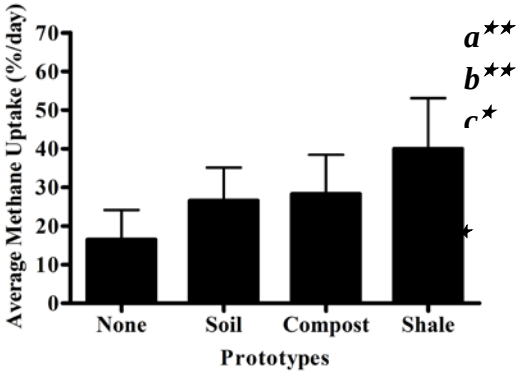

Figure 24. Average methane uptake by a four-layered biotarp prototype with various additives. *a* indicates a statistically significant difference from prototypes with no additive. *b* indicates a statistically significant difference from prototypes with a soil additive. *c* indicates a statistically significant difference from prototypes with a compost additive. p<0.05, unless indicated by ★ (p<0.01) or ★★ (p<0.001). Error bars represent the standard deviation of replicate numbers previously stated.

EPS Detection Controls from Batch Incubations. To confirm that the visualization technique for EPS would work, some positive controls were prepared from biotarps incubated in jars with methane headspace. The controls stained positive for EPS when both fluorochromes were used (Concanavalin A-Alexa Fluor 488 fluoresced red and Concanavalin A-Alexa Fluor 594 fluoresced green) (Fig 25).

The fiber structure of the geotextile could clearly be distinguished from the background, indicating that EPS coated the fibers and resulted in either green or red fluorescence. Since the culture was almost exclusively methanotrophs, it is presumed that the EPS is of methanotroph origin, although no further work was done to confirm this. Negative control geotextiles that were not inoculated with cells showed virtually no fluorescence. Together, these images confirm that the stain was binding selectively and did not bind to the geotextile or embedding material.

Individual geotextile fibers could be distinguished in both methanotroph incubated samples, suggesting the bacterial cells are associated with the fiber surface. Furthermore, the presence of EPS around the fibers in Fig. 25 suggests that it is mediating cell attachment, as would be expected.

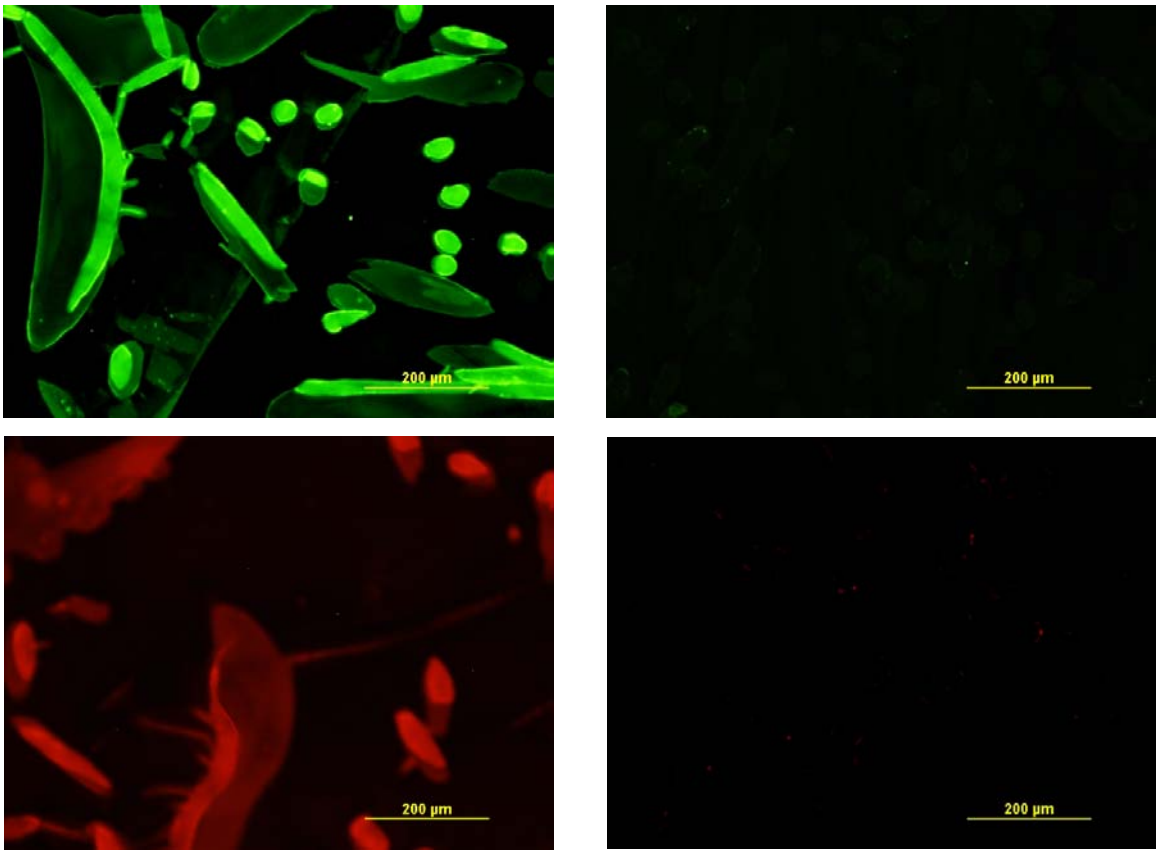

Figure 25. Concanavalin A staining for methanotroph EPS. A) **Geotextile sample incubated for one week with methanotrophs and stained with Concanavalin A-Alexa Fluor 488.** B) **Negative control geotextile (no cells) stained with Concanavalin A-Alexa Fluor 488.** C) **Geotextile sample incubated for one week with methanotrophs and stained with Concanavalin A-Alexa Fluor 594.** D) **Negative control geotextile (no cells) stained with Concanavalin A-Alexa Fluor 594. All sections were viewed a 100X magnification.**

Methanotroph Detection Controls from Batch Incubations. To confirm that the fish probes were able to properly detect their targets, pure cultures of Type I (LW13) and Type II (Methylocystis parvus OBBP) methanotrophs were inoculated on geotextile swatches and incubated in batch under methane headspace. When the biotarp samples were subjected to FISH using probes specific for Type I (red fluorescence) and II (green fluorescence) methanotrophs, the probes

fluoresced appropriately (Fig 26). There was no fluorescence from the negative control, which was a swatch of geotextile incubated without cells.

The microscopy also indicates that attachment was higher on *M.* parvus OBBP geotextile sections, as almost all cells appeared to be associated with the geotextile fibers. On the other hand, there was significant amount of Type I probe hybridization independent of the

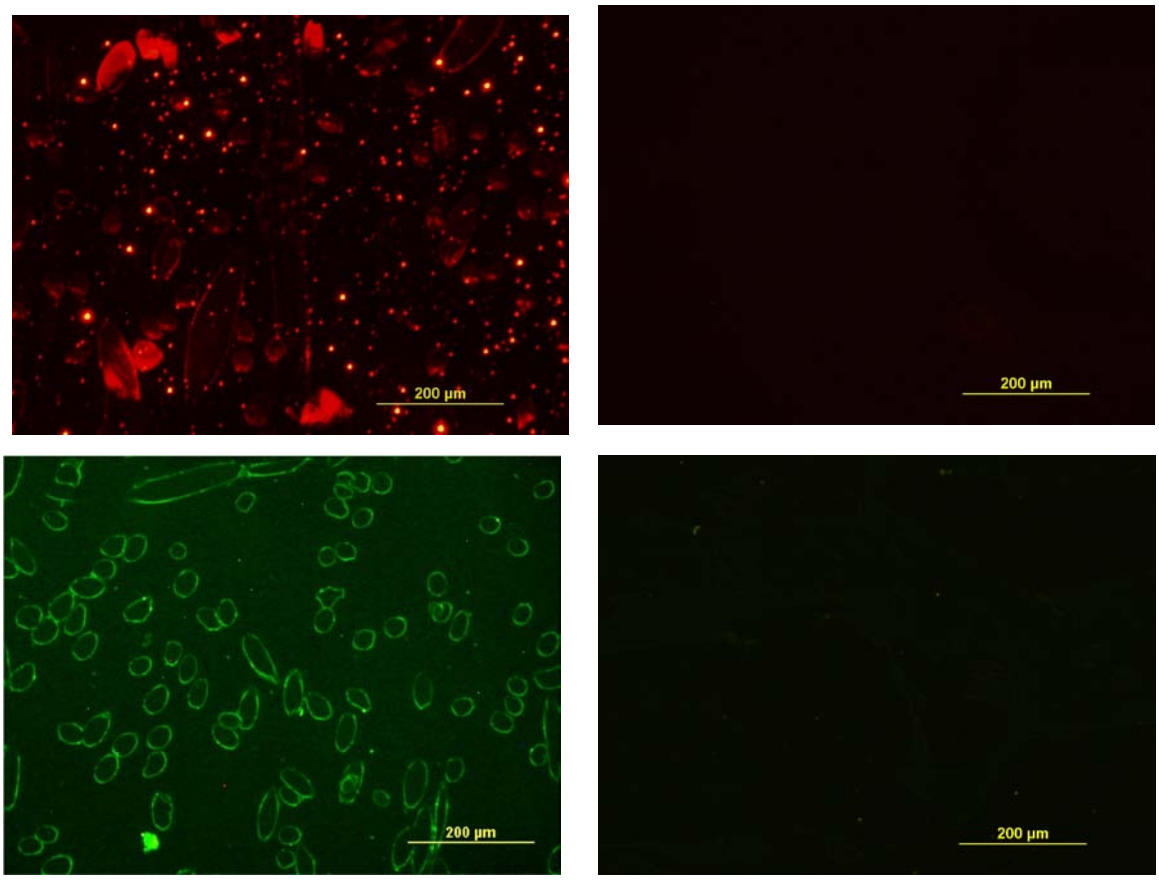

Figure 26. Fluorescent *In Situ* Hybridization controls on synthetic geotextile sections. A) **Type I positive control methanotroph LW13 hybridized with CY-3 (red) tagged RNA probes.** B) **Type I negative control (no cells) hybridized with CY-3(red) tagged RNA probes.** C) **Type II positive control methanotroph *Methylocystis parvus* OBBP hybridized with FLUOR (green) tagged RNA probes.** D) **Type II negative control (no cells) hybridized with FLUOR (green) tagged RNA**

geotextile fibers. Such difference may be the result of differences in the propensity of attachment or EPS production between the two strains. As sections were viewed at 100X magnification, the fluorescent points are not single cells, but rather cell aggregates. It is not certain if the unattached cells were an artifact of the embedding and slicing, or were never attached to the fibers at all. It is possible that not all cells became associated with the geotextile fibers, but some remained suspended in the NMS liquid trapped between fibers.

Biotarp Incubations in Continuous Flow Chambers. The combined EPS and cell visualization techniques were applied to subsamples of shale amended tarps that either received no incubation; that were incubated without methanotrophs; or that were active biotarps treated with the methanotroph population. Negative control biotarp sections, which were incubated in the absence of cells, showed negligible fluorescence from hybridized Type I or II methanotroph RNA probes or from the Concanavalin A probe for EPS (Figs. 27 and 28). This confirmed that in the absence of cells and EPS, there was no nonspecific binding of these molecules in active biotarp samples. When the biotarp prototype inoculated but not incubated with the mixed methanotroph population was probed, there was little EPS and few cells (Figs. 27 and 28). The EPS detected in these sections was likely carried over from culture growth. When multiple fields were examined, cell aggregates appeared to be evenly distributed through the sections. The fiber definition seen in positive controls coated with EPS or methanotroph cells was not evident, indicating that there was no attachment and colonization of the geotextile immediately upon exposure to cells in NMS.

When a sample from an active biotarp was examined after its incubation in a continuous flow chamber, there was significant EPS accumulation in each layer of the prototype (Figs 29and 30). Likewise, methanotrophic cells were present in all layers and at much higher numbers than were observed in the biotarp prototype tested before chamber incubation. Growth was not confluent throughout a section, but the majority of the areas stained positive for methanotrophs co-localized with areas positive for EPS, suggesting that the polymer matrix was generated by associated cells. Furthermore, the shapes of the co-stained areas are consistent with the size and shape of fibers expected in the geotextile. Although most methanotrophs appeared to be attached and surrounded by EPS, both unattached cell aggregates and unpopulated EPS were observed.

There appeared to be more Type I methanotrophs in the middle two layers than in the outer layers of the four layered biotarp, but it was clear that all layers were colonized. This phenomenon was not noticeable in the distribution of Type II methanotrophs. It is possible that the shale placed between the two middle layers of the biotarp added Type I methanotrophs, such that the layers adjacent to the shale were more highly populated. Since continuous flow chambers are not a sterile environment, some of the apparently cell-free EPS may have been due to the presence of other organisms. Similarly, the free cells may have been an artifact of the section preparation or a true phenomenon reflecting that not all methanotrophs were present as attached cells.

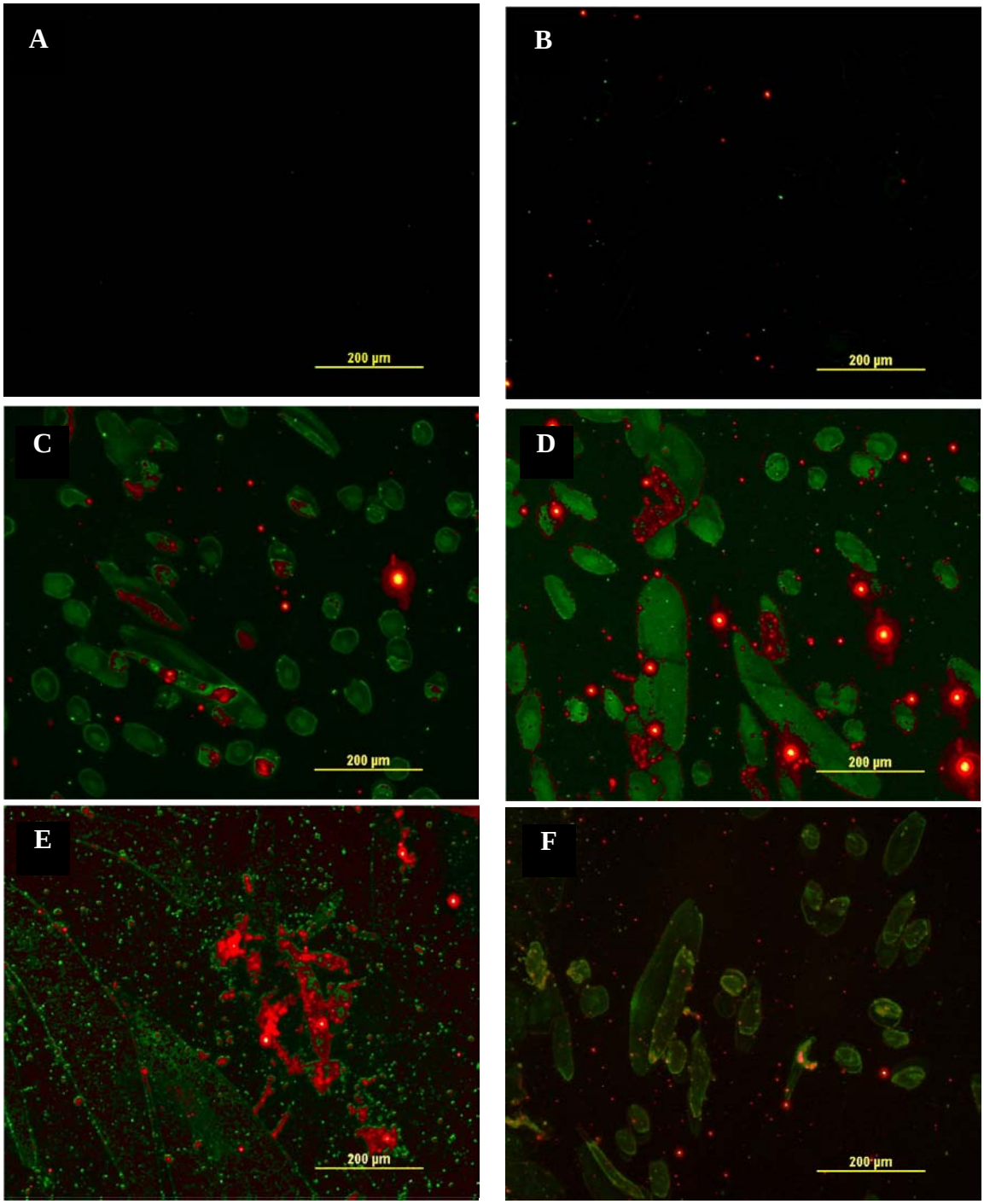

Figure 27. Shale amended biotarp prototype sections stained for Type I methanotrophs (red) using FISH and EPS (green) using Concanavalin A. A) **Negative control biotarp section (no cells).** B) **Initial biotarp sample (fixed immediately after cell application).** C-F) **Biotarp layers from bottom to top, after 9 days incubation in a laboratory continuous flow chamber. All sections viewed at 100X magnification.**

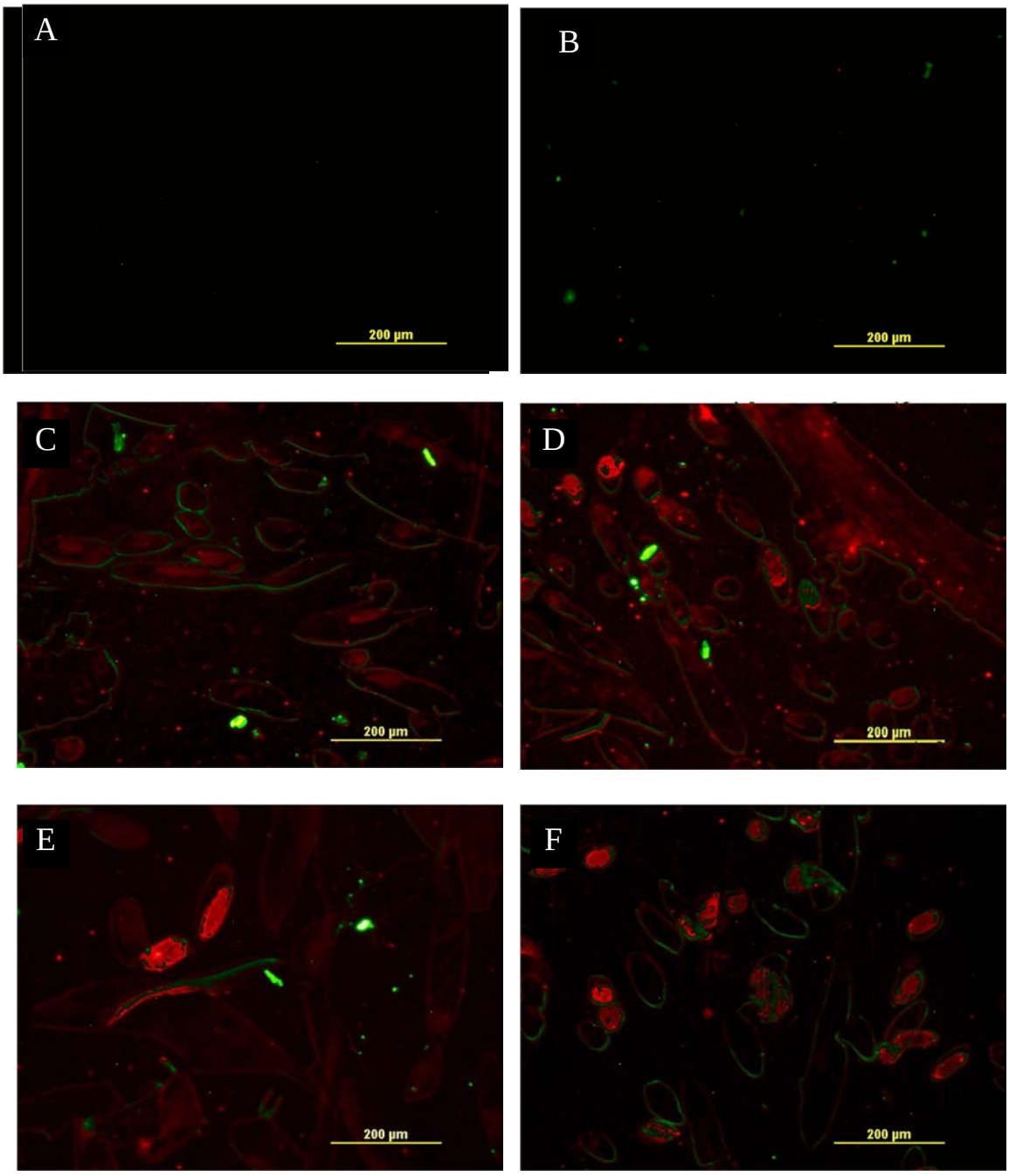

Figure 28. Shale amended biotarp prototype sections stained for Type II methanotrophs (green) using FISH and EPS (red) using Concanavalin A. A) **Negative control biotarp section (no cells).** B) **Initial biotarp sample (fixed immediately after cell application).** C-F) **Biotarp layers from bottom to top, after 9 days incubation in a laboratory continuous flow chamber. All sections viewed at 100X magnification.**

FIELD EVALUATION OF BIOTARP PROTOTYPES

Although the standard protocol for collecting flux data remained unchanged over the course of the field trials, many changes were made in how the biotarps and controls were prepared for testing and in how long they remained in the field before and after flux measurements. This was due, in part, to the fact that field trials began while laboratory simulation experiments were still on-going. The results are reported here as individual experiments to show the evolution of experimental manipulations and differentiate among them. As noted previously, these trials were not conducted atop freshly placed waste. They were conducted on a site that had been topped with 0.3-0.92 m (1-3 ft) of intermediate soil cover about one year before the experiments began. This was done to ensure the safety of students collecting flux measurements and to avoid inconveniencing the haulers and landfill operators working at the open cell.

Experiment 1: Baseline Flux Conditions (11/9-12/07/07)

The aim of the first field experiments was to collect baseline flux measurements from the waste buried below the intermediate cover. Six holes were dug through the soil down to the waste layer, and the flux chamber bases were installed. Flux measurements were collected at each of the six chambers over a one-month period in winter 2007. The fluxes varied widely among the six chambers although they were all within a 20 m x 20 m 65 ft x 65 ft) area (Table 5). Mean fluxes ranged from 422.5 to 5398 g m^{-2} d^{-1}. As expected, there was also day to day variation for a given site, with standard deviations generally about 10% of the mean. Overall, it was clear that methane emissions were occurring and could be used to assess biotarp performance.

Table 5: Methane flux measurements over one year old buried waste

	Day 1	Day 2	Day 3	Day 4	Day 5		
	11/9/2007	11/14/2007	11/16/2007	11/30/2007	12/7/2007		
Chamber	Flux ($g\ m^{-2}\ d^{-1}$)	Flux ($g\ m^{-2}\ d^{-1}$)	Flux ($g\ m^{-2}\ d^{-1}$)	Flux ($g\ m^{-2}\ d^{-1}$)	Flux ($g\ m^{-2}\ d^{-1}$)	Average	Stan Dev
1	1,056	1,175	1,385	998.7	1,041	**1,131**	156.3
2	2,575	2,610	2,569	2,631	3,102	**2,697**	227.5
3	6,522	4,601	5,664	5,188	5,015	**5,398**	734.9
4	2,611	1,899	4,364	1,829	2,338	**2,608**	1,033
5	4,672	3,796	4,311	4,102	4,819	**4,340**	416.2
6	596.9	348.8	325.9	418.4		**422.5**	122.8

Experiment 2: Biotarps tested over buried waste (12/13-12/20/2007)

- Biotarps were dual layers of TenCate^{tm} #6 osy geotextile
- Controls: DI water only

The 6osy material was tested because it proved to successful support biotic methane oxidation in the early material comparison trials. It is a 1.2 cm (0.46 in) thick nonwoven geotextile composed of polypropylene fibers, and it was tested here at double thickness. In three chambers, the methane flux through biotarps impregnated with methanotrophs in nutrient broth was measured, and in three chambers the flux through DI wetted geotextile (controls) was measured. The tarps were put in place in the flux chamber base early on Day 1 and allowed to remain (uncovered) overnight to simulate the real process of placing the tarp on the trash at the end of the work day (about 5 pm). Flux measurements were made at the end of Day 2, and the tarps were collected for return to the laboratory. Baseline fluxes with no tarp in place were also measured on Day 2.

Since the methane fluxes from chamber to chamber varied, the percent change in methane flux was calculated to better compare the treatments (Table 6). The control tarps appeared to outperform the biotarps, although the differences were not significant at $p<0.10$. (Although statistical significance is typically assessed at a probability level of $p<0.05$, the number of replicates and the variability between them here warranted the use of a larger p value in order to have more statistical power.)

Table 6: CH_4 flux reductions through a dual layer 6 osy geotextile biotarp over buried waste

Treatment	Chambers	Baseline	Geotextile	% decrease	Mean % Decrease	Stan Dev
2 layer 6osy w/ DI water	1	940	317	**66.3**		
2 layer 6osy w/ DI water	2	2276	637	**72.0**		
2 layer 6osy w/ DI water	3	4368	1363	**68.8**	**69.0**	**2.9**
2 layer 6osy w/ MT	4	2502	1387	**44.6**		
2 layer 6osy w/ MT	5	3173	1076	**66.1**		
2 layer 6osy w/ MT	6	402	153	**61.9**	**57.5**	**11.4**
		Flux ($g\ m^{-2}\ d^{-1}$)				

Experiment 3: Biotarps tested over intermediate cover (1/15-1/16/08)

- Biotarps were dual layers of TenCate^{tm} #6 osy geotextile
- Controls: DI water only

Experiment 3 followed the same protocol as Experiment 2, except that the chambers were installed on top of the intermediate cover instead of on top of the waste. Dr. Jean Bogner, President of Landfills+, Inc. has reported that she measured open cell fluxes that ranged from 100-200 g m^{-2} d^{-1}. It was reasoned that any uptake by the biotarps may have been too small to be detected with such large fluxes occurring, and with lower, more representative baseline fluxes, biotarp activity might be detected. Again, tarps were left in the field overnight and collected after the second day. The baseline readings were measured on the same day as the tarp readings; immediately after removing a tarp, a second measurement is taken over bare soil.

The measured fluxes ranged from 3.07-49.83 g m^{-2} d^{-1}, which was lower than the targeted values. Also, the percent removal rates varied widely among chambers in the same treatment, and in almost all cases, methane fluxes were higher with the geotextile (biotarp or control) in place than through bare soil (Table 7). Two of the biotarps showed some trend to methane uptake, but the wide variability among replicates rendered the differences statistically insignificant ($p<0.10$). It is difficult to explain how the presence of a tarp could contribute to higher flux readings than would occur over bare soil, and it was presumed that the low baseline flux levels led to distortion effects when small differences were measured.

Table 7: CH_4 flux reductions through a dual layer 6 osy geotextile biotarp over intermediate cover

Treatment	Chambers	Baseline	Geotextile	% decrease	Mean % Decrease	Stan Dev
2 layer 6osy w/ DI water	1	14.11	16.85	**-19.4**		
2 layer 6osy w/ DI water	2	49.83	53.08	**-6.5**		
2 layer 6osy w/ DI water	3	4.96	7.29	**-46.9**	**-24.3**	**20.6**
2 layer 6osy w/ MT	4	23.98	23.08	**3.8**		
2 layer 6osy w/ MT	5	3.07	4.77	**-55.2**		
2 layer 6osy w/ MT	6	26.56	21.03	**20.8**	**-10.2**	**39.9**
		Flux ($g\ m^{-2}\ d^{-1}$)				

Experiment 4: Biotarps tested over intermediate cover (2/7-2/15/08)

- Tarps were a single layer of TenCate^{tm} #IR26 osy geotextile
- No biotarps; treatments were DI wetted tarp and dry tarp

Experiment 4 was conducted to obtain some baseline readings on a different tarp material, IR26, which is thicker (1.78 cm; 0.7 in) and has a high water holding capacity (Table 2). One side of the tarp is fused during production, creating a thick "skin-like" surface on the top to slow down the permeation of gas and increase retention time, allowing bacteria to have more time to oxidize methane. The tarp was tested dry and wetted to see how much physical resistance it offered before adding any biological effect from the presence of methanotrophs. Placement was again on top of the intermediate cover. Tarps were left in the field overnight and collected after the second day of testing.

Again the baseline fluxes were very low (Table 8), but there was a significant difference ($p<0.10$) between the mean changes due to wet tarps and dry tarps. This suggests that even a wetted tarp with a fused surface could reduce the rate at which methane entered the atmosphere. The experiment also confirmed that there was no effect of dry tarps on methane emissions.

Table 8: CH_4 flux reductions through TenCate[tm] #IR26 dry or DI wetted on intermediate cover

Treatment	Chambers	Baseline	Geotextile	% decrease	Mean % Decrease	Stan Dev
Single layer IR26 w/ DI water	1	6.40	4.35	32.0		
Single layer IR26 w/ DI water	2	24.48	13.88	43.32		
Single layer IR26 w/ DI water	3	7.10	2.26	68.25	47.8	18.6
Single layer IR26 Dry	4	39.40	45.16	-14.61		
Single layer IR26 Dry	5	19.57	17.56	10.3		
Single layer IR26 Dry	6	0.86	0.87	-1.45	-1.92	12.5
		Flux ($g\ m^{-2}\ d^{-1}$)				

Experiment 5: Biotarps tested recessed in intermediate cover (2/20-2/21/08)

- Tarps were a single layer of TenCate[tm] #IR26 OR #S1600 geotextiles
- No biotarps; treatments were DI wetted #IR26 OR DI wetted #S1600

Experiment 5 was conducted to repeat Experiment 4 with two changes. One change was to move the flux chambers again to try to get in a more representative flux range (100-200 g m^{-2} d^{-1}). The flux chambers were recessed about 20 cm (8 in) below the intermediate cover, which put them about 46 cm (18 in) above the buried waste. Second, an additional tarp material was tested in parallel to IR26. TenCate[tm] material S1600 had high water holding capacity and good methane oxidation performance (Tables 2 and 3) in batch tests, and it is made from a needle-punched nonwoven material composed of polypropylene fibers. It did not have a fused surface. Tarps were incubated in the field overnight, and samples for flux measurement were collected on the following day.

The fluxes measured in the six chambers ranged from 1.25-897.7 g m^{-2} d^{-1} (Table 9), moving some of the chambers (but not all) into a higher baseline flux range. Again the IR26 performed well, reducing emissions 77.5% here (compared to 47.8% in Experiment 4). The S1600 geotextile decreased methane emissions an average of 54%, and the performance difference between the materials was not statistically significant ($p<0.1$).

Table 9: CH_4 flux reductions through TenCate[tm] wetted #IR26 and wetted S1600 (recessed chambers)

Treatment	Chambers	Baseline	Geotextile	% decrease	Mean % Decrease	Stan Dev
IR26 w/ DI	1	897.7	238.3	73.5		
IR26 w/ DI	2	200.6	28.64	85.7		
IR26 w/ DI	3	12.03	3.22	73.2	77.5	7.1
S1600 w/ DI	4	1.25	0.37	70.7		
S1600 w/ DI	5	2.65	1.20	54.8		
S1600 w/ DI	6	57.93	36.84	36.4	54.0	17.2
		Flux ($g\ m^{-2}\ d^{-1}$)				

Experiment 6: Biotarps tested recessed over intermediate cover (2/28-2/29/08)

- Tarps were a dual layer composite of TenCate^{tm} IR26 and S1600
- No biotarps; treatments were tested in duplicate: dry tarps and DI wetted tarps

Experiment 6 was conducted to obtain some baseline readings on composite tarp prototypes that combined IR 26, a fused tarp, with S1600, a high water holding capacity tarp. Laboratory testing showed that one layer did not provide sufficient retention time to allow treatment, and this was confirmed in the early field experiments. Duplicate wetted composite tarps were tested against duplicate dry composite tarps. Tarps were tested with the chambers recessed 8 in below the intermediate cover surface. They were allowed to remain in the open chamber bases overnight, and samples were collected the following day.

The baseline flux readings were very low, despite the fact that the chambers were now recessed. Three of the four readings were below 10 g m^{-2} d^{-1}, and the highest reading was 34.89 (Table 10). There was no statistical significance ($p<.010$) between the treatments, and the performance of the wetted tarps was much lower than in previous experiments. The low flux readings were probably related to a recent rain, which liked clogged the soil pores and prevented methane migration. This, combined with the same sample size resulted in little information being gleaned from this experiment.

Table 10: CH_4 flux reductions through wetted and dry composite tarps (recessed chambers)

Treatment	Chambers	Baseline	Geotextile	% decrease	Mean % Decrease	Stan Dev
IR26+S1600 w/ DI	3	6.16	3.82	38.0		
IR26+S1600 w/ DI	4	5.60	4.47	20.2	29.1	12.6
IR26+S1600 Dry	5	1.40	0.91	35.1		
IR26+S1600 Dry	6	34.89	39.00	-11.8	11.7	33.1
		Flux ($g\ m^{-2}\ d^{-1}$)				

Experiment 7: Composite biotarps with soil tested recessed over intermediate cover (3/13-4/17/08)

- Tarps were a four-layer composite of two layers of IR26 and two layers of S1600
- Two biotarps, two biotarps with a layer of landfill cover soil, and two wetted controls

Experiment 7 introduced testing of four layer tarps, because on-going laboratory experiments suggested the retention time offered by thicker tarps was needed to obtain 25-40% methane uptake rates. Since the laboratory tests were showing that a layer of landfill cover soil in the tarp stimulated methane uptake, such a layer was tested here, too. The purpose of the soil layer was to

add nutrients for the bacteria; additional moisture; and perhaps some additional methanotrophs. Since the methanotroph slurry used to inoculate the tarps was already a dense mix of methanotrophs, the methanotroph contribution from the soil was likely negligible. The four layers forming the composite prototype consisted of two layers of IR26 alternating with two layers of S1600. The treatments that were compared were: two four-layer composite biotarps and two four-layer composite biotarps with a layer of soil in the middle of the four layers. Additionally, two four-layer composites with DI water only were tested as controls. Tarps were left in the field overnight and collected two days later.

The flux from all of the chambers was more robust than in Experiment 6, ranging from 9.1 to 1189 g/day/m^2 (Table 11). There were no significant differences ($p<0.10$) between the treatments, which is not surprising considering the low number of samples compared. The control replicates yielded the highest mean methane removal rate, but it was in this treatment that the very low baseline flux occurred, which may have skewed the results.

Table 11:CH4 flux reductions through four-layer biotarps with and without soil (recessed chambers)

Treatment	Chambers	Baseline	Geotextile	% decrease	Mean % Decrease	Stan Dev
4 layers (IR26+S1600) w/ MT and soil	1	1185	178.2	**85.0**		
4 layers (IR26+S1600) w/ MT and soil	2	181.3	73.75	**59.3**	**72.1**	**18.1**
4 layers (IR26+S1600) w/ MT	3	208.1	123.3	**40.8**		
4 layers (IR26+S1600) w/ MT	4	1609	540.1	**66.4**	**53.6**	**18.2**
4 layers (IR26+S1600) w/ DI water	5	9.10	2.51	**72.4**		
4 layers (IR26+S1600) w/ DI water	6	169.6	30.28	**82.1**	**77.3**	**6.9**
		Flux ($g\ m^{-2}\ d^{-1}$)				

Experiment 8: Composite biotarps with compost tested recessed over intermediate cover (4/25-4/28/08)

- Tarps were a four-layer composite of two layers of IR26 and two layers of S1600
- Two biotarps, two biotarps with a layer of compost, and two wetted controls

Experiment 8 repeated the manipulations in Experiment 7 except that two of the biotarps had an additional layer of compost rather than soil in the middle of the four geotextile layers. The treatments were: two four-layer composite biotarps and two four-layer composite biotarps with a mid-layer of finished compost. Two four-layer composites with DI water only were tested as controls. Tarps were incubated overnight and tested the following day.

The baseline fluxes were again robust in the treatment chambers, ranging from 212.3-2902 g/day/m^2 (Table 12). The baseline fluxes in the chambers used to test the controls were an order of magnitude lower, at 21.92 and 86.74 g/day/m^2. It is unclear whether or not this was a confounding variable. There was no significant difference between the biotarps with and without

compost added. The control tarps showed higher methane mitigation than either of the bioactive treatments, but the differences were not statistically significant ($p<0.10$).

Table 12: CH_4 flux reductions by four-layer biotarps with and without compost

Treatment	Chambers	Baseline	Geotextile	% decrease	Mean % Decrease	Stan Dev
4 layers (IR26+S1600) w/ MT and Compost	1	2902	1264	**56.5**		
4 layers (IR26+S1600) w/ MT and Compost	2	212.3	109.0	**48.6**	**52.6**	**5.5**
4 layers (IR26+S1600) w/ MT	3	631.1	92.87	**85.3**		
4 layers (IR26+S1600) w/ MT	4	2819	1440	**48.9**	**67.1**	**25.7**
4 layers (IR26+S1600) w/ DI water	5	21.92	4.87	**77.8**		
4 layers (IR26+S1600) w/ DI water	6	86.74	13.65	**84.3**	**81.0**	**4.6**
		Flux ($g\ m^{-2}\ d^{-1}$)				

Experiment 9: Composite biotarps and two types of controls tested recessed over intermediate cover (5/22-6/6/08)

- Tarps were a four-layer composite of two layers of IR26 and two layers of S1600
- Six biotarps, six controls wetted with DI, and six controls wetted with NMS biotarps with a layer of landfill cover soil, and two wetted controls

Experiment 9 was a troubleshooting exercise to investigate the hypothesis that the trend for control tarps with DI water to perform as well or better than active biotarps might be related to the DI water used for controls. It was reasoned that the DI water was able to dissolve and absorb more methane than the liquid salts medium in which the methanotrophs were applied to the tarp. The medium used to support methanotroph growth was Whittenbury's Nitrate Mineral Salts (NMS). Therefore, control tarps with DI water and also with NMS were compared to active biotarps. All tarps were composite four-layer tarps of IR 26 and S1600. The testing occurred over three separate days of trials so that six replicates could be tested in each condition. Tarps were placed in the field during the day, left overnight night, and then gas samples were collected the following day.

Over the three dates of testing, the baseline fluxes for a given chamber ranged widely (Table 13). For example, while Chamber 1 baseline fluxes varied from 214 to 1537 to 848 g/day/m^2 on the three test dates, Chamber 6 remained quite steady at 81, 77, and 66 g/day/m^2 over the same three days. Chamber 5 fluxes remained below 10 g m^{-2} d^{-1} throughout the trials. One data point in each set was discarded as an outlier (Chamber 2 in the DI controls, and Chamber 5 in the NMS and biotarp tests), and paired t-tests were used to compare the treatments. The results disproved the hypothesis, showing that there was no statistically significant difference between using DI water or NMS for control tarps ($p<0.10$), but that the methane emission reductions achieved with the controls (81%) were significantly higher than those achieved with the biotarps (60%). On Chamber 6, where the day-to-day baseline fluxes were

most similar, the reductions were 90%, 84%, and 63% for the DI water, NMS, and active biotarps respectively.

These results led to further consideration of the factors that could be leading to the poor performance of the biotarps relative to the controls. One of the factors noted included short-circuiting of gases because the tarps were so thick. Gas may have been passing through only one or two layers of the biotarp and then up the edges of the chamber base. Another factor was the rate of growth of the methanotrophs. It may be that their exposure to the methane flux was not long enough for them to move from a lag phase to a high growth phase. A third possibility was that ammonia gas in the emissions was toxic to the methanotrophs, so that their oxidation activity was inhibited. Some of these factors were investigated in subsequent experiments.

Table 13: CH_4 emissions reductions by composite biotarps, DI controls, and NMS controls

_Treatment	Chambers	Baseline	Geotextile	% decrease	Mean % Decrease	Stan Dev
4 layers (IR26+S1600) w/ DI water	1	214.3	24.41	**88.6**		
4 layers (IR26+S1600) w/ DI water	2	4.98	4.91	**1.5**		
4 layers (IR26+S1600) w/ DI water	3	57.62	21.44	**62.8**		
4 layers (IR26+S1600) w/ DI water	4	1363	361.8	**73.5**		
4 layers (IR26+S1600) w/ DI water	5	9.40	0.66	**93.0**		
4 layers (IR26+S1600) w/ DI water	6	81.02	8.96	**88.9**	**68.0**	**34.6**
4 layers (IR26+S1600) w/ NMS	1	1537	176.1	**88.5**		
4 layers (IR26+S1600) w/ NMS	2	601.1	130.7	**78.3**		
4 layers (IR26+S1600) w/ NMS	3	684.8	171.8	**74.9**		
4 layers (IR26+S1600) w/ NMS	4	2208	443.0	**79.9**		
4 layers (IR26+S1600) w/ NMS	5	8.76	20.82	**-137.8**		
4 layers (IR26+S1600) w/ NMS	6	76.95	12.60	**83.6**	**44.6**	**89.5**
4 Layers (IR26+S1600) w/ MT	1	847.9	539.7	**36.4**		
4 Layers (IR26+S1600) w/ MT	2	398.1	143.1	**64.0**		
4 Layers (IR26+S1600) w/ MT	3	447.2	190.1	**57.5**		
4 Layers (IR26+S1600) w/ MT	4	3483	749.0	**78.5**		
4 Layers (IR26+S1600) w/ MT	5	2.43	6.81	**-180.2**		
4 Layers (IR26+S1600) w/ MT	6	66.32	24.57	**62.9**	**19.8**	**99.0**
		Flux ($g\ m^{-2}\ d^{-1}$)				

Experiment 10: Effect of longer acclimation time on biotarp performance (tested recessed over intermediate cover) (6/27-7/22/08)

- Tarps were a four-layer composite of two layers of IR26 and two layers of S1600
- Three biotarps and three NMS controls, with all tarps left in place for seven days

Experiment 10 was a troubleshooting experiment to assess whether or not methanotroph acclimation to field conditions might be a factor in the poor biotarp performance observed. Tarps were left on the field for one week before sample collection to optimize microbial

acclimatization to the field conditions. All of the baseline fluxes were within a fairly narrow range (92-216 g m^{-2} d^{-1}) except for Chamber 5, which remained below 10 g m^{-2} d^{-1} (Table 14). However, there was high variability among replicates within each treatment, and neither showed emission reduction rates as high as those seen in Experiment 10. This was likely due to the fact that some of the moisture evaporated from the tarps, so that water blockage or absorption of gas was reduced and microbial activity was reduced in the biotarps. Nevertheless, the trend of poor performance by the biotarps relative to the controls persisted, although the differences between any of the treatments were not statistically significant ($p<0.10$).

Table 14: CH4 flux reductions by four-layer biotarps and NMS controls

Treatment	Chambers	Baseline	Geotextile	% decrease	Mean % Decrease	Stan Dev
4 layers (IR26+S1600) w/ NMS	1	92.38	18.65	**79.8**		
4 layers (IR26+S1600) w/ NMS	2	93.87	61.36	**34.6**		
4 layers (IR26+S1600) w/ NMS	4	108.4	53.2	**50.9**	**55.1**	**22.9**
4 layers (IR26+S1600) w/ MT	3	105.7	72.71	**31.2**		
4 layers (IR26+S1600) w/ MT	5	4.33	1.50	**65.3**		
4 layers (IR26+S1600) w/ MT	6	215.7	179.0	**17.0**	**37.8**	**24.8**
		Flux ($g\ m^{-2}\ d^{-1}$)				

Experiment 11: Composite biotarps with shale tested recessed over intermediate cover (7/28-7/31/08)

- Tarps were a four-layer composite of two layers of IR26 and two layers of S1600 with a layer of shale in the middle
- Three biotarps+shale and three NMS controls+shale

In laboratory testing, the inclusion of a layer of shale in the middle of the biotarp showed good methane uptake that was superior to that of soil or compost amendment. Shale is a lightweight, highly porous aggregate commonly used for making of concrete. Experiment 11 was conducted to assess the effect of adding a layer of shale to the tarps during field testing. The hypothesis for this step was that the shale could provide increased surface area and greater moisture holding capacity than was present in an unamended biotarp. Tarps were placed and incubated for one week before fluxes were measured.

The baseline fluxes covered a relatively narrow range (48-138 g m^{-2} d^{-1}) except for Chamber 5, which was characteristically below 10 g m^{-2} d^{-1} (Table 15). There was no significant difference ($p<0.10$) between the biotarps with shale and the controls with shale, indicating that any effects observed were likely due to solubility and absorption or the physical barrier presented by the geotextiles. The lower percentage decreases in methane emissions in all cases was likely due to the drying of the tarps.

Table 15: CH_4 methane emissions reduction by four-layer biotarps and controls with shale

Treatment	Chambers	Baseline	Geotextile	% decrease	Mean % Decrease	Stan Dev
4 layers (IR26+S1600) w/ NMS+Shale	1	47.65	21.03	**55.9**		
4 layers (IR26+S1600) w/ NMS+Shale	2	138.3	98.24	**29.0**		
4 layers (IR26+S1600) w/ NMS+Shale	4	48.13	25.93	**46.1**	**43.7**	**13.6**
4 layers (IR26+S1600) w/ MT+Shale	3	136.1	80.41	**40.9**		
4 layers (IR26+S1600) w/ MT+Shale	5	4.42	1.80	**59.3**		
4 layers (IR26+S1600) w/ MT+Shale	6	109.4	86.06	**21.3**	**40.5**	**19.0**
		Flux ($g\ m^{-2}\ d^{-1}$)				

Experiment 12: Repeat test of shale amendment and test of in-situ methanotroph tarp tested recessed over intermediate cover (8/7-8/25/08)

- Four tarps were four-layer composites of two layers of IR26 and two layers of S1600 with a layer of shale in the middle; a tarp incubated in the field to be populated by in situ methanotrophs was also tested
- Two biotarps+shale; two NMS controls+shale; and two and three NMS controls+shale

Experiment 12 was conducted to retest the shale amendment and also to investigate whether a tarp colonized by in situ methanotrophs might be more active and robust than tarps impregnated with a laboratory culture. One 4 m^2 (43 ft^2) tarp soaked in NMS was allowed to incubate atop the intermediate landfill cover soil for about one month. It was hoped that bacteria would colonize the tarp, become well established, and then serve to consume emitted methane. After the incubation period, circular pieces were cut to create a four-layer composite for testing in the chambers. Both these tarps and the tarps with shale were placed in the chambers and allowed to incubate for one week before gas samples were collected. The range of baseline fluxes was again fairly narrow (22-210 g m^{-2} d^{-1}), with even Chamber 5 yielding a larger flux than was typically measured (Table 16). Unfortunately, the low sample size and high performance variability among the biotarps with shale again yielded no statistically significant differences ($p<0.10$) between the biotarps and control tarps. The performance of the tarps incubated in situ was also variable and low. There was no evidence that the tarp+NMS incubated in the field offered better methane uptake than biotarps.

Table 16: CH_4 emission reductions by tarps amended with shale and methanotrophs grown in-situ

Treatment	Chambers	Baseline	Geotextile	% decrease	Mean % Decrease	Stan Dev
4 layers (IR26+S1600) w/ NMS+Shale	1	120.4	71.8	**40.4**		
4 layers (IR26+S1600) w/ NMS+Shale	2	210.0	114.8	**45.3**	**42.8**	**3.5**
4 layers (IR26+S1600) w/ MT+Shale	3	165.7	97.3	**41.3**		
4 layers (IR26+S1600) w/ MT+Shale	4	60.0	7.5	**87.5**	**64.4**	**32.7**
4 layers (IR26+S1600) w/ Land	5	22.0	24.3	**-10.5**		
4 layers (IR26+S1600) w/ Land	6	166.0	92.4	**44.3**	**16.9**	**38.7**
		Flux ($g\ m^{-2}\ d^{-1}$)				

Experiment 13: Test of multiple treatments on the same chamber in one day (9/19/08 and 10/3/08)

- Tarps were two layers of IR26 and two layers of S1600. Biotarps and controls with NMS-only were tested on an individual chamber.
- All six chambers were tested for bare soil flux, flux with NMS control tarp in place, and flux with biotarp in place.

Experiment 13 was repeated on two occasions, with the results from the second trial shown here (Table 17). It was performed to see if any response could be discerned between the treatments without any confounding issues related to overnight incubations or comparisons of treatments tested on different chambers. Therefore, a measurement of bare soil flux was taken, and then an NMS-only tarp was emplaced and the methane flux was measured. Then a new bare soil flux was measured, and the flux with a biotarp in place was measured. After one trial yielded some unusable concentration curves (R^2 <0.9), a second trial was conducted where only two data points are missing.

The baseline reading shown for a treatment and a chamber is the one taken just before the tarp was put in the chamber. For example, the methane flux from the bare soil in Chamber 2 was 122.1 g m^{-2} d^{-1}, which changed to 106.1 g m^{-2} d^{-1} after the NMS-only control was put in the chamber for a flux reading. After this control tarp was removed, the flux from the bare soil was measured to be 98.23 g m^{-2} d^{-1}. When the biotarp was placed in the chamber, the flux measurement was 38.41 g m^{-2} d^{-1}. The data show that the control tarp reduced the base flux by 13.1%, while the biotarp reduced the baseline flux by 60.9%. However, the overall data set show that in some cases the biotarp outperformed the control, in some cases there was no significant difference, and in other cases the effect was reversed.

Table 17: CH_4 Flux Reductions by Treatments Tested Sequentially on Each Chamber

Treatment	Chambers	Baseline	Geotextile	% decrease	Mean % Decrease	Stan Dev
4 layers (IR26+S1600) w/ NMS	2	122.1	106.1	**13.1**		
4 layers (IR26+S1600) w/ NMS	4	111.7	80.62	**27.8**		
4 layers (IR26+S1600) w/ NMS	3	330.1	428.3	**-29.8**		
4 layers (IR26+S1600) w/ NMS	6	17.75	32.56	**-83.4**	**-18.1**	**50.0**
4 layers (IR26+S1600) w/ MT	1	4.11	4.73	**-15.1**		
4 layers (IR26+S1600) w/ MT	2	98.23	38.41	**60.9**		
4 layers (IR26+S1600) w/ MT	4	115.8	94.67	**18.3**		
4 layers (IR26+S1600) w/ MT	3	99.7	126.7	**-27.1**		
4 layers (IR26+S1600) w/ MT	5	22.62	13.19	**41.7**		
4 layers (IR26+S1600) w/ MT	6	95.92	91.72	**4.4**	**13.8**	**33.5**
		Flux ($g\ m^{-2}\ d^{-1}$)				

This experiment revealed the high variability that could occur between sequential readings on a single chamber. One would expect that within the 2-3 hours required for these tests that the baseline flux for a chamber would be fairly constant. For chambers 2 and 4 this was the case. But for chambers 3 and 6 there was very high variability from one baseline reading to another. Chamber 3 yielded a flux of 330 g m^{-2} $d^{-1}$the first time it was measured and a flux of 99.7 g m^{-2} d^{-1} the second time it was measured. Likewise, chamber 6 baseline fluxes were 17.8 g m^{-2} d^{-1} and 95.9 g m^{-2} d^{-1}. There were several instances where the flux rose after a tarp was emplaced, and this could certainly be due to the fluctuating baseline fluxes in a given chamber. Two additional experiments were designed. The first, Experiment 14, was performed to vary the order in which the treatments were tested to eliminate any "position" effects that might be associated with repeated measures at a given chamber. The second, Experiment 15, was performed to conduct repeated measures of the same treatment at a given chamber to assess the variability among the consecutive readings.

Experiment 14: Test of multiple treatments on the same chamber in one day (10/23-11/24/08)

- Tarps for five of the chambers were two layers of IR26 and two layers of S1600. In one chamber, a three-layer tarp of a new product (#3W) from TenCate^{tm} was tested. Biotarps, controls with NMS-only and dry tarp controls were tested on an individual chamber.
- All six chambers were tested for bare soil flux, flux with dry tarp in place, flux with NMS control tarp in place, and flux with biotarp in place. The treatments were tested in varied order.

As noted above, Experiment 14 was a troubleshooting experiment to assess whether the order in which the treatments were tested affected the results. The baseline fluxes were always taken first and between treatment tests, but the order in which the NMS-only or biotarp was tested was randomized.

Table 18 shows that there were relatively large changes in the baseline flux from reading to reading in a given chamber. For example, in Chamber 1, the first baseline reading was 1885 but the second was 1470, a 22% change within 30 min. In chamber 4, the baseline flux changed from 854-1321g m^{-2} d^{-1}, an increase of 35%. Averaging the results of the positive percent decreases for the control and biotarp, the NMS-only control had a mean percent decrease of 28.1% but a standard deviation of 26.7. The biotarp had a mean percent decrease of 32.2% and a standard deviation of 19.1. Although this result suggests that the biotarp performance exceeds that of the controls, the results are suspect, considering the inclusion of the very low percent decrease value (0.49 g m^{-2} d^{-1}) and the high variability among the control readings.

Table 18: CH_4 Flux Reductions by Treatments Tested Sequentially in Different Orders

Treatment	Chambers	Baseline	Geotextile	%decrease	Mean % Decrease	Stan Dev
4 layers (IR26+S1600) w/NMS	1	1886	1319	**30.0**		
4 layers (IR26+S1600) w/NMS	2	273.0	328.7	**-20.4**		
4 layers (IR26+S1600) w/NMS	3	473.6	585.8	**-23.7**		
4 layers (IR26+S1600) w/NMS	4	854.2	850.0	**0.5**		
4 layers (IR26+S1600) w/NMS	5	75.6	35.0	**53.7**	**8.0**	**33.3**
4 layers (IR26+S1600) w/MT	1	1470	1060	**27.9**		
4 layers (IR26+S1600) w/MT	2	508.4	382.7	**24.7**		
5 layers (IR26+S1600) w/MT	3	558.2	522.4	**6.4**		
6 layers (IR26+S1600) w/MT	4	1321	681.9	**48.4**		
4 layers (IR26+S1600) w/MT	5	85.5	39.7	**53.6**	**32.2**	**19.1**
		Flux ($g\ m^{-2}\ d^{-1}$)				

Experiment 15: Test of replicate methane flux readings at a single chamber(4/27/09 and 6/22/09)

- Six repeated measures of the bare soil flux were collected at Chamber 6, and then six repeated measures of NMS-only controls were collected at Chamber 6.

Experiment 15 was a troubleshooting experiment to determine the variability that existed within six consecutive repeated flux measurements from the same chamber. While it had been documented early in the experiments that there was day-to-day variability for a given chamber, no experiments had been conducted to determine the degree of variability between measurements taken repeatedly at a given flux chamber. If the variability was very high, that could explain why

the results from experiment 14 showed such different baseline fluxes each time they were measured within the period of one hour.

Tests were conducted on two different days using a single chamber (#6). On one date the bare soil flux in the chamber was measured six different times, leaving about 5 minutes between the end of one measurement and the start of the next (Figure 29a). On a second date the flux through a single layer of dry tarp was again measured the same way (Figure 29b). The mean bare soil flux on the first date was 102.5 g m^{-2} d^{-1} with a standard deviation of 37.4; when the dry tarps were tested the mean was 180.7 g m^{-2} d^{-1} with a standard deviation of 33.6. When the bare soil fluxes were measured, the first and second readings were quite different, the third and fourth were similar to one another, and the fifth and sixth were similar to one another, but not similar to the prior four measurements. When the dry tarp fluxes were measured, the first and second readings differ by almost 31%, while other readings are quite similar to one another.

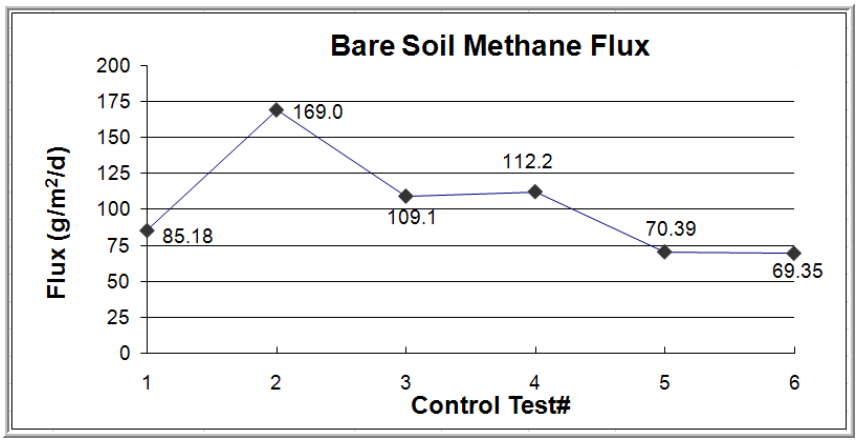

(a)

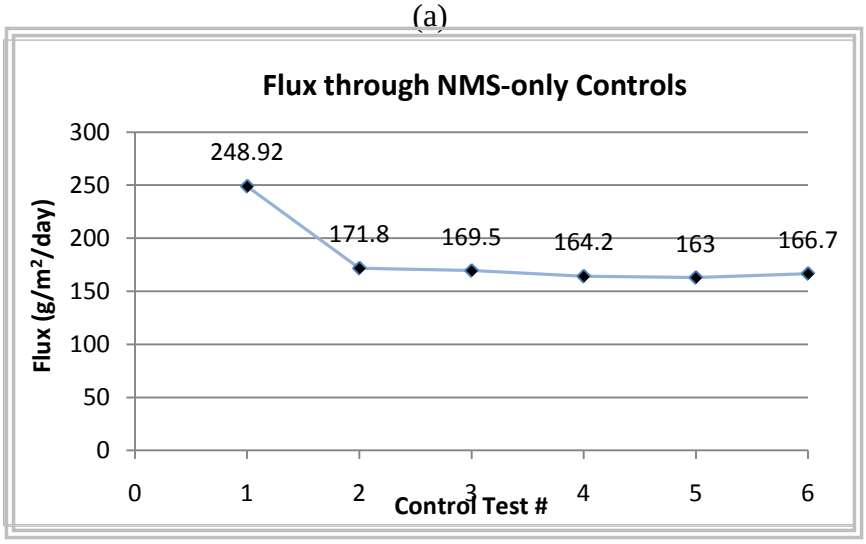

(b)

Figure 29: Repeated measures on a given flux chamber for (a) bare soil and (b) NMS-only control tarps.

CONCLUSIONS AND RECOMMENDATIONS

The aim of this study was to assess the feasibility of immobilizing methane oxidizing bacteria into a tarp-like matrix that could be used for alternative daily cover at open landfill cells. It began with creating a culture of mixed methanotrophs that could be used to inoculate prospective tarp matrices. Although methanotroph isolation can be challenging, a modification of previously published methods was used here and proved to be relatively straightforward procedurally and successful for generating liquid cultures of methanotrophs from soil samples. Use of a microarray test, which permits identification of methanotroph species in the mix without first culturing the bacteria, showed that both Type I and Type II methanotrophs were present. It also revealed that Methylobacter, Methylosinus, and Methylocystis species were all present.

The liquid cultures were used to inoculate a variety of potential supports that were either suitable for creating a tarp or suitable for incorporation into a tarp. The cultures were also used to embed the cells in alginate gel beads and to immobilize them in the core of liquid core gel capsules. Testing of the methane oxidation activity of cells immobilized in all of these ways showed that the adsorption of the cells into a synthetic geotextile matrix was easy and yielded good methane oxidation activity in batch studies. The key factor among the materials that performed well as a methanotroph matrix appeared to be good water holding capacity. Hence, geotextile and natural sponge yielded the highest methane uptake activity, while glass beads and plastic trickling filter supports did not. When a series of candidate geotextiles was compared, two were identified that had good water holding capacity and good methane oxidation activity (140-294 mL $CH_4/10^8$ cells inoculated.)

Methane oxidizers adsorbed to geotextile to create a biotarp showed a typical mesophilic response to temperature, which means they will likely be less active in a biotarp during colder months of the year. There is some evidence that population shifts may allow biotarp cultures to adapt to changing temperature, but that phenomenon was not investigated here. Biotarps showed a distinct drop in activity during batch starvation experiments, where they were exposed to alternating conditions of 12 h with and without methane in the headspace. When biotarp swatches were exposed to strenuous washing (to simulate heavy rainfall), about 70% of the cells could be removed. However, the 30% that remained provide to be quite resistant to removal, suggesting that a biotarp could repopulate after heavy rainstorms. Molecular staining of biotarp specimens to examine the microbial architecture of methane oxidizers in the tarp showed that there was a notable build up of exopolymer substances (EPS), which is known to encase the methanotrophs and inhibit their methane oxidation capacity. It is possible that under field conditions, this EPS may be sloughed off during rain events and serve to revitalize the underlying biofilm.

In laboratory simulations of landfill conditions, where biotarp prototypes were exposed to a continuous flow of methane (22 g m^{-2} d^{-1}) and carbon dioxide from below and air from above, the highest methane uptake observed was 50%, and this was with a four-layer composite biotarp made with two types of geotextile and a layer of methanotroph-inoculated shale layered with the

geotextiles. Without an external amendment, methane uptake was highest initially and then tapered off as the days of incubation increased. Amendments such as landfill soil, compost, and shale appeared to maintain steadier uptake rates over nine days of incubation.

In field tests, biotarp prototype samples were tested as 12 in circles in static flux chambers installed in intermediate cover at a nearby landfill. Control tarps were dry tarps or tarps wetted with either DI or NMS media. The flux chambers were recessed into the intermediate cover to the point where the measured fluxes generally fell in the range of 100-200 g m^{-2} d^{-1}. Six chambers were used within a 20x20 ft area. It was difficult to draw reliable conclusions from the field experiments. Some of the phenomena observed were: (i) there was high variability in flux readings from chamber to chamber; from day-to-day for a given chamber; and even within 15 minute intervals of readings from a given chamber; (ii) wetted tarps used for controls showed good reductions of methane emissions, and these reductions were often equal to or better than reductions by biotarp samples; (iii) rainfall events confounded the data collected, because some chambers appeared to be more influenced by wet conditions than others. A variety of manipulations were undertaken to improve biotarp performance, but the high variability of field readings and frequent rain events during the field test campaign required that testing be terminated before satisfactory biotarp performance could be demonstrated. Another experimental paradigm will likely be needed to obtain more conclusive data about biotarp performance. Specifically, an engineered system to deliver subsurface synthetic landfill gas upward through a field scale prototype tarp will be needed to eliminate all of the confounding variables of active field conditions, where rainfall and atmospheric pressure changes make statistically meaningful testing comparisons very difficult to obtain.

Some of the issues that remain for future testing are whether or not other geotextiles or even other matrices would provide better configurational or nutritional support for methanotrophs. The four-layer design used here appeared to be required to enhance the contact time between methane and the biotarp. If a lighter but thicker matrix could be found, the additional gas retention time it could provide would likely increase methane oxidation without making the tarp too cumbersome to place and remove. Methanotrophs in a biotarp may also benefit from a source of organic material or the presence of other microorganisms, if synergistic effects are important. The addition of soil, compost and shale to composite biotarps were not thought to be major sources of additional bacteria, and yet they did prolong steady-state methane uptake in the laboratory reactors. Also, the staining of EPS and methanotrophs suggested that the methanotrophs were not confluent on the geotextile fibers, so that their density could be further increased.

Overall, the findings suggest that a methanotroph embedded biotarp appears to be a feasible strategy to mitigate methane emission from landfill cells, although the performance of field-tested biotarps was not robust here. The problem addressed here – fugitive methane emissions from open landfill cells – is still an important one. While great effort and expense target landfill cover engineering, emissions from open cells proceed unabated. Interferences from high flux variability and weather conditions limited the amount and reliability of the data

collected for this study. A different and more controlled testing paradigm is needed to unequivocally show biotarp performance under field conditions. Also, continued modification of the biotarp prototypes to provide nutrient replenishment or a source of synergistic heterotrophs is recommended. It may be possible to design desiccation resistant capsules for timed release of nutrients, which was beyond the scope of the work here, that would stimulate greater biotarp activity.

Finally, the biotarp concept can be extended to include interception of other compounds beyond methane. Landfills are well-known for emitting a variety of non-methane organic compounds, such as aromatic hydrocarbons and chlorinated solvents that are volatile and travel with carbon dioxide and methane into the atmosphere. It has already been shown in the laboratory that some of these hazardous air pollutants can be cometabolized by methanotrophs[143]. Also, the biotarp concept offers a unique opportunity for sensor applications. In addition to being microbially active, it could be embedded with remote real-time sensors that could deliver information about emissions from open cells or atop intermediate cover.

REFERENCES

[1] **U.S. EPA**. 2006. Global Mitigation of Non-CO_2 Greenhouse Gases, EPA 430-R-06-005

[2] **U.S. EPA**., 2009. U.S. Inventory of Greenhouse Gas Emissions and Sinks: 1990-2007, EPA 430-R-09-004.

[3] **U.S. EPA.** 2006. Municipal Solid Waste in the United States. Office of Solid Waste. EPA-530-R-06-011.

[4] **Tchobanoglous, G., F. L. Burton, and H. D. Stensel**. 2003. Wastewater Engineering Treatment and Reuse, 4 ed. McGraw-Hill, New York.

[5] **Tchoubanoglous, G., H. Theisen, and H. Vigil.** 1993. Integrated Solid Waste Management Principles: Engineering Principles and Management, McGraw-Hill.

[6] Personal communication, Dr. Jean Bogner, Landfills +, Inc, Wheaton, IL.

[7] **Bogner, J., M. Meadows, and P. Czepiel.** 1997. Fluxes of Methane between Landfills and the Atmosphere: Natural and Engineered Controls. Soil Use and Management 13:268-277.

[8] **Haughey, R. D.** 2001. Landfill alternative daily cover: conserving air space and reducing landfill operating cost. Waste Management and Research **19**:89-95.

[9] **Hilger, H.A. and Huber-Humer, M.** 2003. Biotic landfill cover treatments for mitigating methane emissions, Environmental Monitoring and Assessment, Special Edition on Innovative Technologies and Policies for Waste Management, **84**:71-84.

[10] **Scheutz, C., Bogner, J**. 2003. Comparative oxidation and net emissions of CH4 and selected non-methane organic compounds in landfill cover soils, Environmental Science and Technology **37**:5143-5149.

[11] **Huber-Humer, M., J. Gebert, and H. Hilger.** 2008. Biotic systems to mitigate landfill methane emissions. Waste Management Research **26:**33-46.

[12] **Humer, M., and P. Lechner.** 2001. Microbial methane oxidation for the reduction of landfill gas emissions. Journal of Solid Waste Technology and Management **27:**147-151.

[13] **Huber-Hummer, M.** 2004. Abatement of Landfill Methane Emissions by Microbial Oxidation in Biocovers made of Compost. University of Natural Resources and Applied Life Sciences (BOKU), Vienna.

[14] **Dever, S. A., G. E. Swarbrick, and R. M. Stuetz.** 2005. Passive drainage and biofiltration of landfill gas using recycled waste materials, under Australian conditions, Tenth International Waste Management and Landfill Symposium, Cagliari, Italy.

[15] **Figueroa, R. A.** 1996. Landfill gas treatment by biofilters, p. 535-559. *In* T. H. Christensen, R. Cossu, and R. Stegmann (ed.), Landfilling of Waste: Biogas E&FN Spoon, London.

[16] **Straka, F., J. Crha, M. Musilova, and M. Kuncarova.** 1999. LFG-Biofilters on old landfills, Seventh International Waste Management and Landfill Symposium Cagliari, Italy.

[17] **Sly, L. I., L. Y. Bryant, J. M. Cox, and J. M. Anderson.** 1993. Development of a biofilter for the removal of methane from coal mine ventilation atmospheres. Journal of Applied Microbiology and Biotechnology **39:**400-404.

[18] **Maurice, C., and A. Lagerkvist.** 2004. Assessment of the methane oxidation capacity of soil. Waste Management and Research **22:**42-48.

[19] **Gebert, J., A. Groengroeft, and G. Miehlich.** 2003. Kinetics of microbial landfill methane oxidation in biofilters. Waste Management **23:**609-619.

[20] **Park, S., K. W. Brown, and J. C. Thomas.** 2002. The effect of various environmental and design parameters on methane oxidation in a model biofilter. Waste Management and Research **20**.

[21] **Powelson, D. K., J. Chanton, T. Abichou, and J. Moreles.** 2006. Methane oxidation in water spreading and compost biofilters. Waste Management and Research **24:**528-536.

[22] **Du Plessis, C. A., J. M. Strauss, E. M. T. Sebapalo, and K.-H. J. Tiedel.** 2003. Empirical model for methane oxidation using composted pine bark biofilter. Fuel **82:**1359-1365.

[23] **Melse, R. W., and A. Van der Werf.** 2004. Biofiltration for mitigation of methane emission from animal husbandry. Environmental Science and Technology **39:**5460-5468.

[24] **Petit, J. R., J. Jouzel, D. Raynaud, N. I. Barkov, J.-M. Barnola, I. Basile, M. Bender, J. Chappellaz, M. Davis, G. Delaygue, M. Delmotte, V. M. Kotlyakov, M. Legrand, V. Y. Lipenkov, C. Lorius, L. PÉpin, C. Ritz, E. Saltzman, and M. Stievenard.** 1999. Climate and atmospheric history of the past 420,000 years from the Vostok ice core, Antarctica. Nature **399:**429-436

[25] **Streese, J., and R. Stegmann.** 2003. Microbial oxidation of CH_4 from old landfills in biofilters. Waste Management **23:**573-580.

[26] **Powelson, D. K., J. Chanton, T. Abichou, and J. Moreles.** 2006. Methane oxidation in water spreading and compost biofilters. Waste Management and Research **24:**528-536.

[27] **Wrangstadh, M., P.L. Conway, and S. Kjelleberg.** 1986 The production and release of an extracellular polysaccharide during starvation of a marine *Pseudomonas* sp. and the effect thereof on adhesion. Archives of Microbiology **145**, 220-227.

[28] **Chen, J**. 2004. Efficient immobilization of whole cells of Methylomonas sp. Strain GYJ3 by sol-gel entrapment. Journal of Molecular Catalysis **30**:167-172.

[29] **Kierstan, M., and C. Bucke**. 1977. The immobilization of microbial cells, subcellular organelles, and enzymes in calcium alginate gels. Biotechnology and Bioengineering **19**:387-397.

[30] **Williams, R. A., and H. W. Blanch**. 1994. Covalent immobilization of protein monolayers for biosensor applications. Biosensors and Bioelectronics **9**:159-167.

[31] **Tampion, J., and M. D. Tampion**. 1987. Immobilized Cells: Principles and Applications. Cambridge University Press, New York.

[32] **Pashova, S., L. Slokoska, E. Krumova, and M. Angelova**. 1999. Induction of polymethylgalacturonase biosynthesis by immobilized cells of Aspergillus niger **26**. Enzyme and Microbial Technology **24**:535-540.

[33] **Newby, D. T., D. W. Reed, L. M. Petzke, A. L. Igoe, M. E. Delwiche, F. F. Roberto, J. P. McKinley, M. J. Whiticar, and F. S. Colwell.** 2004. Diversity of methanotroph communities in a basalt aquifer. FEMS Microbiology Ecology **48:**333-344.

[34] **Mallick, N.** 2002. Biotechnological potential of immobilized algae for wastewater N, P and metal removal: A review. BioMetals **15:**377-390

[35] **Bhamidimarri, S. M. R.** 1990. Adsorption and attachment of microorganisms to solid supports, p. 29-43. *In* R. D. Tyagi and K. Vembu (ed.), Wastewater Treatment by Immobilized Cells. CRC Press, Inc., Boca Raton, FL.

[36] **Pethica, B. S.** 1961. The physical chemistry of cell adhesion. Experimental Cell Research Suppl **8:**123-140.

[37] **Mozes, N., F. Marchal, M. P. Hermesse, J. L. Van Haecht, L. Reuliaux, A. J. Leonard, and P. G. Rouxhet.** 1987. Immobilization of microorganisms by adhesion: Interplay of electrostatic and nonelectrostatic interactions. Biotechnology and Bioengineering **30:**439-450.

[38] **Michaux, M., M. Paquot, B. Baijot, and P. Thonart.** 1982. Continuous fermentation: Improvement of cell immobilization by zeta potential measurement, p. 475-484. *In* E. L. Gaden Jr. (ed.), Biotechnology and Bioengineering Symposium 12. John Wiley, New York.

[39] **Klotz, S. A., D. J. Drutz, and J. E. Zajic.** 1985. Factors governing adherence of *Candida* species to plastic surfaces. Infection and Immunity **50:**97-101.

[40] **Klein, J., and H. Ziehr.** 1990. Immobilization of microbial cells by adsorption. Journal of Biotechnology **16:**1-15.

[41] **Slabova, O. I., and D. I. Nikitin.** 2005. Immobilization of oligotrophic bacteria by absorption on porous carriers. Microbiology **74:**371-373

[42] **Wang, L., H. Chua, S. N. Sin, Q. Zhou, D. M. Ren, and Z. L. Li.** 2004. A Combined bioprocess for integrated removal of copper and organic pollutant from copper-containing municipal wastewater. Journal of Environmental Science and Health, Part A: Toxic/Hazardous Substances & Environmental Engineering **39:**223-235.

[43] **Saeed, A., and M. Iqbal.** 2006. Immobilization of blue green microalgae on loofa sponge to biosorb cadmium in repeated shake flask batch and continuous flow fixed bed column reactor system. World Journal of Microbiology and Biotechnology **22:**775-782

[44] **Tse, S.-W., and J. Yu.** 2003. Adsorptive immobilization of a *Pseudomonas* strain on solid carriers for augmented decolorization in a chemostat bioreactor. Biofouling **19:**223-233.

[45] **Marcipar, A., N. Cochet, L. Brackenridge, and J. M. Lebeault.** 1979. Immobilization of yeasts on ceramic supports. Biotechnology Letters **1:**65-70.

[46] **Navarro, J. M., and G. Durand.** 1977. Modification of yeast metabolism by immobilization onto porous glass. Applied Microbiology and Biotechnology **4:**243-254.

[47] **Champluvier, B., B. Kamp, and P. G. Rouxhet.** 1988. Immobilization of β-galactosidase retained in yeast: adhesion of the cells on a support. Applied Microbiology and Biotechnology **V27:**464-469.

[48] **Stewart, P. S., and C. R. Robertson.** 1988. Product inhibition of immobilized *Escherichia coli* arising from mass transfer limitation. Applied and Environmental Microbiology **54:**2464-2471.

[49] **Willaert, R., and G. Baron.** 1993. Growth kinetics of gel-immobilized yeast cells studied by on-line microscopy. Applied Microbiology and Biotechnology **39:**347-352.

[50] **Zobell, C. E.** 1937. The influence of solid surfaces upon the physiological activities of bacteria in sea water. Journal of Bacteriology **33:**86.

[51] **Mateo, C., O. Abian, R. Fernandez-Lafuente, and J. M. Guisan.** 2000. Reversible enzyme immobilization via a very strong and nondistorting ionic adsorption on support-polyethylenimine composites. Biotechnology and Bioengineering **68:**98-105.

[52] **Kolot, F. B.** 1981. Microbial carriers - strategy for selection. Process Biochemistry **16:**2-9, 30-46.

[53] **Atkinson, B., G. M. Black, and A. Pinches.** 1980. Process intensification using cell support systems. Process Biochemistry **15:**24-32.

[54] **Manohar, S., C. K. Kim, and T. B. Karegoudar.** 2001. Enhanced degradation of napthalene by immobilization of *Pseudomonas* sp. strain NGK1 in polyurethane foam. Applied Microbiology and Biotechnology **55:**311-316.

[55] **Guiraud, J. P., A. M. Bajon, P. Chautard, and P. Galzy.** 1983. Inulin hydrolysis by an immobilized yeast-cell reactor. Enzyme and Microbial Technology **5:**185-190.

[56] **Gomez, J. M., D. Cantero, and C. Webb.** 2000. Immobilization of *Thiobacillus ferroxidans* cells on nickel alloy fibre for ferrous sulfate oxidation. Applied Microbiology and Biotechnology **54**.

[57] **Marcipar, A., N. Cochet, L. Brackenridge, and J. M. Lebeault.** 1979. Immobilization of yeasts on ceramic supports. Biotechnology Letters **1:**65-70.

[58] **Opara, C. C., and J. Mann.** 1988. Development of ultraporous fired bricks as support for yeast cell immobilization. Biotechnology and Bioengineering **31:**470-475.

[59] **Kovalenko, G. A., and V. D. Sokolovskii.** 1992. Epoxidation of propene by microbial cells immobilized on inorganic supports. Biotechnology and Bioengineering **39:**522-528.

[60] **O'Toole, G., H. B. Kaplan, and R. Kolter.** 2000. Biofilm formation as microbial development. Annual Reviews in Microbiology **54:**49-79.

[61] **Dunne, W. M.** 2002. Bacterial adhesion: seen any good biofilms lately? Clinical Microbiology Reviews **15:**155-166.

[62] **Jefferson, K. K.** 2004. What drives bacteria to produce a biofilm? FEMS Microbiology Letters **236:**163-173.

[63] **Mozes, N., and P. G. Rouxhet.** 1992. Influence of surfaces on microbial activity, p. 125-136. *In* M. L.F., T. R. Bott, M. Fletcher, and B. Capdeville (ed.), Biofilms. Kluwer Academic Publishers, Dordrecht.

[64] **Lipscomb, J. D.** 1994. Biochemistry of the soluble methane monooxygenase. Annual Review of Microbiology **48:**371-399.

[65] **Wittlich, P., E. Capan, M. Schlieker, K.-D. Vorlop, and U. Jahnz.** 2004. Entrapment in Lentikats®, p. 53-63. *In* V. Nedovic and R. Willaert (ed.), Fundementals of Cell Immobilisation Biotechnology. Kluwer Academic Publishers, Netherlands.

[66] **Lozinsky, V. I., and F. M. Plieva.** 1998. Poly(vinyl alcohol) cryogels employed as matrices for cell immobilization. D. Overview of recent research and developments. Enzyme and Microbial Technology **23:**227-242.

[67] **Jekel, M., A. Buhr, T. Willke, and D. Vorlop.** 1998. Immobilization of biocatalyst in LentiKats®. Chemical Engineering and Technology **21:**275-278.

[68] **Rebros, M., M. Rosenberg, R. Stloukal, and L. Kristofikova.** 2005. High efficiency ethanol fermentation by entrapment of *Zymomonas mobilis* into LentiKats®. Letters in Applied Microbiology **41:**412-416.

[69] **Hsieh, Y.-L., S.-K. Tseng, and Y.-J. Chang.** 2002. Nitrification using polyvinyl alcohol-immobilized nitrifying biofilm on an O_2-enriching membrane. Biotechnology Letters **24:**315-319.

[70] **Martins, R. F., F. M. Plieva, A. Santos, and R. Hatti-Kaul.** 2003. Integrated immobilized cell reactor-adsorption system for β-cyclodextrin production: a model study using PVA-cryogel entrapped *Bacillus agaradhaerens* cells. Biotechnology Letters **25:**1537-1543.

[71] **Trelles, J. A., L. Bentancor, A. Schoijet , S. Porro, E. S. Lewkowicz, J. V. Sinisterra, and A. M. Iribarren.** 2004. Immobilized *Escherichia coli* BL21 as a catalyst for the synthesis of adenine and hypoxanthine nucleosides. Chemistry and Biodiversity **1:**280-288.

[72] **Trelles, J. A., E. S. Lewkowicz, J. V. Sinisterra, and A. M. Iribarren.** 2004. Free and immobilised *Citrobacter amalonaticus* CECT 863 as a biocatalyst for nucleoside synthesis. International Journal of Biotechnology **6:**376 - 384

[73] **Li, F., P. Xu, J. Feng, L. Meng, Y. Zheng, L. Luo, and C. Ma.** 2005. Microbial desulfurization of gasoline in a *Mycobacterium goodii* X7B immobilized-cell system. Applied and Environmental Microbiology **71:**276-281.

[74] **Vingerhoeds, M. H., and P. F. H. Harmsen.** 2004. Proteins: Versatile materials for encapsulation, p. 73-102. *In* V. Nedovic and R. Willaert (ed.), Fundamentals of Cell Immobilisation Biotechnology. Kluwer Academic Publishers, Netherlands.

[75] **de Graaf, L. A.** 2000. Denaturation of proteins from a non-food perspective. Journal of Biotechnology **79:**299-306.

[76] **Vingerhoeds, M. H., and P. F. H. Harmsen.** 2004. Proteins: Versatile materials for encapsulation, p. 73-102. *In* V. Nedovic and R. Willaert (ed.), Fundamentals of Cell Immobilisation Biotechnology. Kluwer Academic Publishers, Netherlands.

[77] **Tolstoguzov, V. B.** 1993. Thermoplastic extrusion - the mechanism of the formation of extrudate structure and properties. Journal of the American Oil Chemists' Society **70:**417-424.

[78] **Reid, A. A., J. C. Vuillemard, M. Britten, Y. Arcand, E. Farnworth, and C. P. Champagne.** 2005. Microentrapment of probiotic bacteria in a Ca^{2+}-induced whey protein gel and effects on their viability in a dynamic gastro-intestinal model. Journal of Microencapsulation **22:**603 – 619.

[79] **Plessas, S., A. Bekatorou, M. Kanellaki, C. Psarianos, and A. Koutinas.** 2005. Cells immobilized in a starch-gluten-milk matrix usable for food production. Food Chemistry **89:**175-179.

[80] **Sungur, S., R. Al-Taweel, O. Yıldırım, and E. Loğoğlu.** 2006. Immobilization of *Saccharomyces cerevisiae* in gelatin cross-linked with Chromium ions for conversion of sucrose by intracellular invertase. Polymer-Plastics Technology and Engineering **45:**929 – 934.

[81] **Melvik, J. E., and M. Dornish.** 2004. Alginate as a carrier for cell immobilization, p. 33-51. *In* V. Nedovic and R. Willaert (ed.), Fundamentals of Cell Immobilisation Biotechnology Kluwer Adademic Publishers, Netherlands

[82] **Onsøyen, E.** 1996. Commercial applications of alginates. Carbohydrates in Europe **14:**26-31.

[83] **Kushal, R., S. K. Anand, and H. Chander.** 2006. *In vivo* demonstration of enhanced probiotic effect of co-immobilized *Lactobacillus acidophilus* and *Bifidobacterium bifidum*. International Journal of Dairy Technology **59:**265-271.

[84] **Takeno, K., Y. Yamaoka, and K. Sasaki.** 2005. Treatment of oil-containing sewage wastewater using immobilized photosynthetic bacteria. World Journal of Microbiology and Biotechnology **21:**1385-1391.

[85] **Li, P., X. Wang, F. Stagnitti, L. Li, Z. Gong, H. Zhang, X. Xiong, and C. Austin.** 2005. Degradation of phenanthrene and pyrene in soil slurry reactors with immobilized bacteria *Zoogloea* sp. Environmental Engineering Science **22:**390-399.

[86] **Khor, E., W.-F. Ng, and C.-S. Loh.** 1998. Two-coat system for encapsulation of *Spathoglottis plicata* (Orchidaceae) seeds and protocorms. Biotechnology and Bioengineering **59:**635-639.

[87] **Kierstan, M., and C. Bucke.** 1977. The immobilization of microbial cells, subcellular organelles, and enzymes in calcium alginate gels. Biotechnology and Bioengineering **19:**387-397.

[88] **Quirasco, M., M. Remaud-Simeon, P. Mansan, and A. Lopez-Munguia.** 1999. Experimental behavior of a whole cell immobilized dextransucrase biocatalyst in batch and packed bed reactors. Bioprocess Engineering **20:**289-295.

[89] **Read, T.-A., D. R. Sorensen, R. Mahesparan, P. O. Enger, R. Timpl, B. R. Olsen, M. H. B. Hjelstuen, O. Haraldseth, and R. Bjerkvig.** 2001. Local endostatin treatment of gliomas administered by microencapsulated producer cells. Nature Biotechnology **19:**29-34.

[90] **Seki, M., and S. Furusaki.** 1985. Effect of intraparticle diffusion on reaction by immobilized growing yeast. Journal of Chemical Engineering of Japan **18:**461-463.

[91] **Seki, M., K. Shigematsu, and S. Furusaki.** 1990. Cell growth and reaction characteristics of immobilized *Zymomonas mobilis*. Annals of the New York Academy of Sciences **613:**290-302.

[92] **Tanaka, H., S. Irie, and H. Ochi.** 1989. A novel immobilization method for prevention of cell leakage from gel matrix. Journal of Fermentation and Bioengineering **68:**216-216

[93] **Klein, J., J. Stock, and K.-D. Vorlop.** 1983. Pore size and properties of spherical Ca-alginate biocatalysts. European Journal of Applied Microbiology and Biotechnology **18:**86-91.

[94] **Spikermann, P., K. D. Vorlop, and J. Klein.** 1987. Animal cells encapsulated within Ca-alginate hollow spheres. Proceedings of the 4th European Congress on Biotechnology **3**.

[95] **Nigam, S. C., I. Tsoa, A. Sakoda, and H. Y. Wang.** 1988. Techniques for preparing hydrogel membrane capsules. Biotechnology Techniques **2:**271-276.

[96] **Calhoun, A., and G. M. King.** 1998. Characterization of root-associated methanotrophs from three freshwater macrophytes: *Pontederia cordata*, *Sparganium eurycarpum*, and *Sagittaria latifolia*. Applied and Environmental Microbiology **64**:1099-1105.

[97] **Kallmeyer, J., and A. Boetius**. 2004. Effects of Temperature and Pressure on Sulfate Reduction and Anaerobic Oxidation of Methane in Hydrothermal Sediments of Guaymas Basin. Applied and Environmental Microbiology **70**:1231-1233.

[98] **Laursen, A. E., C. F. Kulpa, M. F. Niedzielski, and M. C. Estable**. 2007. Bacterial cultures capable of facultative growth on methane under thermophilic or thermotolerant conditions Journal of Environmental Engineering and Science **6**:643-650.

[99] **Wise, M. G., J. V. McArthur, and L. J. Shimkets.** 1999. Methanotroph diversity in landfill soil: Isolation of novel type I and type II methanotrophs whose presence was suggested by culture-independent 16S ribosomal DNA analysis. Applied and Environmental Microbiology **65:**4887-4897.

[100] **Whittenbury, R., K. C. Phillips, and J. F. Wilkinson.** 1970. Enrichment, isolation and some properties of methane-utilizing bacteria. Journal of General Microbiology **61:**205-218

[101] **Stralis-Pavese, N., A. Sessitsch, A. Weilharter, T. Reichenauer, J. Riesing, J. Csontos, J. C. Murrell, and L. Bodrossy.** 2004. Optimization of diagnostic microarray for application in

analyzing landfill methanotroph communities under different plant covers. Environmental Microbiology **6:**347-363.

[102] **Knaebel, D. B., K. E. Stromo, et al.** 1997. Immobilization of bacteria in macro- and microparticles. Methods in Biotechnology: Bioremediation Protocols. D. Sheehan. Totowa, NJ, Humana Press Inc.

[103] **Koyama, K., and S. Seki.** 2004. Evaluation of mass-transfer characteristics in alginate-membrane liquid-core capsules prepared using polyethylene glycol. Journal of Bioscience and Bioengineering **98**:114-121.

[104] **Arcangeli, J.-P., and E. Arvin**. 1997. Modelling the growth of a methanotrophic biofilm Water Science Technology **36**:199-204.

[105] **Arcangeli, J.-P., and E. Arvin**. 1999. Modelling the growth of a methanotrophic biofilm: Estimation of parameters and variability. Biodegradation **10**:177-191.

[106] **Bodrossy, L., E. M. Holmes, A. J. Holmes, K. L. Kovacs, and J. C. Murrell**. 1997. Analysis of 16S rRNA and methane monooxygenase gene sequences reveals a novel group of thermotolerant and thermophilic methanotrophs, *Methylocaldum* gen. nov. Archives of Microbiology:493–503.

[107] **Chen, Y., M. G. Dumont, N. P. McNamara, P. M. Chamberlain, L. Bodrossy, N. Stralis-Pavese, and J. C. Murrell.** 2008. Diversity of the active methanotrophic community in acidic peatlands as assessed by mRNA and SIP-PLFA analyses. Environmental Microbiology **10**:446-459.

[108] **Gunther, G. R., J. L. Wang, I. Yahara, B. A. Cunningham, and G. M. Edelman**. 1973. Concanavalin A derivatives with altered biological activities. Proceedings of the National Academy of Sciences **70**:1012-1016.

[109] **Mandal, D. K., and C. F. Brewer.** 1993. Differences in the binding affinities of dimeric concanavalin A (including acetyl and succinyl derivatives) and tetrameric concanavalin A with large oligomannose-type glycopeptides. Biochemistry **32**:5116-5120.

[110] **Chida, K., G. Shen, T. Kodama, and Y. Minoda**. 1983. Acidic polysaccharide production from methane by a new-methane oxidizing bacterium H-2 Agricultural and Biological Chemistry **47**:275-280.

[111] **Hou, C. T., A. I. Laskin, and R. N. Patel.** 1978. Growth and polysaccharide production by *Methylocystis parvus* OBBP on methanol. Applied and Environmental Microbiology **37**:800-804.

[112] **Wyss, O., and E. J. Moreland**. 1968. Composition of the capsule of obligate hydrocarbon-utilizing bacteria. Applied and Environmental Microbiology **16**:185.

[113] **Eller, G., S. Stubner, and P. Frenzel**. 2001. Group-specific 16S rRNA targeted probes for the detection of type I and type II methanotrophs by fluorescence *in situ* hybridisation. FEMS Microbiology Letters **198**:91-97.

[114] **Gulledge, J., A. Ahmad, P. A. Steudler, W. J. Pomerantz, and C. M. Cavanaugh**. 2001. Family- and genus-level 16S rRNA-targeted oligonucleotide probes for ecological studies of methanotrophic bacteria. Applied and Environmental Microbiology **67**:4726-4733.

[115] **Hanson, R. S., and T. E. Hanson**. 1996. Methanotrophic bacteria. Microbiological Reviews **60**:439-471.

[116] **Joergensen, L., and H. Degn**. 1983. Mass spectrometric measurements of methane and oxygen utilization by methanotrophic bacteria. FEMS Microbiology Ecology **20**:331-335.

[117] **Amaral, J. A., and R. Knowles**. 1995. Growth of methanotrophs in methane and oxygen counter gradients. FEMS Microbiology Letters **126**:215-220.

[118] **Czepiel, P. M., B. Mosher, P. M. Crill, and R. C. Harriss**. 1996. Quantifying the effect of oxidation on landfill methane emissions. Journal of Geophysical Research **101**:16721-16729.

[119] **Radajewski, S., G. Webster, D. S. Reay, S. A. Morris, P. Ineson, D. B. Nedwell, J. Prosser, and J. C. Murrell. 2002**. Identification of active methylotroph populations in an acidic forest soil by stable isotope probing. Microbiology **148**:2331-2342.

[120] **Bodrossy, L., N. Stralis-Pavese, M. Konrad-Köszler, A. Weilharter, T. G. Reichenauer, D. Schöfer, and A. Sessitsch**. 2006. mRNA-based parallel detection of active methanotroph populations by use of a diagnostic microarray. Applied and Environmental Microbiology **72**:1672–1676.

[121] **Auman, A. J., S. Stolyar, A. M. Costello, and M. E. Lidstrom.** 2000. Molecular characterization of methanotrophic isolates from freshwater lake sediment. Applied and Environmental Microbiology **66:**5259-5266.

[122] **Dedysh, S. N., M. Derakshani, and W. Liesack.** 2001. Detection and enumeration of methanotrophs in acidic sphagnum peat by 16S rRNA fluorescence in situ hybridization, including the use of newly developed oligonucleotide probes for *Methylocella palustris*. Applied and Environmental Microbiology **67**:4850-4857.

[123] **Kolb, S., C. Knief, S. Stubner, and R. Conrad**. 2003. Quantitative detection of methanotrophs in soil by novel *pmoA*-targeted real-time PCR assays. Applied and Environmental Microbiology **69**:2423-2429.

[124] **Bodelier, P. L. E., M. Meima-Franke, G. Zwart, and H. J. Laanbroek**. 2005. New DGGE strategies for the analyses of methanotrophic microbial communities using different combinations of existing 16S rRNA-based primers. FEMS Microbiology Ecology **52**:163-174.

[125] **Wise, M. G., J. V. McArthur, and L. J. Shimkets**. 2001. *Methylosarcina fibrata* gen. nov., sp. nov. and *Methylosarcina quisquiliarum* sp. nov., novel type 1 methanotrophs. International Journal of Systematic and Evolutionary Microbiology **51**:611–621.

[126] **Henckel, T., P. Roslev, and R. Conrad**. 2000. Effects of O2 and CH4 on presence and activity of the indigenous methanotrophic community in rice field soil. Environmental Microbiology **2**:666-679.

[127] **Rosch, J. W., J. Sublett, G. Gao, Y.-D. Yang, and E. I. Tuomanen**. 2008. Calcium efflux is essential for bacteria survival in the eukaryotic host. Molecular Microbiology **70**:435-444.

[128] **King, G. M**. 1992. Ecological aspects of methane oxidation, a key determinant of global methane dynamics, p. 431-468. *In* K. C. Marshall (ed.), Advances in Microbial Ecology, vol. 12. Plenum, New York.

[129] **Borjesson, G., and B. H. Svensson**. 1997. Seasonal and diurnal methane emissions from a landfill and their regulation by methane oxidation. **15**:33-54.

[130] **Whalen, S. C., W. S. Reeburgh, and K. A. Sandbeck**. 1990. Rapid methane oxidation in a landfill cover soil. Applied and Environmental Microbiology **56**:3405-3411.

[131] **Boeckx, P., O. van Cleemput, and I. Villaralvo**. 1996. Methane emission from a landfill and the methane oxidising capacity of its covering soil. Soil Biology and Biochemistry **28**:1397-1405.

[132] **De Visscher, A., M. Schippers, and O. V. Cleemput**. 2001. Short-term kinetic response of enhanced methane oxidation in landfill cover soils to environmental factors. Biology and Fertility of Soils **33**:231-237.

[133] **King, G. M., and A. P. S. Adamsen**. 1992. Effects of temperature on methane consumption in a forest soil and in pure cultures of the methanotroph *Methylomonas rubra*. Applied and Environmental Microbiology **58**:2758-2763.

[134] **Visvanathan, C., D. Pokhrel, W. Cheimchaisri, J. P. A. Hettiaratchi, and J. S. Wu**. 1999. Methanotrophic activities in tropical landfill cover soils: effects of temperature, moisture content and methane concentration, p. 313-323, vol. 17.

[135] **Gebert, J., A. Groengroeft, and G. Miehlich**. 2003. Kinetics of microbial landfill methane oxidation in biofilters. Waste Management **23**:609-619.

[136] **Gebert, J., M. Alawi, and L. Bodrossy**. 2006. Influence of temperature on the activity and community composition in a biofilter used for the oxidation of landfill methane, Intercontinental Landfill Research Symposium, Gällivare, Sweden.

[137] **Yamamoto, S., J. B. Alcauskas, and T. E. Crozier**. 1976. Solubility of methane in distilled water and seawater. Journal of Chemical & Engineering Data **21**:78-80.

[138] **Whittenbury, R., S. L. Davies, and J. F. Davey.** 1970. Exospores and cysts formed by methane-utilizing bacteria. Journal of General Microbiology **61**:219-226.

[139] **Reed, W. M., J. A. Titus, P. R. Dugan, and R. M. Pfister**. 1980. Structure of *Methylosinus trichosporium* exospores. Journal of Bacteriology **141**:908-913.

[140] **Hanson, R. S., and E. Wattenburg**. 1991. The ecology of methane oxidizing bacteria, p. 325-349. *In* I. Goldberg and J. S. Rokem (ed.), Biology of Methylotrophs. Butterworths Publishers, London, UK.

[141] **Huber-Humer, M., J. Gebert, and H. Hilger**. 2008. Biotic systems to mitigate landfill methane emissions. Waste Management Research **26**:33-46.

[142] **Gebert, J., A. Groengroeft, and G. Miehlich**. 2003. Kinetics of microbial landfill methane oxidation in biofilters. Waste Management **23**:609-619.

[143] **Scheutz, C., Bogner, J**. 2003. Comparative oxidation and net emissions of CH_4 and selected non-methane organic compounds in landfill cover soils, *Environmental Science and Technology* **37**:5143-5149.